Master's thesis

NTNU
Norwegian University of Science and Technology
Faculty of Natural Sciences
Department of Chemistry

Jostein Zakariassen Nilsen

Evaluation of chloride and sodium ion selective electrodes (ISEs) for use in biological regenerative life support systems

Master's thesis in MSENVITOX
Supervisor: Øyvind Mikkelsen
Co-supervisor: Øyvind Mejdell Jakobsen
June 2022

NTNU
Norwegian University of
Science and Technology

Jostein Zakariassen Nilsen

Evaluation of chloride and sodium ion selective electrodes (ISEs) for use in biological regenerative life support systems

Master's thesis in MSENVITOX
Supervisor: Øyvind Mikkelsen
Co-supervisor: Øyvind Mejdell Jakobsen
June 2022

Norwegian University of Science and Technology
Faculty of Natural Sciences
Department of Chemistry

NTNU
Norwegian University of
Science and Technology

Abstract

Interest in longer range and duration manned extraterrestrial missions are on the rise, and have been made possible by technological leaps in recent decades. Recirculating hydroponic systems are researched as a method of providing regenerative sources of food, oxygen and clean water. For these purposes accurate and low-maintenance monitoring methods for water quality and nutrient solution levels in hydroponic systems are necessitated. One possible method of monitoring individual nutrients is the use of potentiometric sensors, like ion-selective electrodes (ISEs).

In this thesis ion selective electrodes for chloride (HACH ISECl181) and sodium (HACH ISENa381) have been evaluated for use in hydroponic systems. The electrodes have been tested with regards to interferences, drift and accuracy. An at-line sampling and analysis method with the electrodes has also been tested, with regards to electrode drift and biofouling. Most ions present in nutrient solutions were found to impact the electrodes. Nitrate and sulphate had the largest impact on the chloride electrode, while potassium and magnesium was found to have the largest impact on the sodium electrode. Interfering ions were determined by the preparation of calibration curves in solutions with analyte and interfering ions, and by an experiment with spiking of interferences into a sodium chloride solution. The chloride electrode was found to drift significantly over a period of 12 days in a synthetic nutrient solution, while the sodium electrode was more stable.

Both electrodes were used to analyze the chloride and sodium contents in samples collected from a hydroponic experiment. Neither electrode provided sufficient accuracy when compared to the alternative methods, ion chromatography for chloride and ICP-MS for sodium. Two flow cells for the electrodes were designed and implemented at-line in a hydroponic system, and an experiment was conducted over a period of 4 weeks and 5 days. When compared to alternative methods the electrodes still had subpar accuracy, and biofouling of the chloride electrode was observed after 4 weeks. No biofouling was observed on the sodium electrode over the duration of the experiment.

More research into the influence of interference on specific ion selective electrodes is recommended before implementation into hydroponic systems. Flow cell design should be improved, the volume used minimized, and anti-biofouling methods that do not negatively impact plant health should be investigated.

Sammendrag

Interessen for lengre bemannede utenomjordiske oppdrag er økende, og muliggjort av teknologiske sprang de siste tiårene. Resirkulerende hydroponiske systemer er forsket på som en regenerativ kilde for mat, oksygen og rent vann. Med disse bruksområdene oppstår også behovet for nøyaktige metoder, med lave vedlikeholdskrav, for overvåkning av vannkvalitet og næringsstoffnivåer i hydroponiske systemer. En mulig metode for overvåkning av individuelle næringsstoffer er bruken av potentiometriske sensorer, slik som ioneselektive elektroder(ISEr).

I denne masteroppgaven har ioneselektive elektroder for klorid(HACH ISECl181) og natrium(HACH ISENa381) blitt evaluert for bruk i hydroponiske system. Elektrodene har blitt testet med hensyn til interferenser, drift og nøyaktighet. En at-line prøvetakings- og analysemetode med elektrodene har også blitt testet, med hensyn på drift og begroing. De fleste tilstedeværende ionene i næringsløsning påvirket elektrodene. Nitrat og sulfat hadde den største påvirkningen på kloridelektroden, mens kalium og magnesium viste seg å ha størst påvirkning på natriumelektroden. Interfererende ioner ble bestemt ved bruk av kalibreringskurver i løsning med analytt og interferenser, og ved et eksperiment hvor interferenser ble spiket inn i en natriumklorid løsning. Klordielektroden ble vist å drifte betydelig over en periode på 12 dager i en syntetisk næringsløsning, mens natriumelektroden var mer stabil.

Begge elektrodene ble brukt til å analysere klorid- og natriuminnholdet i prøver samlet fra et hydroponisk eksperiment. Ingen av elektrodene ga tilstrekkelig nøyaktighet når de ble sammenlignet med de alternative metodene, ionekromatografi for klorid og ICP-MS for natrium. To flytceller for elektrodene ble designet og implementert at-line i et hydroponisk system, og et eksperiment ble utført over en periode på 4 uker og 5 dager. Når sammenlignet med alternative metoder hadde elektrodene fortsatt manglende nøyaktighet, og begroing ble observert på kloridelektroden etter 4 uker. Ingen begroing ble observert på natriumelektroden over eksperimentets varighet.

Mer forskning på påvirkningen av interferenser på spesifikke ioneselketive elektroder anbefales, før implementering i hydroponiske systemer. Flytcelledesign bør forbedres, volum brukt bør minimeres, og antibegriongsmetoder som ikke påvirker plantehelsen bør undersøkes.

Acknowledgements

I would like to thank both my supervisors for their invaluable help and supervision through this project. Øyvind Mikkelsen for his support, guidance, and IC analysis, and Øyvind Jakobsen for support and all practical help and considerations. None of this would be possible without either. I would also like to thank Geir Solem at the NTNU Faculty of Science workshop for all his help with design and production of the flow cells used in this thesis. Anica Simic and Kyyas Seyitmuhammedov also deserve thanks for the ICP-MS analyses provided, as well as help with regards to ICP-MS questions. I would also like to thank Roger Aarvik for help with the procuring of chemicals and equipment used.

I would also like to thank my family and friends, for being there for me in what has been an exceptional year. Thank you to everyone who helped keep me sane, when I struggled staying so myself. A special thanks, and congratulations, to my girlfiend, Sofie, is also in order, as we both complete these final stages of our formal education this year. I'm proud of us. Thank you to everyone.

And lastly, a special thanks to the poor student reading this. You may, through the year, struggle to see the excitement in your work, to see the worth of your thesis, or the end of your education. We all do. Remember this; what you're doing is cool as shit, and you've never been this close to graduating. If I can do it, so can you. I believe in you.
Good luck, and happy writing.

Contents

1 Background **1**

2 Theory **2**
2.1 Hydroponics . . . 2
2.1.1 Nutrient film technique . . . 2
2.1.2 Contents and nutrients . . . 3
2.1.3 Hydroponics in extraterrestrial travel . . . 5
2.2 Potentiometry . . . 7
2.2.1 Ion Selective Electrodes . . . 7
2.2.2 Interferences . . . 10
2.2.3 ISEs in hydroponics . . . 11
2.3 Ion exchange-chromatography . . . 13
2.4 Inductively coupled plasma mass spectrometry . . . 15
2.5 Spectrophotometry . . . 16
2.6 Quality assurance and quality control . . . 17
2.7 Statistical analysis . . . 18

3 Materials and Methods **19**
3.1 Ion selective electrodes . . . 19
3.2 Interferences calibration curves . . . 20
3.3 Interference spiking . . . 21
3.4 Electrode behavior over a 12 day span of time . . . 22
3.5 Hydroponic samples . . . 23
3.6 Flow Cell experiment . . . 24
3.6.1 Pump testing . . . 25
3.6.2 Experimental conditions . . . 25
3.7 Ion Chromatography . . . 28
3.8 ICP-MS . . . 28

4 Results & Discussion **30**
4.1 Interference calibration curves . . . 33
4.2 Interference Spiking . . . 42
4.3 Electrode behavior over a 12-day span of time . . . 46
4.4 Hydroponic samples . . . 52
4.5 Flow cell experiment . . . 57
4.5.1 Pump testing . . . 57
4.5.2 Experiment results . . . 59

5 Further Work **67**

6 Conclusion **69**

References **76**

Appendix **77**

A Appendices **77**
A.1 Hydroponic samples - theoretical nutrient concentrations 77
A.2 Hydroponics samples batch 1, calibration curves 78
A.3 Hydroponic samples batch 2, calibration curves 79
A.4 Flow cell experiment, calibration curves 81
A.5 Ion chromatography results 83
A.5.1 Hydroponic samples, Batch 1 83
A.5.2 Hydroponic samples, Batch 2 92
A.5.3 Flow cell experiment 101
A.6 ICP-MS Results 111
A.6.1 Hydroponic samples, Batch 1&2 111
A.6.2 Flow cell experiment 115

Acronyms and Abbreviations

CHS1	Shorthand for specific hydroponic nutrient solution
CIRiS	Centre for Interdisciplinary Research in Space
CRLSS	Closed Regenerative Life Support Systems
EC	Electrical conductivity
ESA	European Space Agency
HACH HQ40d	Data logger unit
HACH ISECl181	Chloride electrode
HACH ISENa381	Sodium electrode
HDPE	High density polyethylene
IC	Ion Chromatography
ICP-MS	Inductively coupled mass spectrometry
ISA	Ionic strength adjuster
ISE	Ion-selective electrodes
ISS	International Space Station
KHP	Potassium hydrogen phthalate
MELiSSA	Micro-Ecological Life Support System
MES	2-Morpholinoethanesulfonic acid monohydrate
NASA	National Aeronautics and Space Administration
NFT	Nutrient film technique
POM	Polyoxymethylene
QA	Quality assurance
QC	Quality control
RSD	Relative standard deviation
TBT	Tributyltin
UV	Ultraviolet

1 Background

With the leap in technologies longer distance and duration extraterrestrial missions are becoming a real possibility. Longer missions call for regenerative methods for production of food, oxygen and pure water. The use of plants for these purposes are a key area of scientific research, and hydroponics is considered one of the main methods for regenerative plant growth and production on manned space flight missions[1], due to having control of the entire growth and process, as well as allowing for recirculating of water and nutrients. Recirculating hydroponic systems are researched as the best approach, where water and nutrient solutions are re-used through the system, and this gives rise to the need for sensors for monitoring and controlling water quality.

Water quality and nutrient solution levels are classically analyzed using off-line techniques, such as ion chromatography. More advanced applications, such as space travel, necessitates the use of sensors for monitoring of individual nutrients in hydroponic solutions, using low-maintenance, accurate methods[2]. Preferably these solutions could be implemented at-line or in-line in hydroponic systems. A way of monitoring individual nutrient ions that has been tested, and warrants further investigation, is the use of ion selective electrodes (ISEs). ISEs are considered cheap, reliable and to have low maintenance requirements. Individual nutrients are of research interest, but certain other ions that can have negative impact on plant growth are also of interest, such as sodium and chloride.

NTNU Social Research Centre for Interdisciplinary Research in Space (CIRiS) are among the many institutions conducting research into advances of hydroponics, and the use of sensors for monitoring nutrient concentrations in recirculating hydroponic systems, not only for use in extraterrestrial travel, but also in general and specialized applications. CIRiS has successfully demonstrated the use of optical sensors for monitoring of nitrate. In-line ISE implementation in hydroponic systems has also been tested, but found to be susceptible to biofouling and drift[2].

The objective of this master thesis is to examine the use of ISEs for sodium and chloride monitoring in hydroponic systems. ISE viability with regards to drift and interferences will be evaluated, with ion chromatography and inductively coupled plasma mass spectrometry as alternative methods. An at-line implementation of ISEs for monitoring will also be tested, with regards to drift and biofouling of sensors.

2 Theory

2.1 Hydroponics

Hydroponics is a term used for the soilless growing of crops and plants, using a nutrient solution instead of traditional nutrient filled soils. The technique is viewed by many as a method for future agricultural cultivation, due to being less resource and area intensive than traditional techniques[3]. Traditional farming techniques are faced with challenges, and are especially prone to failure to climate changes[4]. Hydroponics can address many of these issues, as hydroponic growth facilities require less area, they are more efficient in terms of water and nutrient use, leading to a decrease of use in fertilizer and water resources, while also reducing pollution of local water resources[3][5][6]. Systems using hydroponic techniques also allow for the recirculation of water and nutrients, as the used nutrient solution can be easily captured and reused without restricting crop yields[4]. This makes hydroponics ideal for use in future agricultural practices in a more challenging climate, but also in manned space travel as a self-sufficient food source.

2.1.1 Nutrient film technique

There are several ways of implementing hydroponic growth in practice, either by anchoring of plants into an inert substrate that holds the water, or more direct, strict hydroponic methods where only nutrient solution and air are in contact with the root systems. One such strict hydroponic technique is the nutrient film technique (NFT)[7], which will be briefly expanded upon here.

NFT is what can be called a "water culture" method. In certain other hydroponic techniques, the plant root system is suspended in a substrate, which ensures that the root zone is supplied nutrients. These substrate based techniques require irrigation at set, semi-frequent times[7]. NFT, and other "water culture" methods such as aero hydroponics and deep-flow technique systems, are continuous irrigation methods. Here the root zone is submerged in the bulk flow of the nutrient solution, where the flow is either supplied by pumps, or induced by bubbled air into the solution[7].

In NFT systems the plants are kept on a slanted trough, where the width is dependent on the plant species grown. Typically the trough is 1-20cm wide, and on an angle of 0.5-2 degrees. Nutrient solution flows in at the top of the trough, and is allowed to flow down to the end of the trough, where it is typically collected for reuse. The flow is adjusted to keep the nutrient solution flowing as a thin layer around the roots, almost like a film, hence the name nutrient film technique. The flow rate in NFT systems must be kept at a level to allow a thin layer to form, but must not be too low. A too low flow rate would introduce problems for the plants on the lowest part of each trough, as the concentration of nutrients decreases down the trough, as root system of plants higher in elevation absorb nutrients. This can lead to malnourished plants in the bottom part of the trough if the flow rate is not high enough[7].

Nutrient film technique systems have some advantages, as compared to other hydroponic techniques, such as dramatically reduced water and nutrient use, low use of materials, combined with high levels of control of the root system, high levels of automation possible, and the technique is adaptable to a wide variety of crops[8]. These advantages make it a great choice for research and specialized purposes, as well as a good choice for all-round hydroponics. However, the technique also requires a great deal of maintenance and care, almost continuously. The trough design of the technique also means that there is no buffer between plants, which enables root borne diseases to rapidly spread if introduced. The technique is also susceptible to interruptions in the flow of water and nutrients[7]. These disadvantages have led to other techniques being primarily used in commercial applications[7].

2.1.2 Contents and nutrients

For the growth of plants 17 nutrients are thought to be essential[3]. These can be further broken down depending on the need for them. Those who are needed in relatively large amounts are called macronutrients, while the others are needed in much smaller amounts and are referred to as micronutrients[7]. As such, in hydroponic nutrient solutions, the macronutrients much be present in high concentrations, while micronutrients are present in much lower concentrations. In addition to these there are other elements and nutrients that are not essential to the growth, but can impede or further facilitate growth. A selection of needed macro- and micronutrients used in hydroponics are presented in table 2.1 below.

Table 2.1: Table of elements used in hydroponic nutrient solutions, their available forms, and classification of these into macro- or micronutrients[3][7]

Classification	**Element**		**Available to plants as**
Macro	Nitrogen	(N)	NO_3^-, NH_4^+
	Phosphrous	(P)	HPO_4^{2-}, $H_2PO_4^-$
	Potassium	(K)	K^+
	Calcium	(Ca)	Ca^{2+}
	Magnesium	(Mg)	Mg^{2+}
	Sulfur	(S)	SO_4^{2-}
Micro	Iron	(Fe)	Fe^{2+}, Fe^{3+}
	Boron	(B)	H_3BO_3, HBo_3^-
	Manganese	(Mn)	Mn^{2+}
	Copper	(Cu)	Cu^+, Cu^{2+}
	Zinc	(Zn)	Zn^{2+}
	Molybdenum	(Mo)	MoO_4^{2-}
	Chloride	(Cl)	Cl^-
	Nickel	(Ni)	Ni^{2+}

In addition to those presented in table 2.1, there are three more macronutrients. These are carbon, oxygen and hydrogen. These are not supplied in nutrient solutions[7]. In addition certain micronutrients like nickel and chlroide are not added to nutrient solutions, as their concentrations are assumed to be sufficient in water supply[3]. The function of specific macro- and micronutrients will not be discussed in detail here.

The concentrations of nutrients can vary from hydroponic system to system, depending on a range of factors such as application, cultivar, system, user and/or manufacture if the nutrient solution is premade[4]. An example composition used in this thesis work is the CHS1 nutrient solution presented by Jakobsen et al., 2021[9]. The concentrations used in the CHS1 nutrient solution is presented in the table 2.2.

Table 2.2: Concentrations of nutrients added to the CHS1 nutrient solution[9]. ppm/b concentrations are rounded to the nearest whole digit ppm/b.

Macronutrients	**Conc.(mM)**	**Conc.(ppm, mg/L)**
N as NO_3^-	7.0	434
N as NH_4^+	0.5	9
P	1.0	31
K	3.5	137
Ca	2.0	80
Mg	1.0	24
S	1.0	32
Micronutrients	**Conc.(µM)**	**Conc.(ppb, μ g/L)**
Fe, chelated DTPA	36	2010
B	24	259
Cu	1.4	89
Zn	6.6	432
Mn	15	824
Mo	0.9	86

The concentrations of micro- and macronutrients must be kept at a desired level to ensure optimal plant growth[10]. This can be done by addition of more nutrient solution, or direct addition of salts during the growing period[4]. Classically the amount of nutrients are measured by the electrical conductivity (EC) of the solution[3]. This gives a total measure of total dissolved salts in solution, or the salinity[7]. This is accomplished by measuring the conductivity through solution, through applied voltage using electrodes, and is typically measured in millisiemens per cm(mS/cm)[7]. Desired salinity levels are typically dependent on the plant species and cultivar, but normally range from 1-3 mS/cm[11]. High salinity has been shown to be detrimental to plant growth[7].

Another normally controlled parameter in hydroponic systems is pH. Typically plants are grown in solutions with pH ranging from 5.5-6.5, but this depends on the plant species and cultivar[3]. Lettuce is for instance typically grown at pH in the ranges of 5.4 to 5.6[9]. It has also been shown that lower pHs can facilitate higher uptake of calcium and phosphorus, dependent on plant species, cultivar and conditions[3]. The pH is typically measured using pH-meters[12], which is a potentiometric method for selectively measuring hydrogen ion concentration in solution[2]. The pH is typically managed in hydroponic systems, by addition of alkaline or acidic buffers[3].

Sodium chloride has been shown to accumulate in closed hydroponic systems[13], and can lead to change in nutritional status of crops, depending on the plant species[14]. However, relatively high sodium chloride concentrations in hydroponics have been shown to have little effect on growth of for instance lettuce, while enhancing root elongation[15]. The conditions do however need to be adapted to the different cultivars grown, as different cultivars of lettuce have been shown to respond differently to sodium chloride concentrations[16]. The sodium chloride concentration must be considered in hydroponic systems, as too high concentration can lead to adverse effects in grown crops, depending on the species[17]. Of special concern is when the sodium concentration becomes significantly higher than the potassium concentration[9]. This, among other factors, stipulates a need for more advanced monitoring methods in hydroponics, measuring not only the total content of nutrients in solution, but concentrations of specific

nutrients, in order to keep growth conditions optimal[2][18].

2.1.3 Hydroponics in extraterrestrial travel

The many advantages of hydroponics lead to it being considered a key component in the future of long-range extraterrestrial travel. Here hydroponics is considered the prime candidate for biological Closed Regenerative Life Support Systems (CRLSS), where hydroponic systems form the basis for growth of higher plant life during missions, both for use as food source, but also oxygen production[1]. Hydroponics for use in extraterrestrial applications has been extensively researched, but is still an area in need of exploration for future use.

Both the European Space Agency (ESA) and the U.S. National Aeronautics and Space Administration (NASA) consider research into closed loop hydroponics key to the future of longer range and duration missions, as well as in-orbit installations such as the ISS (the International Space Station), and manned missions to other planets[19]. The ESA initiated the Micro-Ecologocial Life Support System (MELiSSA) project in 1989, which aims to establish CRLSS systems based on resource recycling, which includes the need for recirculating systems of plant growing[20]. The NASA has also devoted significant amounts of research to this through different research projects[21].This area is not limited to the ESA and NASA but is a heavily researched area for many space agencies, researchers, and commercial actors around the globe[22].

One of the areas found to be in need of further research as part of the process of developing regenerative life support systems is the ability to control the nutrient ions in nutrient solutions[23]. This also stipulates the need for methods of monitoring these nutrients, as well as other ions which could have a detrimental effect on plant nutrition[24]. As discussed earlier, only basic parameters like the total salinity and pH of the nutrient solutions are measured in-situ, while more detailed parameters are typically measured in off-site laboratories[2]. This is however a laborious and time-consuming process, and such off-site measurements will possibly not be available during extraterrestrial travel. More advanced control and monitoring could lead to increased yields, but are also a necessity in space travel applications. This is due to the recirculation of water and nutrient solution in these applications. While recirculating water nutrient concentration could decrease, while other ions, like sodium and chloride, could accumulate. Both could lead to reduced plant growth and quality[23].

The on-site, in-situ, monitoring of specific ions will not only have applications in space travel, but also have applications in terrestrial, commercial growing operations. Here off-site measurements are available, but imply a cost and need for expertise that most commercial hydroponic growing operations possibly do not have access to. Off-site measurements also imply infrequent sampling and monitoring frequency, due to the need for posting samples to accredited laboratories, as well as other factors[2]. On-site monitoring would enable the sampling frequency to decrease from weekly to several times a day[24].

Proposed monitoring techniques can not only be used for direct monitoring of nutrients or other ions in hydroponic systems, but can also be employed as early warning systems. Here the concentration can be monitored relative to a set level and provide feedback to a potential user when concentrations reach, or exceed such a level[25]. An early warning system could be especially useful for applications where nutrient solutions and water are recirculated over time, and for ions shown to accumulate under such conditions.

Advanced monitoring and control of nutrients in solution can lead to increased crop yields, quality, and growth reliability, while reducing the water and fertilizer use in all applications. Monitoring and

control can also lead to improved system reliability and reduced susceptibility to water source variations in terrestrial applications, and would as such be advantageous for both terrestrial and extraterrestrial hydroponic systems[24].

2.2 Potentiometry

Potentiometry is a widely used electroanalytical method, where the potential between two electrodes in a solution or over a membrane is measured[26]. Typically potentiometry is a static, or high-ohmic electroanalytical method, where information on sample composition is obtained applying negligible current to the sample[26]. As such, measurements can be made without sample composition changes, which typically make potentiometric methods useful for non-destructive quantitative measurements[27].

2.2.1 Ion Selective Electrodes

In modern electroanalytical chemistry, the most common use-case for potentiometry is in ion selective electrodes (ISEs). ISEs are potentiometric electrodes that are capable of selectively measuring the activity of the analyte ion[26]. A potentiometric measurement device requires a reference electrode, an indicator electrode, and a device to measure the potential. A diagram of a typical potentiometric system, or cell, is included in figure 2.1. The figure has been collected from Wang, 2006[26].

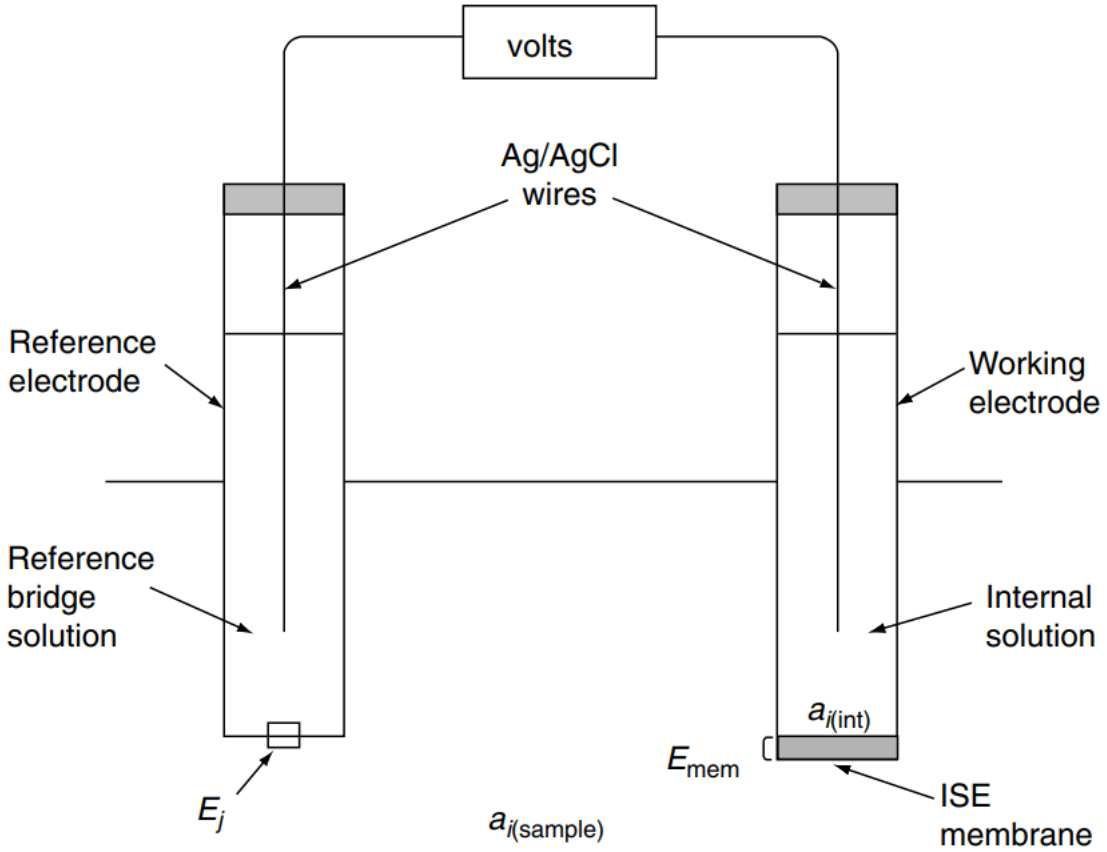

Figure 2.1: Diagram of a general potentiometric cell, including a reference electrode, and a typically selective indicator electrode[26].

The reference electrode should provide a highly stable potential over time, that should not be influenced by analytes in solution[26]. The indicator is an ISE which selectively responds to the activity of the analyte ion in solution. ISEs typically provide a low response time, a wide linear range and are not affected by turbidity and color of the solution[26]. Modern ISEs are typically delivered as a complete system in a combined electrode, for the sake of practicality[27]. This means that the reference electrode

is typically placed inside the indicator electrode in one package.

There are different types of ISEs[27], but the most commonly used, are membrane-based ion selective electrodes. In these ISEs the membrane is typically made of a permselective ion-conducting material, which separates the sample and the inside of the electrode. Inside the electrode there is typically also an internal solution of constant activity. The membranes are typically nonporous, insoluble in water and mechanically stable, and are designed to yield a potential primarily due to the analyte ion in solution[26].

When the ISE is inserted into a sample containing the analyte ion, selective binding processes occur at the membrane-sample interface, which generates a phase boundary potential. Another phase boundary potential develops on the inside of the electrode, where the internal reference solution interfaces with the inside of the membrane. The potential difference over the membrane, or boundary potential, can be expressed as

$$E = \frac{RT}{zF} \ln \frac{a_s}{a_{ref}} \tag{2.1}$$

Where E is the potential over the membrane, R is the universal gas constant, T is the absolute temperature, z is the charge of the analyte ion and F is the Faraday constant. a_s and a_{ref} are the activities of the analyte ion in the sample and the internal reference solution respectively. Equation 2.1 is derived from the Nernst equation[26].

The potential measured by an ISE is the potential across the membrane, relative to the potential measured by the reference electrode, as well as a small contribution from an asymmetry potential. The asymmetry potential is often negligible[27]. Since the potential of the reference electrode is fixed, and the activity of the inner solution is constant, the measured potential reflects the boundary potential, and can as such be related to the activity of the measured ion using the Nernst equation[28]:

$$E = E_i + \frac{2.303RT}{zF} \ln a_s \tag{2.2}$$

Where E is still the boundary potential, E_i is a constant which includes all sample independent contributions and is influenced by the design of the specific ISE, z is the charge of the analyte ion, while a_s is the activity of the analyte ion in the sample. The other constants are the same as in equation 2.1.

Equation 2.2 shows that the membrane potential is proportional to the logarithm of the activity of the ion measured[26]. The equation also shows that a tenfold increase in activity of a monovalent analyte ion at room temperature (25°C) would ideally result in a change of |59.16| mV. Divalent ions would have an ideal change of half this, per tenfold increase or decrease in activity, at |29.58| mV per decade[28]. ISEs that behave in this way, showing the appropriate change in potential with analyte activity, are characterized as showing Nernstian behavior. If the electrode shows a significantly smaller change, it is characterized as showing sub-Nernstian behavior[26].

It must also be noted that the ISE measures the activity of the analyte ion, while most applications in the real world are more concerned with the present concentration of the analyte in the sample. The activity of an ion is related to the concentration by the equation

$$a = fc \tag{2.3}$$

Where a is the activity of a given ion, f is the activity coefficient of that given ion, and c is the concentration. The activity coefficient is given by the Debye-Hückel equation

$$logf = \frac{-0.51z^2\sqrt{\mu}}{1 + 3.3\alpha\sqrt{\mu}} \tag{2.4}$$

Where f is the activity coefficient, z is the charge of the ion, μ is the ionic strength of solution, and α is the effective diameter of the hydrated ion[27]. In dilute solutions the activity coefficient approaches unity, and the activity can be approximated to be the concentration[26], but that is not the case for most hydroponic samples, as the ionic strength in water used for hydroponics is generally high[29].

In most use-cases the activity of an analyte in solution is not of interest, but the concentration present. The easiest and most used way to convert from potential measured using the activity of an ion to the concentration is by using an empirical calibration curve[26]. Such a curve is obtained by recording the electrode potentials of standard solutions of known concentrations, and then plotting them on a semi-log scale, plotting the potential vs the logarithm of standard concentrations. A hypothetical calibration curve for sodium, or any monovalent cation, is presented in figure 2.2. The curve has a slope of 59.2 mV per decade, and is for an electrode exhibiting Nernstian behavior. The figure has been collected from Wang, 2006[26].

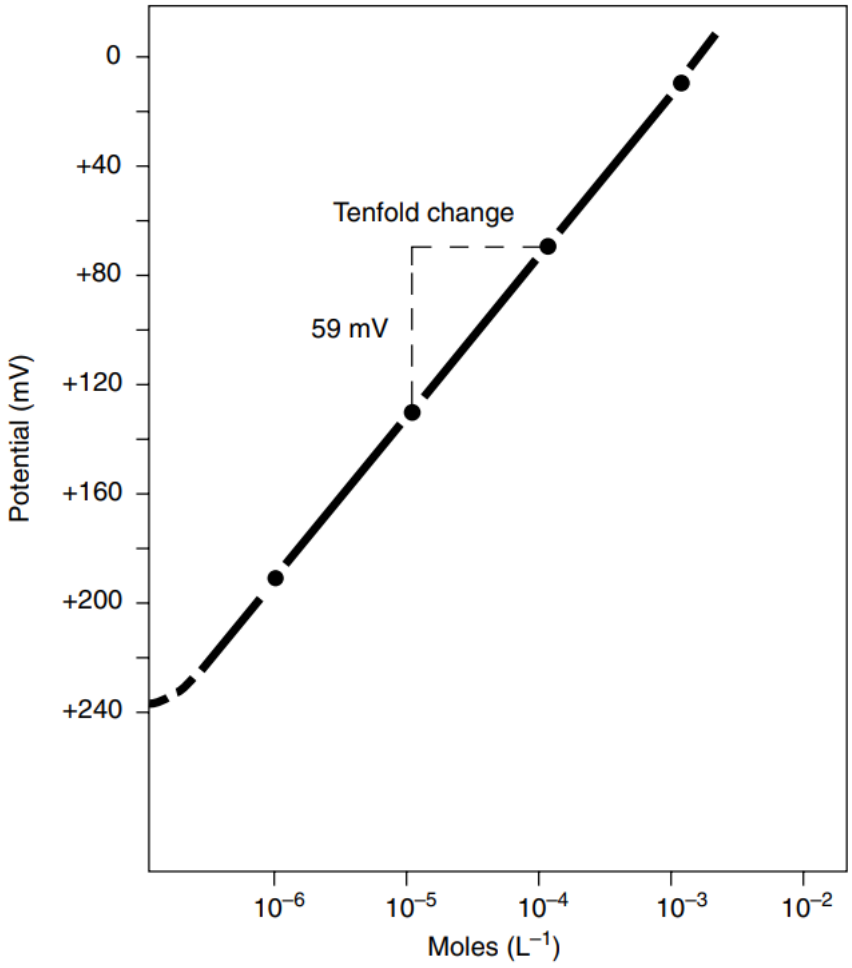

Figure 2.2: A hypothetical, ideal calibration curve for a sodium ion selective electrode, or any monovalent cation ISE. Figure collected from Wang, 2006[26].

When using ISEs it is also important to have approximately the same ionic strength, and as such an ionic strength adjuster (ISA) should be used for samples and standards[26].

Several different ISE membranes have been developed, implemented and used over the years[26]. Here two types are of special concern. The two used electrodes in this experiment have membranes made of

glass[30] and solid-state crystal[31]. These two membrane types will be briefly discussed here.

A glass membrane ISE is typically shaped with a bulbous tip, where the bulb is a thin membrane consisting of glass doped to give response to the analyte ion[27]. Historical glass membrane ISEs have been used for pH measurements, due to their responsiveness to the hydrogen cation. However, these electrodes were shown to have a responsiveness to other monovalent cations in alkaline conditions. Deliberate doping of the glass to enhance these responses, as well as changing of the internal reference solution, have given rise to glass ISEs selective for small monovalent cations, such as sodium, ammonium and potassium. The glass composition is complicated, and the mechanism for electrode response is complex, but compared to pH electrodes, the glass in these ISEs have anionic seats with a weaker electrostatic field, which shows a greater affinity to cations rather than protons[26]. With these ISEs it is important that the pH is adjusted to such a level that hydrogen ions in solution does not interfere with the measurement of cations[30]. This varies from electrode to electrode. It is also important that the thin glass membrane is kept hydrated in order to ensure no loss of performance[26].

Membranes of solid state crystals are selective towards anions in the same way that glass is selective towards cations[27]. Crystalline membranes contain cationic seats that attracts anions. The selectivity of these seats can be enhanced by doping of the crystalline membrane[26]. Most halide crystalline membrane ISEs consist of silver halide crystals, where the halide is the same as the ISE analyte[27]. This allows for selectivity towards the analyte, but also opens for interference from anions of similar size and charge.

2.2.2 Interferences

While ion selective electrodes are a cheap method of measurements, that can provide great responses over a wide linear range, while showing great selectivity, they are only ion-selective, not ion-*specific*[27]. As briefly discussed earlier, other constituents in the sample can influence the measurements made by ISEs. This will be discussed in greater detail here.

Ions of similar size, charge and other physical characteristics can also elicit a response from an ISE, not just the analyte ion. The ISE response in a solution containing analyte ion and one interfering ion can be expressed by expanding equation 2.2 into

$$E_b = E_i + \frac{2.303RT}{zF} \ln(a_s + k_{si} a_i^{\frac{z_i}{z_s}}) \tag{2.5}$$

This is the Nicholskii-Eisenmann equation, and accounts for interference from an interfering ion i. a_i is the activity of the interfering ion in solution, $\frac{z_i}{z_s}$ accounts for a potential charge difference between the analyte and interfering ion, while k_{si} is the selectivity coefficient of the interfering ion i for the analyte ion s[32]. The selectivity coefficient, k, is a measure for the response of the ISE stemming from the interfering ion. For instance, if the ISE is 100 times more selective towards the analyte ion, s, than to the interfering ion, i, the selectivity coefficient k_i would be 0.01. A selectivity coefficient value of 1 would indicate that the ISE has the same response to the interfering ion, as the analyte ion. For an ideal ISE the selectivity coefficient would be zero, and there would be no interference, but typically commercially available ISEs have selectivity coefficients of less than one[26]. The selectivity coefficient is assumed to be constant, and the Nicholskii-Eisenmann equation assumes a Nernstian response for the analyte and interfering ions[32]. In most applications of potentiometry there are however not only two ions in solution. The Nicholskii-Eisenmann equation should be expanded with as many interfering ions as there are present in the matrix. The expanded equation can be expressed as

$$E_b = E_i + \frac{2.303RT}{zF} \ln(a_s + \sum_i k_{si} a_i^{\frac{z_i}{z_s}}) \tag{2.6}$$

Where the interfering ions can be expressed as individual terms in the sum $\sum_i$, for i interfering ions[29]. The selectivity coefficient for a certain ISE can be experimentally determined, but it is condition dependent[33].

2.2.3 ISEs in hydroponics

Potentiometry has been suggested as a method for cheap, fast and accurate measurements of nutrients in hydroponic systems[2]. ISEs provide a method for potentially determining the levels of macro- and micro nutrients in solution, which is beneficial for hydroponic implementations in a wide variety of fields, such as monitoring recirculating water in regenerative life support systems in space applications[2], or monitoring nutrient solutions on the ground[34], in order to properly regenerate solutions ensuring optimal growth[35]. Potentiometric monitoring using ISEs can also be a low effort, low cost method for nutrient monitoring on-site, and can as such be used as an alternative to sampling and off-site analysis[2][24].

There are, however, limitations to this approach. For implementation of ISEs in hydroponic systems, certain issues must be addressed.

One such limitation is the possibility of biofouling and sensor degradation in the hydroponic system. Biofouling is a term for the degradation caused by the growth of biofilms and organisms on surfaces in contact with water. Biofouling typically leads to the degradation of the primary purpose of the item being fouled[36]. Biofouling and biofilm growth are caused by many different species of algae and small organisms, but the growth is dependent on factors such as nutrient availability, temperature and light[37][38]. Hydroponic systems are as such good environments for the growth of algae and organisms, and exhibit factors beneficial to biofilm growth, such as high levels of nutrients and organic matter[39]. Biofouling on potentiometric sensors, such as ISEs, can lead to drift and direct interference in measurements, due to growth on, and fouling of, the sensor membrane[40]

Several anti-biofouling measures have been researched and employed, however the vast majority of these have been used in marine environments[36]. The most commonly used methods would not be applicable in hydroponic systems. Historically anti-fouling measures have been based on the use of biocides, like the now regulated tributyltin, TBT, which has been found to be bioaccumulative and negatively impact marine environments[41], and copper, which has been found to be toxic to plant life in high concentrations[42]. These biocides are typically used in anti-fouling coatings, where they would release small amounts of anti-fouling material, such as copper, to inhibit the growth of algae and biofilms[43]. The use of biocide based anti-fouling measures in hydroponic systems should be seriously considered before use, as these could have harmful effects on plant health. The fact that most hydroponic systems are used as food sources must also be taken into consideration. Non-biocide based coatings are also being researched as non-toxic alternatives[44].

Other anti-fouling methods exists and can be used, such as mechanical cleaning using brushes[45] or the removal of biofilms and algae from the sensors using pressure and water jets[46]. These can however be damaging to the sensors and lead to shortened lifespans[47]. Ultraviolet (UV) radiation can also be used to inhibit algae and biofilm growth, or damage and remove existing growths[48]. As such this can also be used as an anti-fouling measure. UV radiation has also been applied successfully in hydroponic systems previously to inhibit algae and biofilm growth[39].

Research has also been devoted to the direct application of anti-fouling to ISEs. Newer studies have shown that direct applications of anti-fouling technologies into newer ISEs, or onto existing sensors can

prevent fouling and lead to longer sensor lifespan in difficult environments[40]. One such method is the direct doping of the ISE membrane with anti-fouling agents, in order to avoid sensor fouling[49]. For existing technology and sensors, the membrane could potentially be surface coated with anti-fouling coatings. This method can have little effect on the measurements made, but is highly dependent on both the membrane and the coating[40]. Caution should still be applied when considering these for use in hydroponic systems, especially with recirculating systems. Release of anti-fouling agents could have detrimental impact on both plants and consumers.

Measurement drift in ISE applications can also be a source of errors in measurement accuracy and sensitivity. This can be combated by proper storing and use of ISEs, as well as with frequent calibration[47].

ISE technology has already been applied successfully in hydroponic systems. Complex systems have been tested, using multiple ISEs to measure the concentrations of the most common macronutrients in hydroponic systems[18][50]. ISEs have also been successfully applied in environmental monitoring, and have seen use for the monitoring of trace metals in rivers and lakes[51]. For long time monitoring of hydroponic systems direct submersion of ISEs into the system has also been tested. This in-line solution has been found to be non-satisfactory, with biofouling and drift being the main sources of data interference for the monitoring of macronutrients[2]. At-line monitoring is recommended, housing the ISEs in separate chambers to the hydroponic system, with the introduction of nutrient solution through pumps. This has been tested in literature, and found to give longer sensor lifespan, with the ISEs stored in a low concentration standard solution[29]. At-line ISE application with frequent calibration has been shown to work for certain ISEs and macronutrients, and has been used to create systems for monitoring and managing concentrations of important macronutrients in hydroponic systems[34][52].

2.3 Ion exchange-chromatography

Ion exchange-chromatography (hereby referred to as ion chromatography, IC) is a method introduced in the 1970s, used for separating small anions and cations after exchange, based on their retention in an analytical column of opposing charge. IC has many applications in biochemistry and medicinal chemistry, but it is now regarded as the most common separation technique for small inorganic ions[53]. Applications of the latter will be discussed here. Ion chromatography is a commonly used method due to the high reliability, selectivity, speed, efficiency and good tolerance to sample matrices[54].

Separation of inorganic ions in ion chromatography is based on the retention of desired ions on a separation column. Depending on the analyte ions, whether they are cations or anions, different separation columns and suppressors are used, as well as eluent. For anion analysis low concentration (2 mM) carbonate or bicarbonate solutions are used as eluents, or mobile phase. Here the cations are exchanged and retained in the suppressor, typically a suppression column, while the carbonate forms carbonic acids which has low conductance[55]. The anions are separated on the separation column, which has a stationary phase of immobilized ions of opposite charge. The cationic seats in the stationary phase forms electrostatic interactions with the anions in the mobile phase, which forms the basis for retention. The retention is based on the affinity of the ions to the stationary phase, and typically a stationary phase and column is chosen based on the desired analytes[53]. The affinity of an analyte anion, A^- can be expressed using the equilibrium to the stationary phase, SP^+, and a competing ion, E^- in equation 2.7, and the equation for the selectivity coefficient of the analyte ion, equation 2.8, which describes the preference of the stationary phase for one ion over a competing ion[53].

$$SP^+E^- + A^- = SP^+A^- + E^- \tag{2.7}$$

$$K_E^A = \frac{[A_s][E_m]}{[A_m][E_s]} \tag{2.8}$$

Here $[A_s]$, $[A_m]$ and $[E_s]$, $[E_m]$ are the concentrations of analyte ion A^- and competing eluent ion E^- in the stationary and mobile phase. The selectivity coefficient K_E^A expresses the affinity of anion A^- to the stationary phase over the eluent ion. This can be used to evaluate the selectivity, or affinity to the stationary phase, of different analytes, given the same eluent. Analyte affinity has been found to be stronger for polyvalent ions, compared to monovalent ions, due to stronger electrostatic interactions. For ions of the same charge, the affinity has been found to decrease with an increase in hydrated ion radius. The selectivity coefficient is dependent on the stationary phase, but changes in the order of analyte affinity are small for the commonly used columns[53].

An ion chromatography system consists of the elements described above. The most commonly used complete system is ion chromatography with suppressed conductivity detection[54]. Typically a guard column is also used, in order to protect the usually expensive separation column. Samples of high ionic strength must be diluted before analysis, to avoid contamination of the instrument. In addition samples should be filtered in order to avoid particulate matter in the instrument. The diluted sample is injected into the ion chromatography instrument, and is carried through by the mobile phase. For separation of anions the mobile phase is typically a carbonate solution, normally sodium carbonate, which acts as a pH buffer, and is easily suppressed before detection. Sodium carbonate increases the background conductance of the mobile phase, and must be suppressed to eliminate noise in the conductivity detector[55]. The sample passes the guard column where contaminants, highly retained solutes and particulate matter

is retained[53]. After passing the guard column, the sample passes to the separation column, where separation occurs as described above. As analyte ions elute from the separation column, it passes the suppressor, where the carbonate cations are exchanged using an acid to form carbonic acids with low conductivity. The suppressor thus increases the detector sensitivity and linear range[55]. Several types of detectors can be used in an ion chromatography system, like UV-vis or mass spectrometry detectors[56], but for inorganic ion analysis, a conductivity detector is most commonly used. A conductivity detector consists of two electrodes with applied voltage, which the mobile phase passes through. All changes in conductivity are recorded by the detector[53]. Quantitative analysis can be performed using ion chromatography using empirical calibration curves. A diagram of an ion chromatography system, with the discussed sub-systems, is provided in figure 2.3. The figure has been collected from Worden, 2005[57].

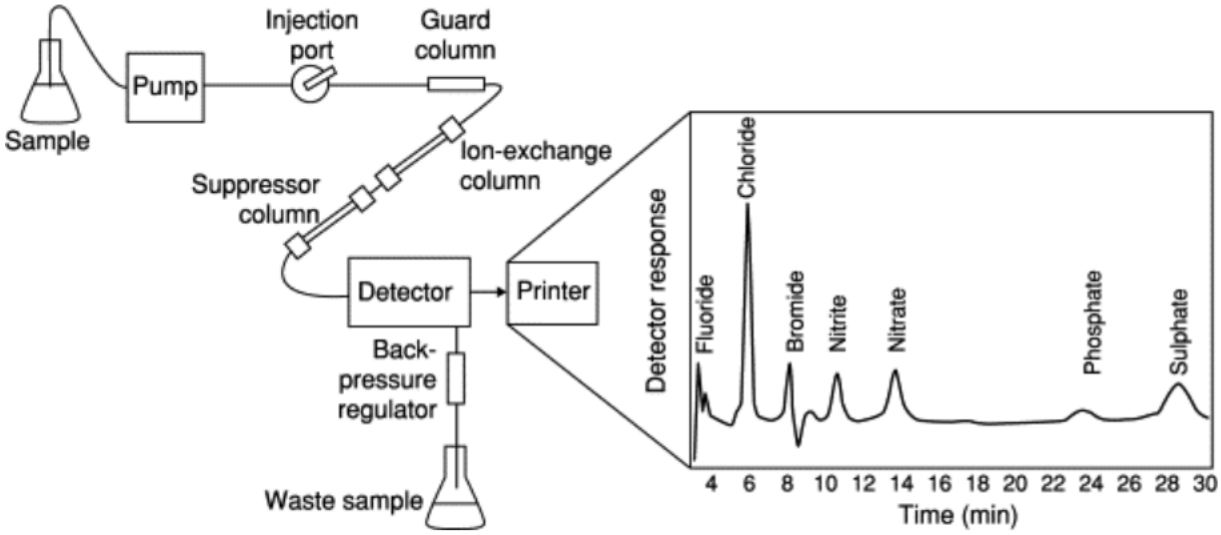

Figure 2.3: The figure shows a schematic representation of a typical ion chromatography system, with a theoretical resulting chromatogram. The figure includes a guard column, a separation column (labeled ion-exchange column), a suppressor and a detector. The figure has been collected from Worden, 2005[57]

Ion chromatography is a widely adapted and used method, but there are limitations and sources of interference in its use. The main source of interferences in IC is the presence of matrix interferences. Here constituents of the sample matrix can lead to heightened or lowered detection of analytes. One such interference is the processes such as co-elution, where other ions elute at the same time as the analyte, leading to overestimation of the analyte concentration[58]. Several methods for elimination of matrix interferences have been discussed and employed over the years, such as the use of solid phase extraction (SPE) cartridges[59]. Matrix interferences are present for the separation and detection of small anions, but are mostly of concern when the analyte ion is present in trace concentrations[58]. Interferences with regards to co-elution can typically be solved using sample dilution or concentration[60]. Deformation of chromatographic peaks are also a source of error in IC analysis. Ideally chromatograms should consists of sharp, distinguishable Gaussian peaks, with no overlap[53]. Overloading of the chromatographic column can lead to the formation of non-Gaussian peaks. Overloading can be due to the injection of too large sample volumes, or sample concentrations being higher than the column exchange capacity[61]. Non-Gaussian peaks can manifest as low, broad bands, peaks exhibiting fronting or tailing, and in extreme cases lead to overlapping analyte peaks in the chromatogram. Peak deformations can lead to difficulties with regards to analyte identification and quantification[61].

2.4 Inductively coupled plasma mass spectrometry

Inductively coupled plasma mass spectrometry (ICP-MS) is a widely used analytical method, especially for trace element analysis. The methods wide adaption is due to its advantages in speed of analysis, ability to characterize several elements in a sample, the isotopic capability and the ability to detect elements in both very low and relatively high concentrations[62]. ICP-MS can detect elements in the span from parts per trillion (ppt) to parts per million (ppm). ICP-MS is a great method with wide applications, however it is complicated and requires special competence to operate, while also being cost inhibitive as the instruments themselves are expensive to acquire and operate.

ICP-MS samples must be liquid, and liquid samples have to be digested using concentrated nitric acid to avoid contamination and damage of the instrument[63]. Nitric acid is used to form stable, water-soluble salts in the sample, which lessens interferences and chance of clogging. Solid ICP-MS samples must be digested or extracted before analysis[64]. The pretreatment of solid samples will not be discussed here.

The ICP-MS instruments works by pumping liquid samples into a nebulizer using peristaltic pumps, where a fine aerosol is created (using argon gas). The fine droplets are separated from the larger ones in a spray chamber, before transferal to a plasma torch. The plasma torch is created using a strong magnetic field and a radio frequency generator, and can reach very high temperatures of upwards to 10 000K. The sample is desolvated, vaporized, atomized and ionized by the torch, before ion extraction and transferal into the interface region. A couple of skimmer cones then transfer the ions into the ion optics, where ions are directed at the mass separation device. Here the remaining neutral species, photons and particulates are lost. The mass separation device separates the species in the ion beam based on their mass-to-charge ratio (m/z)[62]. Typically the mass separation device is a quadrupole, or several in series. A quadrupole mass filter is the most commonly used today, and consists of four rods mounted in parallel and equidistant to the ion beam. AC and DC current can be applied to opposite pairs of rods, only allowing for ions of one m/z ratio to pass the filter at the time. The rod voltages are optimized for only allowing ions of a certain m/z ratio to pass, and the voltage switching process can be rapid, so data collection can be very fast using a quadrupole, scanning the range from 0-300 amu in less than a second[65]. After separation the ions are detected by conversion to an electric signal[62]. Figure 2.4 below shows a general cross section schematic of an ICP-MS instrument. The figure has been collected from Wilschefski et al., 2019[64].

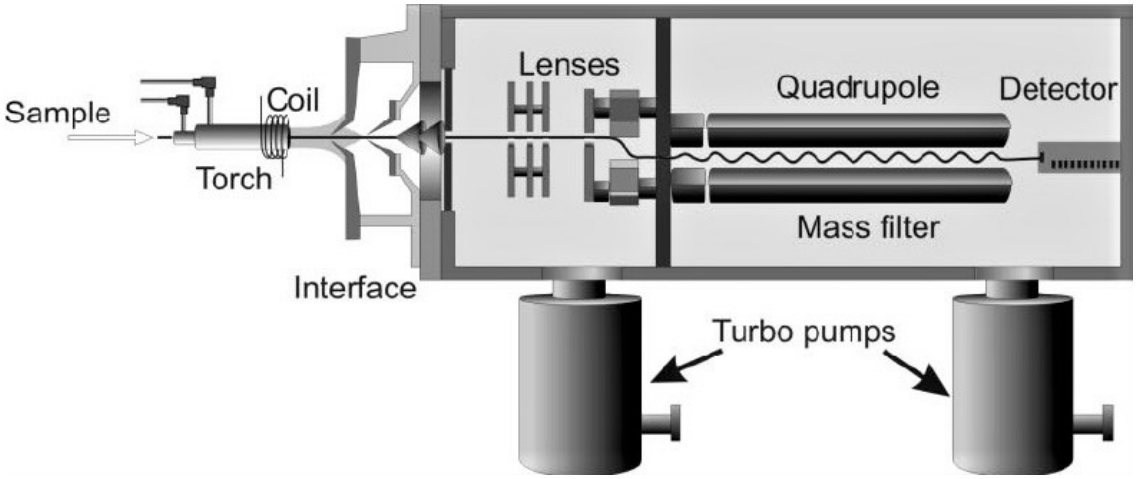

Figure 2.4: Cross section schematic of an ICP-MS instrument. Figure collected from Wilschefski et al., 2019[64].

There are several sources of interferences in ICP-MS. These can mainly be broken down into spectroscopic and non-spectroscopic interferences[64]. The main non-spectroscopic interference is the presence of matrix effects. This is when the analyte signal is either suppressed or enhanced as a result of the constituents in the sample matrix[64]. This can happen in several different ways, and can impact the analysis at nearly every step in the ICP-MS instrument. The sample introduction can be impacted by disturbing the size distribution of droplets in the aerosol, or interfering with the transport efficiency. It can also introduce plasma effects, where the matrix can impact the ionization. Some elements, like carbon, can lead to higher amounts of ionized analyte, or the matrix effect can lead to a lower amount of ionized analyte. Space-charge effects can also occur as a result matrix interferences. Here the ion beam is broadened by repulsion between positively charged ions, which leads to fewer ions reaching the detector[64]. The field of ICP-MS technology is ever changing and improving, and several inventions and ideas have been introduced to reduce these effects. These include chromatography coupled ICP-MS to remove matrix interferences, or more advanced methods such as reaction and collision cells. In these cells chemical reactions and collisions occur, and aim to filter out unwanted ions, or change their spectrum location[64].

Spectroscopic interferences in ICP-MS are the results of analyte and non-analyte ions sharing the same m/z ratio. There are four main types of spectroscopic interference[64], and these will be briefly discussed here. Isobaric interference is the first type of spectroscopic interference, and it is simply when two ions share the same m/z ratio. This leads to a peak at a certain m/z being the result of influence from both the analyte ion, as well as a non-analyte ion. This can lead to an overestimation of the analyte ion. An example here is nickel and boron, which both have isotopes which occur at 58 m/z[64].

Another interference is when ions are created with double charge. While this is rare, and most ions created during the ICP-MS procedure are monovalent, this can result in an element of twice the mass of the analyte ion having the same m/z ratio as the analyte[64]. The high temperature plasma can also create polyatomic atoms, which are ions created in the plasma that are actually made from several atoms. These polyatomic ions can share the same m/z ratio as the analyte ion, and can as such be a source of interference. This can be the result of matrix effects in the torch, be the result of the argon used, or entrained environmental gases in the sample[64].

The last spectroscopic interference that will be discussed here is tailing. This is the result of overlap in the spectrum of ions with similar m/z ratios. This interference can especially be of concern when two analytes of interference have a similar m/z ratio, and one is present in the sample in much higher concentrations than the second [64].

2.5 Spectrophotometry

Spectrophotometry is an application of spectroscopy, and is typically an instrumental method used to measure the transmittance and absorbance of a sample as a function of wavelength. Spectrophotometry is quantitative, and measures the ability of a compound, discussed here as in solution, to absorb or reflect radiation, or transmittance, the ability to allow the radiation to pass through the sample. Most spectrophotometers use radiation in the UV and visible light spectra. The absorbance of a compound is described by the Beer-Lambert law[27]

$$A = \epsilon l c \tag{2.9}$$

Where A is the absorbance of the sample, ϵ is the molar absorptivity coefficient, which describes how strongly a chemical compound absorbs radiation at a given wavelength, l is the length of the optical path

in sample, and c is the concentration of the compound in question[27].

A typical spectrophotometer consists of a light source, capable of emitting both UV and visible light, a wavelength selector, which directs the light of desired wavelength through the sample, and a photometric detector. The light source in a spectrophotometer needs to be able to output a broad range of wavelengths at a very stable power output. Several different types of sources exist, depending on the desired measurement, however they are all required to have a stable output. The wavelength selector is typically a diffraction grating designed to only allow one wavelength, or band of wavelengths to pass. The sample is typically contained in a cuvette. The cuvette material depends on the intended sample, and its absorbance. Glass and plastic is used for normal UV-Vis spectrophotometry, depending on which wavelengths the material transmits, while quartz cuvettes are typically used for samples that need to be analyzed in the far UV-spectrum. The detector in a spectrophotometer is an electro-optical detector, where the signal is detected, amplified and digitized[66]. Quantitative determination using spectrophotometry is typically performed using empirical standard curves, recorded using known standards with known absorbance properties. One example of such a compound is potassium hydrogen phthalate, which absorbs UV-radiation at wavelengths such as 254 nm[67].

The most relevant source of error in spectrophotometry is the presence of stray light, which can give rise to extra signal strength in the measurement. Stray light can have several sources, such as ambient light from outside the spectrophotometer, or light of other wavelengths than the desired one passing through the wavelength selector[66].

2.6 Quality assurance and quality control

Quality management is an important concept in analytical and environmental chemistry, in order to ensure that results obtained are accurate, precise and up to set quality standards. The most important parts of quality management in analytical and environmental chemistry are quality assurance (QA) and quality control (QC).[68]

Quality assurance relates to the overall process of ensuring that quality standards are met. QA can refer to the use of accredited laboratories, or the use of certified reference materials, to guarantee a certain standard[69]. Quality control, on the other hand are operational measures implemented and used to ensure precision and accuracy in results. QC involves the use of blanks during sampling and analysis, as well as the use of standards.

Standards are a vital way of ensuring overall quality control when working with samples. A standard contains a known amount, or concentration, of a specific substance, or substances, and can be broken down into external and internal standards. These are separated by their use and application. Internal standards are added to unknown samples and are used to provide a similar signal to the analyte, while at the same time being sufficiently different enough to provide two distinguishable signals. External standards are similar, in that they have known concentration, or amount, of the specific substance, but are not added to samples, and are analyzed separately. Both standard types are typically used to prepare calibration curves used for quantification, while internal standards are typically also used to check and correct for instrumentation variations during analysis. Internal standards can be used to calculate recovery. Standard addition is a distinct method where known amounts of analytes are added to the samples and are used to correct for matrix effects[69].

Blanks are another important part of QC in environmental and analytical chemistry. Blanks can be used

to identify and quantify contamination during sample extraction (solvent blanks) or from reagents and other analytical methods used (method blanks). They can also be used to establish background levels of analytes present in the sample matrix, by the use of matrix blanks. Field blanks can also be employed, which are clean samples brought and exposed to the sampling environment[69].

When taking and handling samples several precautions must be taken into consideration to ensure good QA. Sampling equipment must be properly cleaned between each sample, preferably using sample material if possible, to avoid potential cross-contamination. Proper sample equipment must also be employed depending on the task. When sampling metals it is important to use equipment with low metal contents to avoid sample contamination. Samples should be properly stored, and if possible preserved, in order to minimize influence from possible chemical reactions or biological activity. This can be done by for instance acidification[68].

2.7 Statistical analysis

Statistical analysis is a tool used to extract data from the results provided from a given analysis. Certain key descriptive statistics are almost ubiquitously used, such as the sample mean (referred to as mean), the standard deviation and relative standard deviation (RSD). Mean is the sum of all sample values, divided by the number of samples. Standard deviation is a measure on the dispersion in a data set. A low standard deviation indicates that values in the set are expected to be close to the calculated mean. Relative standard deviation (RSD) is the ratio between the standard deviation and the mean of the set, expressed as a percentage value[70].

Linear regression is a statistical approach of modelling the linear relationship between one or more explanatory (independent) variables, and an explained (dependent) variable[71]. One type of linear regression is simple linear regression. This model only relies on one explanatory variable, and one explained variable. In analytical and environmental chemistry simple linear regression is typically used to construct calibration curves. Here the response of a detector, or an instrument, is recorded for different concentrations of standards. Through simple linear regression the response (the explained variable) is then predicted as a linear function of the concentrations of standards (the explanatory variable)[72].

The coefficient of determination, R^2, is a numerical value that can be used to evaluate the fit of a linear regression model to the data set it is based on. The coefficient of determination is widely used as a measure of how "well" the linear function fits the data, due to it being relatively simple to calculate and is readily available in most statistical programs[73]. An acceptable R^2 value is dependent on the sample size used for regression. Typically a value of >0.990 is interpreted as the regression being fitted well to the data[73], while R^2 values of <0.990 can be accepted in cases with a large number of samples.

3 Materials and Methods

Table 3.1 below is a comprehensive and exhaustive list of chemicals used in the experimental work presented in this master thesis. The list contains used chemicals, their manufacturer and grade.

Table 3.1: Table of chemicals used through the thesis work. Also included is the manufacturer and grade of chemicals used.

Chemical	**Manufacturer**	**Grade**
Ammonia solution, 25%	Merck	Analytical grade
Ammonium nitrate	VWR Chemicals	Analytical grade
Calcium nitrate	Sigma-Aldrich	ACS grade
Calcium sulphate	Merck Life Sciences	Reagent grade
Dissolvine APN Micronutrients, prod. no. 7305243	Nouryon	N/A
Magnesium sulphate	VWR Chemicals	Reagent grade
2-Morpholinoethanesulfonic acid monohydrate, MES	Merck Millipore	Analytical grade
Potassium chloride	Merck	Analytical grade
Potassium hydrogen phthalate, KHP	VWR Chemicals	Analytical grade
Potassium nitrate	Merck	Analytical grade
Potassium dihydrogen phosphate	VWR Chemicals	Analytical grade
Sodium chloride	VWR Chemicals	Analytical grade

3.1 Ion selective electrodes

Two ion selective electrodes from HACH were used for the lab work presented in this thesis. These were selective for sodium (HACH ISENa381) and for chloride (HACH ISECl181). The sodium electrode uses pH glass, with a Ag/AgCl reference electrode, and uses a 0.02 M NH_4Cl internal reference solution[30]. The chloride electrode used is a solid state crystal membrane electrode, with an Ag/AgCl reference electrode, and a non-refillable Driftek gel reference element as internal reference electrolyte[31].

The electrodes were tested in the lab using 20-30 mL of solution or sample material in separate glass beakers. A magnetic stirrer was always used to provide gentle stirring during measurements. 0.5 mL of 25% ammonia solution was added to the beakers used for the sodium electrode, in order to adjust the pH to above 9 and avoid hydrogen ion influence as per the manufacturer instructions[30]. This was validated for each sample using Fisherbrand pH-fix 0-14 pH indicator paper strips. Both electrodes were left for 15 minutes in each solution before measurements were made, to allow for stabilization. Measurements were repeated five times.

An ionic strength adjuster (ISA) was prepared and used in most measurements. $CaSO_4$ was chosen as ISA, at a 10^{-4}M concentration. A 10^{-2}M solution was prepared, and the final ISA was prepared by dilution. ISA was either added to measured standards, or standards were prepared with ISA during dilution. The ISEs were also allowed to condition before use. The sodium electrode was left over night in tap water, while the chloride electrode was typically left for an hour in a prepared 100 mg/L standard solution.

The electrodes were washed in between samples during the lab work. The chloride electrode was rinsed using deionized (DI) water from a Millipore Elix Essential 5 water purification system, and carefully dried using a paper towel. The sodium electrode was washed in a beaker containing 100 mL ISA with the pH adjusted to >9 using 1 mL 25% ammonia solution, before careful drying using a paper towel.

Calibration curves were recorded using standard solutions prepared by hand. These standards were prepared by dissolving sodium chloride in DI water, to concentrations of 1000 mg/L of sodium and chloride respectively. Lower concentration standards of 100, 10 and 1 mg/L were prepared by dilution with ISA. Calibrations were performed with increasing concentrations, typically from 10 to 1000 mg/L, and under constant gentle stirring from a magnetic stirrer. The calibrations were performed in parallel in separate beakers.

The electrodes were tested in a shared beaker, by recording a calibration curve using sodium chloride dissolved in DI water. The curve was made using concentrations of 10, 100 and 1000 mg/L of sodium, in a 100 mL beaker, with both electrodes. The pH was also adjusted to >9 using ammonia solution.

The selectivity coefficients given for these electrodes are presented in table 3.2 below. The coefficients have been collected from HACH, and are given in the respective electrode manuals[31][30].

Table 3.2: Table of interfering ions and their selectivity coefficients, K, for the ion selective electrodes used in this thesis work. Collected from the respective manuals, published by the Hach company[31][31]

ISENa		**ISECl**	
Interfering ion	**Selectivity coefficient** K	**Interfering ion**	**Selectivity coefficient** K
Ag^+	>1000	I^-	>0.1
H^+	20 (at pH<9)	Br^-	>0.1
Li^+	0.01	Ag^+	>0.1
K^+	0.001	S^{2-}	>0.1
Ti^+	0.0002	CN^-	>0.1

3.2 Interferences calibration curves

Interferences were tested by the construction of three-point calibration curves in standard solutions with interferences. At first a three-point calibration curve was recorded for the used electrode, using respective standards. Two different calibration curves were then recorded for each interference. A calibration curve of varying interference concentration with constant analyte ion concentration was recorded, as well as a calibration curve of constant interference ion-, and varying analyte ion concentration.

The interferences tested were based on the CHS1 nutrient solution described in Jakobsen et al., 2021[9]. The interfering ions are presented in section 2.1.2 table 2.2. Standard solutions of 10, 100 and 1000 mg/L were prepared for each interfering and analyte ion, while solutions of 2x, 20x and 200x CHS1 standard concentrations of the Dissolvine APN Micronutrients solution was prepared. The calibration solutions were prepared by pipetting of 20 mL of interfering solution into a glass beaker, before 20 mL of analyte ion was pipetted into the same beaker. 100 mg/L solution was used as constant concentration. 10, 100 and 1000 mg/L were used as varying concentrations. These concentrations were diluted by half after pipetting into the glass beakers, and the resulting calibration curves were recorded using 5-50-500 mg/L varying concentrations, with a constant concentration of 50 mg/L. Calibration curves were constructed using concentrations of 5, 50 and 500 mg/L of interfering ions with constant concentration

of 50 mg/L of analyte ion in each sample. A second calibration curve was measured afterwards using varying concentrations of 5, 50 and 500 mg/L of analyte ion, with constant concentration of 50 mg/L of interfering ion. The concentrations are expressed in table 3.3.

Table 3.3: Final concentrations used for interference calibration curve recordings. Two calibration curves were recorded per interfering ion, one with varying ion concentration and constant analyte ion concentration, and one with constant interfering ion concentration and varying analyte ion concentration.

Varying interference	
Interfering ion concentration (mg/L)	**Analyte ion (Na/Cl) concentration (mg/L)**
5	50
50	50
500	50
Constant interference	
Interfering ion concentration (mg/L)	**Analyte ion (Na/Cl) concentration (mg/L)**
50	5
50	50
50	500

The same was performed using the Dissolvine APN Micronutrients solution, where 20 mL of each solution was pipetted into glass beakers, before addition of analyte ion. Calibration curves were recorded using concentrations of 0.1x, 1x and 10x standard CHS1 concentrations of micronutrients with 50 mg/L of analyte ion. Calibration curves of 5, 50 and 500 mg/L of analyte ions with 1x CHS1 micronutrient concentration were also recorded.

The measurements for the calibration curves were recorded using the appropriate ISEs. 0.5 mL of 25% ammonia solution was added to the sodium electrode solutions in order to adjust pH>9. Stirring was induced at a constant level for each sample using magnetic stirrers.

3.3 Interference spiking

In order to test the behavior of the ISEs with realistic concentrations of interfering ions, another experiment was prepared. Based on the CHS1 nutrient solution described in Jakobsen et al., 2021[9], solutions of 200 and 100 times normal concentration of interfering ions, the micronutrients and total hydroponic solution were prepared for spiking. A 117 mg/L solution of sodium chloride (2 mM; 46 mg/L sodium, 71 mg/L chloride) with ISA was prepared.

Calibration curves were prepared using sodium and chloride standards of 10 and 100 mg/L respectively. 20 mL of 117 mg/L sodium chloride solution was added to beakers, and electrode response was measured after 15 minutes. After the response in sodium chloride solution was recorded, 100 µL of 200 times nutrient solution concentration of interfering ions was added under constant stirring, and the electrode response was measured after 15 minutes. The process was repeated for 100 times nutrient solution concentration of interfering ions, and for each interference, as well as total hydroponic solution.

The concentrations of nutrients the 117 mg/L sodium chloride solutions were spiked to are shown in table 3.4. Spiking to 1xCHS1 nutrient solutions shown was performed by addition of 100 µL solution containing 200 times the normal nutrient solution (CHS1) concentration. Spiking to 0.5xCHS1 concentrations was

performed by addition of 100 µL solution containing 100 times the normal nutrient solution (CHS1) concentration.

Table 3.4: Concentrations of macronutrients, as CHS1 nutrient solution equivalents, spiked to in the experiment. Spiking was performed by addition of 100 µL of 200 and 100 times CHS1 concentrations into 20 mL 2 mM sodium chloride solution with ISA.

Macronutrient	1xCHS1 (mg/L)	0.5xCHS1 (mg/L)
KNO_3	252	126
KH_2PO_4	136	68
NH_4NO_3	40	20
$MgSO_4$	120	60
$Ca(NO_3)_2$	328	164

In addition to the concentrations in table 3.4, 1x and 0.5x concentrations of micronutrients in the nutrient solution (CHS1) was tested by spiking. Spiking was performed in the same manner as with macronutrients, by addition of 100 µL of 200 and 100 times the micronutrient concentrations described in table 2.2, but for all micronutrients in one solution.

3.4 Electrode behavior over a 12 day span of time

A total CHS1 solution was prepared as described in Jakobsen et al., 2021[9]. 117 mg/L sodium chloride was dissolved in the CHS1 solution. Two 300 mL Erlenmeyer beakers were rinsed with DI water and dried, before filling with 300 mL of CHS1 solution with 117 mg/L of sodium chloride. 3 mL of 25% ammonia solution was added to one of the Erlenmeyer flasks, in order to increase pH over the target level of 9, and the electrodes were placed into solution. These solutions were to be used to evaluate the electrode behavior over time in realistic conditions, in terms of nutrient solution concentrations of interfering ions.

Before the experiment start, two calibration curves were recorded. Two-point calibration curves were recorded for both the sodium and the chloride ISEs in 10 mg/L and 100 mg/L chloride standards. Two standards of 10 and 100 mg/L of chloride, as sodium chloride, dissolved in lab made synthetic CHS1 nutrient solution were prepared, and calibration curves for both the sodium and chloride were recorded in the prepared solutions. For both calibration curves the pH of the sodium ISE samples was adjusted to >9 using 0.5 mL 25% aqueous ammonia solution. All measurements were made under gentle stirring induced by magnetic stirrers.

The sodium ISE was inserted to the pH adjusted Erlenmeyer flask. A gentle stirr was induced in each flask using magnetic stirrers, and was kept constant through the experiment. The Erlenmeyer flasks were sealed using parafilm, ensuring a tight seal around the electrodes and over the top of the flasks.

The electrodes were left to measure in the solution, using the HACH HQ40d meter. Measurements were recorded every 1 minute for 2 hours, before the data was collected. After this measurements were made every 30 minutes over a period of 12 days. The electrodes also measured the temperature of solution at each measuring point. The data was collected every five days, and the electrodes were observed periodically. The electrodes were kept in a fume hood with the lights off for the majority of the period, except for day 10, where the fume hood lights were left on overnight from day 9 until day 11. The

collected data was the relative concentration measured by the electrodes and logger. The experimental setup is shown in figure 3.1, with the chloride electrode to the left, and the sodium electrode on the right.

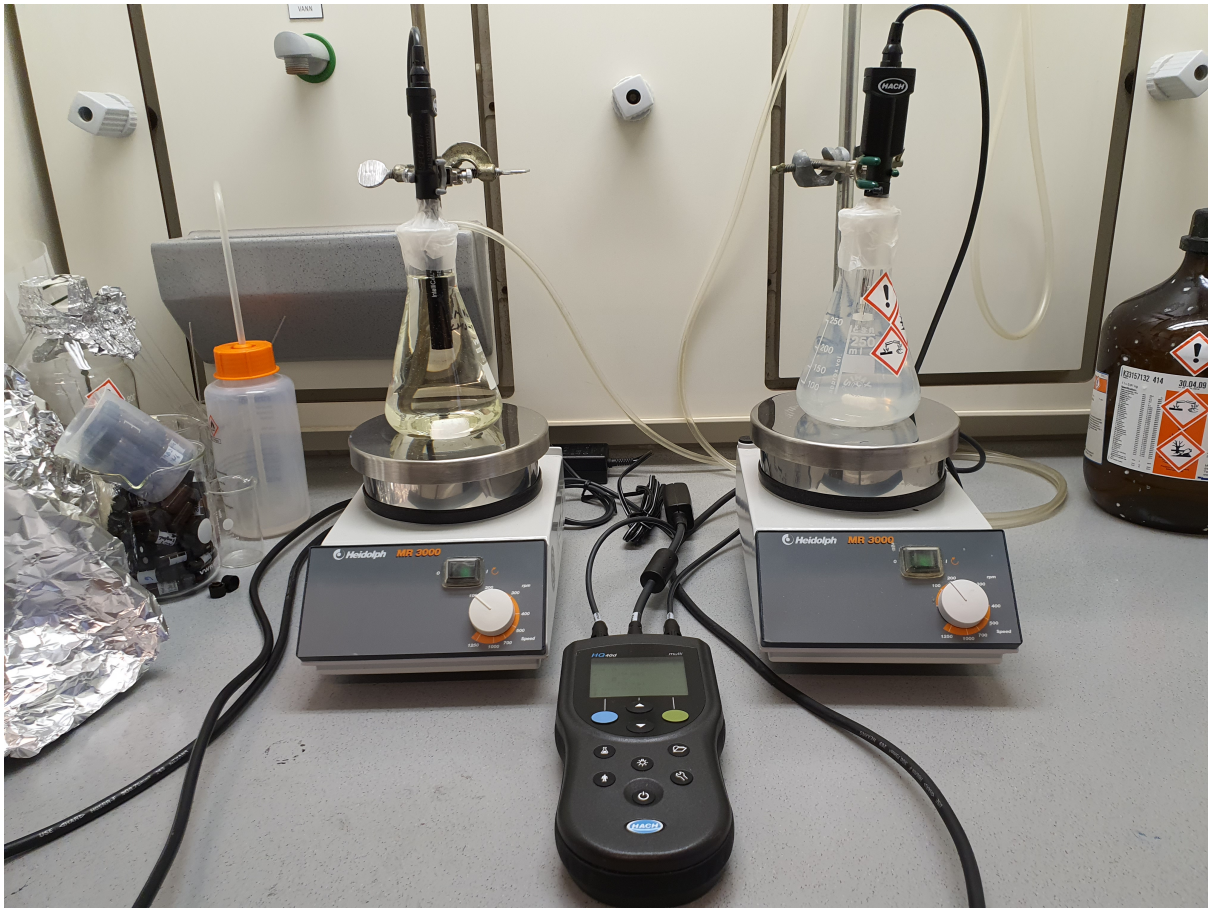

Figure 3.1: Image showing the setup used to evaluate the HACH ISECl181 and ISENa381 electrodes over a 12-day period. On the left is the chloride electrode setup, while the sodium electrode setup is shown on the right, with precipitation from the pH adjustment.

At the end of the 12-day period, a two-point calibration curve was recorded for each electrode, in their appropriate standards.

The electrical conductivity of the CHS1 solution with 117 mg/L sodium chloride was recorded using a WTW Multi 350i handheld meter. At the end of the 12-period the conductivity of the non-pH adjusted solution was recorded, as well as the EC of a CHS1 + 117 mg/L sodium chloride standard solution.

The data was graphed as a function of relative electrode response over time. These are presented in section 4.3.

3.5 Hydroponic samples

Hydroponic sample material was collected from an experiment at NTNU Social Research CIRiS. 8 experiments were running simultaneously, where lettuce was grown in 8 separate hydroponic systems, containing different nutrient solutions with varying nutrient concentrations. Four were added sodium and chloride, while the rest had no additions of sodium and chloride. Complete theoretical concentrations of ions can be found in the Appendix A.1. The experiment ran from 11.11.21 (November 2021) until 06.12.21 (December 2021), and sample material was collected at the first and last day. At the first

sampling, one liter of material was collected from experimental units (EU) 2 through 8, and stored in a dark refrigerated room until analysis. The collected material was not filtered or prepared in any other way. Samples for ICP-MS was collected at the same day, and prepared according to section 3.8. Samples were also prepared for IC as according to section 3.7 at analysis. The sample material was analyzed using the ISEs by direct measurement. 30 mL of sample was prepared in separate glass beakers, and 0.5 mL of 25% aqueous ammonia was added to the sodium electrode samples. Before analysis two two-point calibration curve were prepared. One using sodium and chloride standards of 10 and 100 mg/L, and one using standards of 100 and 1000 mg/L. The samples were analyzed in direct numerical order, from 2 through 8.

The same procedure was repeated at the end of the growth experiment, however due to time constraints the sample material was frozen until analysis about a month after the CIRiS experiment completion. The sample material was frozen on glass bottles at negative 22°C. These bottles unfortunately cracked in the freezing period. The cracked bottles were left to thaw in zipper bags rinsed with DI water, before the sample material was transferred into fresh glass and plastic bottles before analysis. No apparent cross contamination of the sample material was observed. ICP-MS samples were taken before freezing, while IC samples were collected after thawing, both in accordance with sections 3.8 and 3.7. The thawed samples were analyzed using the sodium and chloride electrodes in the same manner as the samples collected in November 2021, but were analyzed going from low to high sodium and chloride concentrations. The samples were analyzed in the order 1, 2, 6, 7, 3, 4, 5 then 8. Before analysis two-point calibration curves of 10 and 1000 mg/L of respective standards were recorded for each electrode.

3.6 Flow Cell experiment

An at-line sampling and monitoring solution was designed and implemented using flow cells.

Two flow cells were designed in cooperation with the NTNU Faculty of Natural Sciences workshop. The two cells were designed to be used for each ISE. The cells were made out of polyoxymethylene, POM. Each individual component was milled out of solid pieces of POM, and glued together. The cells were designed to allow for change of sample using overflow. The cells were designed to keep a volume of 0.1 dm^3 each. The primary cell was designed with two entry spigots, and one exit, in order to allow both hydroponic sample and standard solution to be pumped in. The second cell was designed with one entry spigot, and to be coupled in series with the primary cell. The overflow from the primary cell runs into the second cell, before solution overflows out of the second cell and out to waste. The second cell also included a smaller spigot in order to fit a dosage pump for ammonia addition. Both cells were also fitted with sealable entrances sized for 20 mL VWR HENKE-JECT®syringes aimed at the electrode position in the cell. All spigots, except for dosage pump spigot, were fitted with O-rings to ensure tight seals between hose and spigot.

Tubing with a diameter of 12 mm was used between cells, and from cells to waste. From hydroponic sample and standard solution containers, and to the cell entrance tubing with a diameter of 2 mm was used, in order to minimize the volume of sample and solution in tubing between samples. Tubing size was scaled to 12 mm at the cell entrances using a series of fittings.

Each cell was fitted with lids, including sealable holes for the insertion of electrodes. These were slanted to ensure the electrodes could be introduced into the cell and sample at a slight angle, to avoid air bubbles settling on the electrode sensor surface. The lid was designed to be tightly fitted to the cell body, and sealed using O-rings. The holes used for the electrodes were also fitted with O-rings to ensure

tight seals.

All tubes used for the introduction and transport of hydroponic samples were either solidly dark colored, or covered using dark tape.

Two Verdeflex Peristaltic Electric Operated Positive Displacement (AU R2550120 05) peristaltic pumps were used for introduction of hydroponic sample material and standard solution into the cells. A ProMinent Beta/4 metering pump was used for addition of ammonia solution into the cell with the sodium electrode. All pumps were started and stopped using Biltema Digital weekly timers, art. 35-0107, which regulated the power supplied to the pumps. These timers had a minimum on time of one minute.

3.6.1 Pump testing

The pumps were tested before the experiment. The ability of the peristaltic pumps to exchange the sample volume was tested using the same lengths of tubing as in the experimental flow cell setup. A standard solution of 1 L of 100 mg/L potassium hydrogen phthalate, KHP, was prepared.

The pumps were connected to the primary flow cell, and the second cell was connected in series. DI water was pumped into the cells using one of the peristaltic pumps, until the second cell overflowed into waste. The time used for the pump to exchange this volume was then investigated, by exchange of the DI water with 100 mg/L KHP solution, by recording of the absorbance of the solution in each cell per minute.

The absorbance was recorded using a Shimadzu UV mini 1240 spectrophotometer, with samples contained in Sarstedt plastic UV-transparent micro cuvettes (Fredriksen item number 545150). The spectrophotometer was switched on while the flow cells were set up. The absorbance of pure DI water and the 100 mg/L KHP standard were recorded. The spectrophotometer absorbance was set to zero for the pure DI water sample. After the flow cells were filled with DI water, KHP solution was pumped into the cells at one-minute intervals. The pump was allowed to run for one minute, before being switched off. At each one-minute interval, solution was collected from the center of each cell into a cuvette, using glass pasteur pipettes. New pipettes were used at each interval, and for each cell. This was repeated at each minute interval for five minutes, and before the volume exchange started. Each of these samples were analyzed using the Shimadzu UV mini 1240 spectrophotometer, and the absorbances were recorded.

The volume delivered per minute by the dosage pump was also tested, using the same length of tubing and pump-delivery height as in the flow cell experiment. This was recorded by allowing the dosage pump to deliver DI water for one minute into a previously weighed container. The container with DI water was then weighed again, and the weight of the DI water was recorded. The temperature of the water was recorded before pumping. This was repeated at different dosage pump stroke volumes and stroke intervals. A 10 mL per minute volume was determined and used in the flow cell experiment for addition of 2.5% aqueous ammonia.

3.6.2 Experimental conditions

The flow cell setup was transported to NTNU Social Research CIRiS at NTNU Dragvoll. Here the setup was completed, and the experiment was initiated. A growth tank was prepared according to the method described in Jakobsen et al., 2021[9], but with no harvest over the experiment. One of the peristaltic pumps were set up to pump hydroponic nutrient solution into the cells at required times. The other peristaltic pump was fitted to a 10 mg/L sodium standard solution, with ISA, kept in a 10 L bucket with

lid. The standard was prepared by diluting one liter of 100 mg/L sodium and 0.001M ISA solution to ten liters in the bucket. A 2.5% ammonia solution was prepared by dilution, and placed in a separate room to the plants, with the dosage pump. A two-point calibration curve was recorded for each electrode before transport. The electrode behavior over a 4 hour period in 100 mg/L sodium and chloride standard was also recorded before transport.

The growth tank was prepared with 17 pots on the 20^{th} of April, 2022, according to the method described in Jakobsen et al., 2021[9]. Each pot was populated with two seeds of Lactuca sativa 'Frillice' lettuce (LOG AS, item number 41 29 54 50, batch number 103755757). The tank was filled with 46.5 L of tap water, and covered with a plastic tarp. After five days, on the 25^{th} of April, the plastic tarp was removed, along with one of the seeds. Only one plant was allowed to populate each pot. On the same day nutrient solution standards were added to solution, and nutrient concentrations were adjusted to levels described in table 2.2. The nutrient solution container was also refilled to 46.5 L using tap water. The following Monday, 2^{nd} of May, 50 mL of a prepared 4.65 M sodium chloride solution was added to the growth tank, in order to adjust the sodium chloride concentration in the growth tank to 292 mg/L (115 mg/L sodium, 117 mg/L chloride). The growth tank was also refilled to 46.5 L using tap water, after addition of sodium chloride solution. A week later, on Monday the 9^{th} of May, 100 mL of 4.65 M sodium chloride solution was added, and the tank was refilled again. This adjusted the sodium chloride concentration in the growth tank to 877 mg/L (345 mg/L sodium, 532 mg/L chloride). No further adjustments were made to the solution, nor was the container refilled until the end of the experimental period.

The flow cells were setup next to the growth tank. Each cell contained each their electrode, with the first cell containing the HACH ISECl181 chloride electrode, and the second cell containing the HACH ISENa381 sodium electrode. Each cell was also secured to a magnet stirrer using tape, due to tension with the tubing in the setup, and to ensure that they should not fall over. Two buckets were set up under the bench, one containing the low concentration standard, and one for the collection of waste. Both were covered with lids. The tubing from cell 2 to waste was secured to the bench, and fitted to the bucket to ensure constant fall in the tube. The magnet stirrers were used to ensure constant stirring in each cell.

The sampling was set to happen twice a week, on Mondays and Thursdays. The peristaltic pump was set to start and run for 4 minutes, in order to exchange the standard solution in the cells with hydroponic sample. A minute after complete exchange the dosage pump was set to run for a minute, injecting about 10 mL of 2.5% ammonia solution. The hydroponic sample was left for 4 hours, before the standard solution pump was started, and the sample was exchanged with standard solution for storage. The HACH HQ40d logger was used to record the response of the electrodes, and recorded a data point per electrode every 30 minutes. The data from the logger was collected twice a week, on the same day as ISE sampling, along with samples prepared for IC and ICP-MS in accordance to section 3.7 and 3.8. The overflow was collected as waste. The first week ISE sampling did not happen on Thursday the 21^{st} of April, due to an error with the digital timers used for the pumps. Sample material was pumped into the cells on Friday the 22^{nd} to ensure two sample points were recorded for the first week.

The electrode tips were inspected weekly for biofouling. On the Thursday of the fourth week in the experimental period growth was observed on the chloride electrode, after that days sampling. The electrode was cleaned, and a second sampling was initialized for later on the same day. These two sampling points were both compared to the IC and ICP-MS samples collected on the same day.

A problem relating to the overflow of sample from cell one to cell two was also discovered on Thursday the 21^{st}, where ammonia flowed back from the second cell, and into the primary cell. The primary cell

was raised by a height of about 2 cm to counteract this, and the tubing between the cells was replaced wuth a new joint to ensure enough height difference between the cells. The peristaltic pump runtime was increased from 4 to 5 minutes to counteract the expected loss of pressure over the joint. The figures below shows the setup before (20th of April, figure 3.2) and after adjustments (21st of April, figure 3.3).

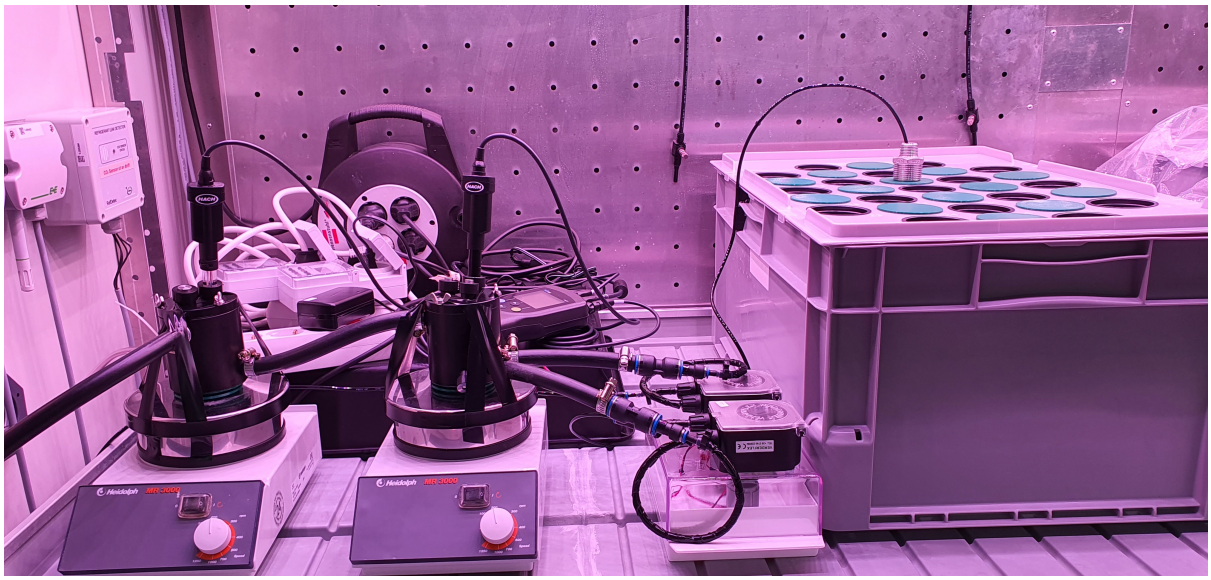

Figure 3.2: Flow cell setup prior to adjustments made the 21st.

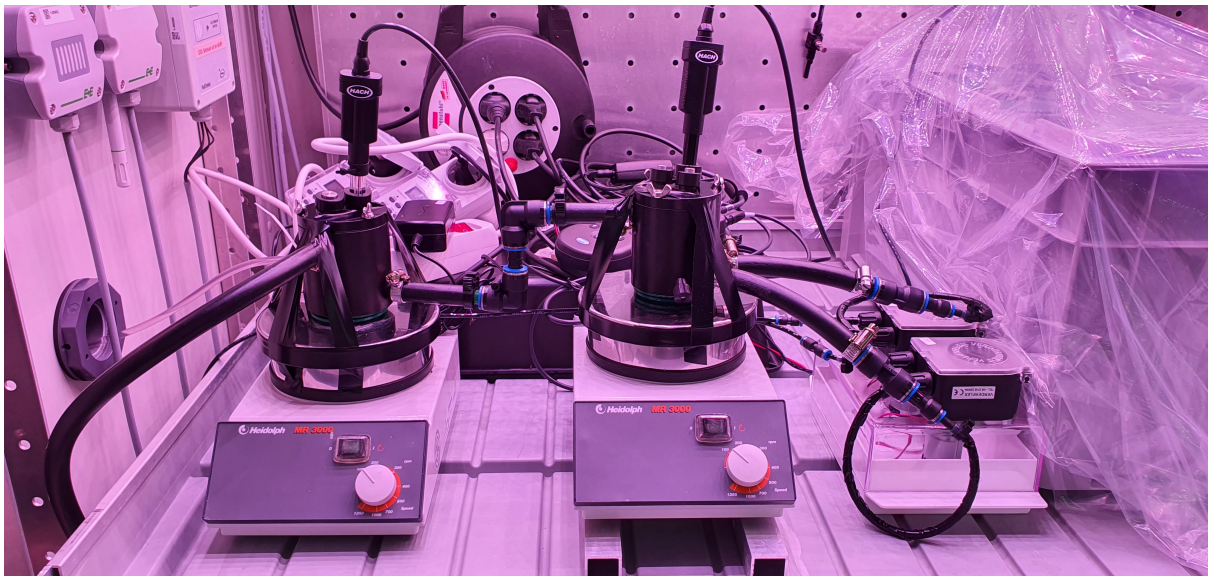

Figure 3.3: Flow cell setup after adjustments were made on the 21st to hinder flow back to the primary cell.

The experiment was conducted over a period of 4 weeks and 5 days, with setup and startup on the 20th of April 2022. The experiment was concluded on the 23rd of May. ISE measurements were made at a frequency of twice a week over the duration of the experiment, as well as sample collection for IC and ICP-MS validation twice a week.

Plant health was prioritized by cleaning of all instruments and items used in the hydroponic setup, using tap water and 70% ethanol solution. Plant growth, growth rate and direct health were not investigated

in this experiment. 16 lettuce plants survived the duration of the experiment, and 1 died in the final days of experiment, most likely due to being broken during IC/ICP-MS sampling procedure. In order to maintain plant health the nutrient solution pH and EC were measured weekly, every Monday after sampling. The pH was measured to ensure it stayed in the range for optimal plant growth, at 5.4-5.6 for the used lettuce cultivar[9]. pH and EC measurements are presented in Appendix table A.4, section A.4. The pH was measured to be within the acceptable range during the experimental period.

3.7 Ion Chromatography

The IC samples were pretreated by filtering using 22 mm syringe filters with 0.45 μm polyethersulfone membranes. The syringe was rinsed three times with DI water and three times with sample material before a filtered sample was obtained. A new filter was used for each sample. The filtered samples were collected in glass sample tubes. The filtered samples were then diluted to ensure none of the analyte anion concentrations were higher than 50 mg/L. Samples from November 2021, the start of the hydroponics experiment, were diluted at a 1:25 ratio, due to high total ion concentration. Samples from December 2021 were filtered and diluted after freezing. These samples were diluted at a 1:12.5 ratio, as the concentration of main ions are assumed to be halved over the time of the experiment. The first five samples collected in the flow cell experiment were diluted at 1:5 ratio, while the last four were diluted at a 1:10 ratio. The filtered and diluted samples were stored in glass sample tubes in a dark refrigerated area (4°C) until analysis.

Sample material collected was analyzed using a Metrohm 940 Professional IC Vario 1 ion chromatography instrument using a Metrohm Metrosep A Supp 7 - 250/4.0 anion separation column, and detected on the Metrohm 950 Professional Vario 1 conductivity detector. Samples were diluted at a ratio of 1:5 by the injection system before transferring to the column. The first five samples from the flow cell experiment were diluted at a 1:10 ratio by the injection system. 3.6 mM sodium carbonate (Na_2CO_3) was used as eluent, and the analysis was run for 38 minutes. The analysis identified chloride, nitrate and sulphate anions in samples.

3.8 ICP-MS

ICP-MS samples were filtered using 22 mm syringe filters with 0.45 μm polyethersulfone membranes. A new filter was used per sample, and the syringe was rinsed using DI water and sample material before filtration. Filtered samples were stored in VWR Metal-Free polypropylene test tubes, with high-density polypropylene caps. Digestion was performed by addition of three drops of 65% nitric acid. Digested samples were stored in a dark refrigerated area before delivery for analysis. Samples were analyzed in order of ionic strength to avoid errors in analysis. Low ionic strength samples were analyzed first, and samples were then analyzed in order of increasing total ionic strength.

Samples were analyzed for elemental composition using 8800 Triple Quadrupole inductive coupled plasma mass spectrometry (ICP-MS) system (Agilent, USA) equipped with prepFAST M5 autosampler (ESI, USA).

The general instrumental parameters are shown in table 3.5

Table 3.5: General parameters used for ICP-MS elemental analysis.

General parameters	
RF Power	1550 W
Nebulizer Gas	0.8 L/min
Makeup Gas	0.35 L/min
Sample depth	8.0 mm
Ion lenses	x-lens
O_2 mode	
O_2 gas flow	0.525 mL/min

The hydroponic samples collected from CIRiS were analyzed for 17 elements; B, Na, Mg, Al, Si, P, S, K, Ca, Mn, Fe, Cu, Zn and Mo. The flow cell experiment samples were analyzed for the elements Na, Mg, K and Ca. Results of ICP-MS analysis for hydroponic batch samples and the flow cell experiment are presented in appendix, section A.6

4 Results & Discussion

All measurements made were repeated five times. After electrode stabilization, five measurements were made in each solution or sample.

The results from the different experiments are presented in the following sections, however certain general observations have also been made over the experiment period. One of the main observations was the formation of precipitate in the sodium samples. The addition of 0.5 mL 25% aqueous ammonia produced precipitate in 25 mL of nutrient solution, both laboratory prepared and samples collected from hydroponic systems. The precipitate formed as a milky white suspension in solution, and would settle as a layer on the bottom of containers if left undisturbed. The stirring induced by the magnetic stirrer kept the precipitate in solution during measurements. The amount of stirring was approximately the same for each sample. Figure 4.1 shows 25 mL of sample material collected in December 2021, with the image on the left showing sample only, while the image on the right shows sample with pH adjusted to >9, by addition of 0.5 mL of 25% aqueous ammonia.

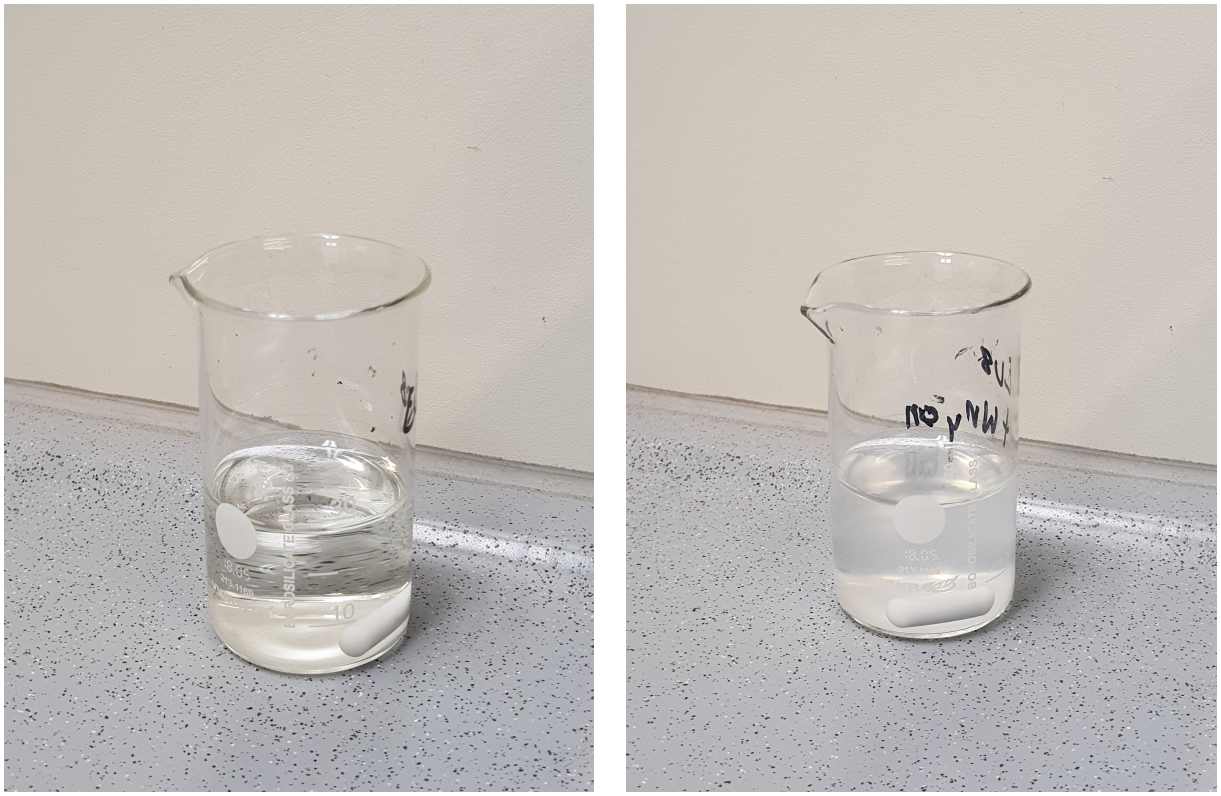

Figure 4.1: Images showing the precipitate formed in hydroponic samples after addition of 0.5 mL 25% aqueous ammonia. Both images show 25 mL of sample material from sample 8, collected in December 2021, after ISE analysis. The left image shows sample only, while the right image shows sample after pH adjustment with 0.5 mL of 25% aqueous ammonia.

Precipitation was observed in all pH adjusted samples, both those collected in November and December of 2021, as well as all laboratory prepared CHS1 samples. Certain samples produced more precipitate than others, such as sample 3 collected in December of 2021.

pH adjustment has little impact on lab-work, but eliminates the possibility of recirculating hydroponic samples, and leads to waste in what preferably should be a closed loop circulation. The formation of

precipitate in both hydroponic samples and prepared solutions could also lead to problems. Precipitate settling on the electrode could lead to measurement problems, by physical blocking of the sensor surface, separating the sensor from the bulk of the solution. Precipitate could also be a potential problem in further uses, with potential impacts on pumping after adjustment to alkaline conditions. Precipitate formed in all hydroponic samples, as well as in nutrient solutions (CHS1) prepared in the lab. Certain samples gave more precipitation than others. For example sample 3 collected in December from CIRiS had about double the precipitate than other samples collected, based on visual inspection. The precipitate is shown in figure 4.1, and was also present in the 12 day experiment. There are many sources for possible precipitation, such as pH adjustments reducing the stability of iron-complexes in nutrient solution[74]. The addition of base also posed problems in regard to the experimental setup and use of flow cells for at-line monitoring.

The response of both electrodes in the same container was also investigated, by the recording of simultaneous three-point calibration curves in one glass beaker. The sample pH was adjusted to >9 using 0.5 mL 25% aqueous ammonia. The resulting calibration curves are graphed in figure 4.2.

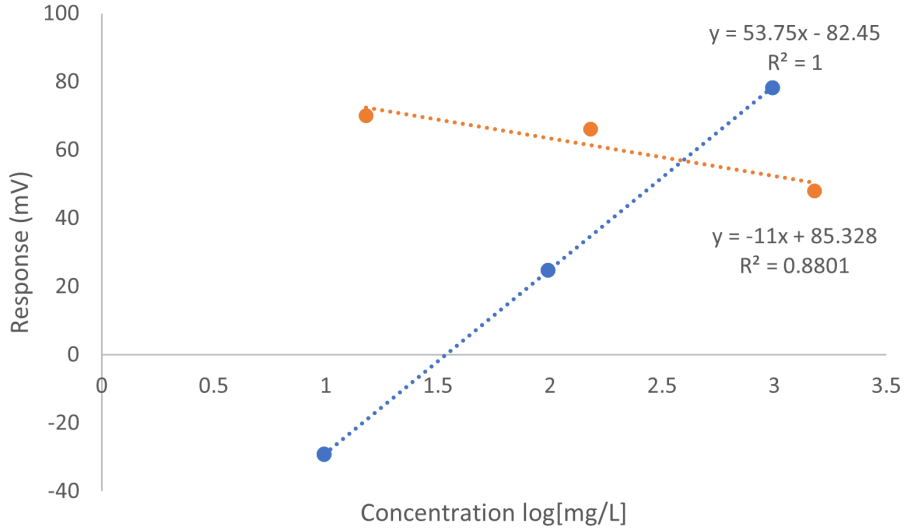

Figure 4.2: Calibration curves of both the sodium (blue) and chloride (orange) electrodes recorded in the same beaker, with basic pH conditions.

The calibration curves in figure 4.2 show that the electrodes need to be kept in separate containers, as the chloride calibration curve is clearly impacted. The sodium calibration curve, shown on the figure in blue, shows an acceptable slope of 53.75 mV per decade, and very good linearity as evident by the determination coefficient of 1. The determination coefficient indicates that the regression is perfectly fitted to the data provided, and could be evidence of overfitting in the model. However, the chloride calibration curve, shown in orange shows significant deviation from the expected. The slope of -11 mV per decade is far from the theoretical value of -59 mV per decade, and it also shows a poor determination coefficient of 0.8801. This is possibly due to the addition of ammonia, even though the chloride electrode should be usable in pH ranges from 1 to 12 as per the manual[30]. The figure shows that this necessarily is not the case. The chloride calibration curve also shows that the electrode records a lower voltage than expected, as evident by the low slope intercept of +85.328 mV. This in turn means that the electrode overestimates the chloride concentration present under such conditions, as the electrode response measured in mV is expected to decrease with increasing chloride concentration. The impacts here show that the chloride

electrode can not be used in pH-adjusted samples, and separate beakers were as such used for the remainder of the experimental work. This also led to the use of individual flow cells in the real time experiment.

4.1 Interference calibration curves

To evaluate the impact of nutrients as interfering ions, calibration curves in the presence of interferences were recorded. These calibration curves are presented in the two next subsections, divided into chloride calibration curves, and sodium calibration curves, for the chloride electrode (HACH ISECl181) and sodium electrode (HACH ISENa381) respectively . Two calibration curves were recorded per interference. One with constant analyte concentration, and varying interfering ion concentration, and one with varying analyte ion concentration and constant interfering ion concentration.

The interference calibration curves provide a way to indicate whether potential interfering ions have an impact on readings made by the ion selective electrodes. For an ideal, non-interfering ion, the first curve (curves A), with constant analyte ion concentration, would give a curve with a slope of 0, and a y-intercept of the mV value for the constant analyte ion concentration. The second curve (curves B), with varying analyte ion concentration, would ideally be the same as the recorded normal calibration curves, shown in figures 4.3 and 4.8.

Chloride calibration curves

A normal calibration curve, using chloride standards of 10, 100 and 1000 mg/L and no ISA was at first recorded. This is presented in figure 4.3.

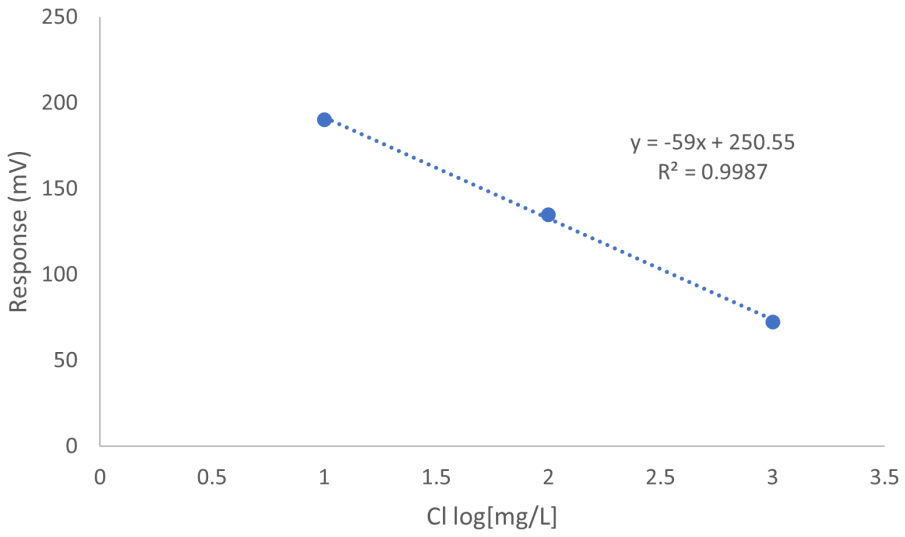

Figure 4.3: Calibration curve recorded using the chloride electrode, in 10, 100 and 1000 mg/L chloride standards.

The calibration curve in the figure has a slope of -59 mV per decade, and a determination coefficient of R^2=0.9987. This curve serves as a reference to the other calibration curves recorded.

Interference calibration curves were based on the previously described CHS1 nutrient solution. Due to the low concentrations and high number of individual micronutrients present in the solution, these were evaluated as one. The calibration curve using varying micronutrient concentration and constant chloride concentrations was recorded using concentrations based on the CHS1 standards. The curve was recorded using 0.1x, 1x and 10x concentrations of micronutrients, based on concentrations for CHS1 given in table 2.2. The calibration curves are presented in figure 4.4.

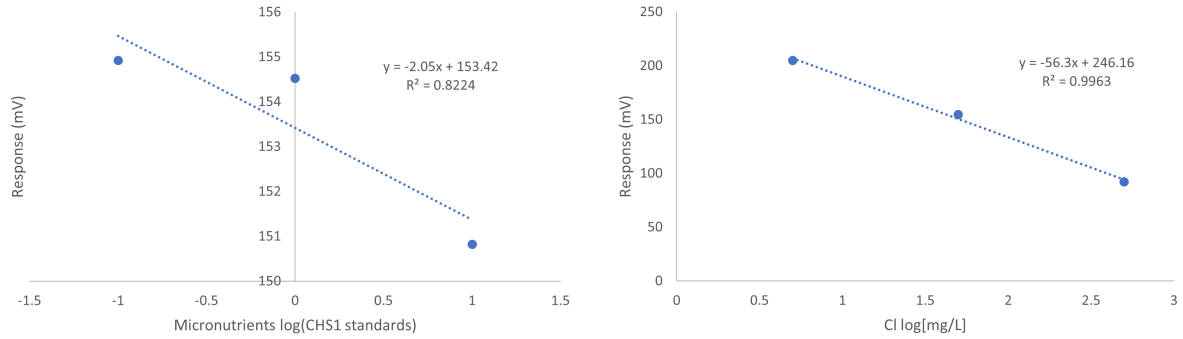

A B

Figure 4.4: Calibration curves recorded in the presence of CHS1 micronutrients. Curve A was recorded using 0.1x, 1x and 10x micronutrient concentrations proportioned by the CHS1 nutrient solution. Curve B was recorded using 1xCHS1 micronutrient concentration, and chloride concentrations of 5, 50 and 500 mg/L.

As shown in the figure, the curve recorded with constant chloride concentrations (curve A, fig. 4.4) has a non-zero slope of -2.05 mV per decade, indicating a deviation from the ideal. The calibration curve recorded with varying analyte concentrations (curve B, fig. 4.4) has a higher slope than the reference presented in figure 4.3, with a slope of -56.3 mV per decade, an increase of 4.6%.

Calibration curves were also recorded for the individual macronutrients present in the CHS1 nutrient solution. These are presented in the figures 4.5, 4.6 and 4.7.

Nitrate calibration curves are presented in figure 4.5. A curve with varying nitrate concentrations of 5, 50 and 500 mg/L and constant chloride concentration of 50 mg/L was recorded (Curve A, figure 4.5). A separate curve with varying chloride concentrations of 5, 50 and 500 mg/L, and constant nitrate concentration of 50 mg/L was also prepared (Curve B, figure 4.5).

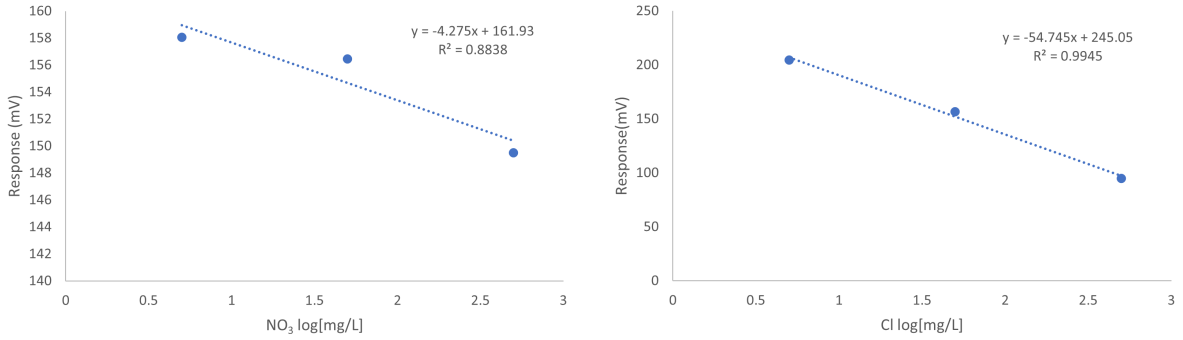

A B

Figure 4.5: Calibration curves recorded in the presence of nitrate. Curve A was recorded using 5, 50 and 500 mg/L standards of nitrate, with 50 mg/L of chloride. Curve B was recorded using 5, 50 and 500 mg/L standards of chloride, with 50 mg/L of nitrate.

In figure 4.5, curve A shows the curve recorded with constant chloride concentration, and varying nitrate concentration. This curve has a slope of -4.275 mV per decade, which indicates that nitrate is an interfering ion. Curve B confirms this, as the varying chloride concentration calibration curve has a slope of -54.745 mV per decade, an increase of 7.2% from the reference slope in figure 4.3.

Calibration curves were prepared for phosphate as an interfering ion. These curves are presented in figure 4.6. A curve with varying phosphate concentrations of 5, 50 and 500 mg/L and constant chloride concentration of 50 mg/L was recorded (Curve A, figure 4.6). A separate curve with varying chloride concentrations of 5, 50 and 500 mg/L, and constant phosphate concentration of 50 mg/L was also prepared (Curve B, figure 4.6).

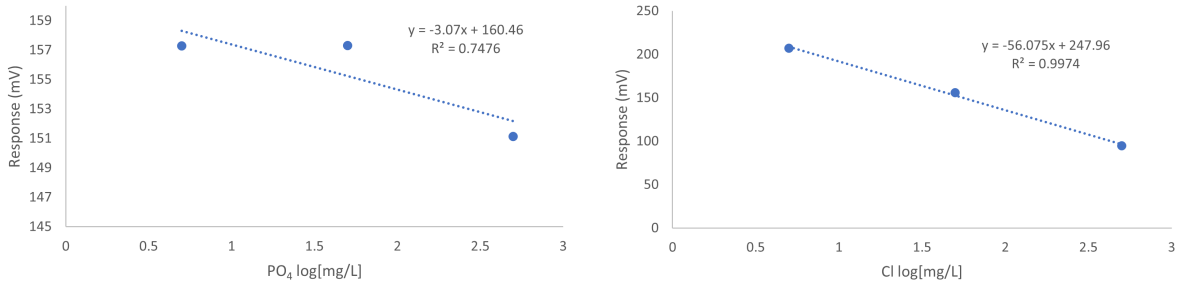

A B

Figure 4.6: Calibration curves recorded in the presence of the interfering ion phosphate. Curve A was recorded using 5, 50 and 500 mg/L standards of phosphate, with 50 mg/L of chloride. Curve B was recorded using 5, 50 and 500 mg/L standards of chloride, with 50 mg/L of phosphate.

Curve A, figure 4.6, is the curve recorded at constant chloride concentrations. The slope here is -3.07 mV per decade. Curve B (fig 4.6) shows an increasing slope compared to the reference in figure 4.3, increasing by 5% to -56.075 mV per decade.

Sulphate was also evaluated as an interfering ion by the recording of calibration curves. These curves are presented in figure 4.7. A curve with varying sulphate concentrations of 5, 50 and 500 mg/L and constant chloride concentration of 50 mg/L was recorded (Curve A, figure 4.7). A separate curve with varying chloride concentrations of 5, 50 and 500 mg/L, and constant sulphate concentration of 50 mg/L was also prepared (Curve B, figure 4.7).

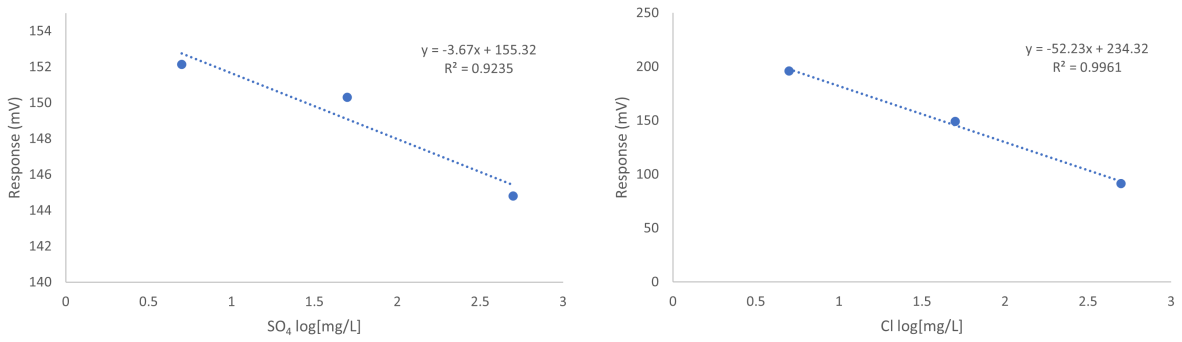

A B

Figure 4.7: Calibration curves recorded in the presence of the interfering ion sulphate. Curve A was recorded using 5, 50 and 500 mg/L standards of sulphate, with 50 mg/L of chloride. Curve B was recorded using 5, 50 and 500 mg/L standards of chloride, with 50 mg/L of sulphate.

Figure 4.7, curve A, shows the curve recorded at varying sulphate concentrations, and constant chloride concentrations. A non-zero slope is presented also here, as the regression curve has a slope of -3.67 mV per decade. Curve B, same figure, shows the calibration curve recorded with varying chloride concentrations

and constant sulphate concentrations. Here the slope has an 11.5% increase compared to the reference presented in figure 4.3.

All recorded chloride calibration curves show departure from ideal behavior, both for curves recorded with constant chloride concentrations, and varying analyte concentrations.

The curves recorded with varying concentrations of interferences (Curves A, figures 4.4, 4.5, 4.6 and 4.7) give slopes $\neq 0$. For a non interfering ion these slopes would expected to be $=0$, as the analyte ion concentration does not change between samples. ion. This indicates that all ions have an interfering effect on the chloride electrode.

Nitrate shows the largest deviation from ideal, with a slope of -4.275 mV per decade, as can be seen in curve A, figure 4.5. All slopes are also less than zero, indicating an increase in measured analyte ion concentration by the electrode with an increase in the interfering ion. Most of these slopes also have rather low determination coefficients, and do, by visual inspection, seem to be mostly impacted by the high concentration readings. All curves A shown in figures 4.4, 4.5, 4.6 and 4.7 have poor determination coefficients, with $R^2<0.990$, indicating that any correlation between the electrode response and interference concentration may be non-linear.

The calibration curves recorded using constant interfering ion concentrations (presented as curve B in figures 4.4, 4.5, 4.6 and 4.7) also show signs of being impacted by the interfering ions. All calibration curve slopes are higher, and have a lower y-intercept, than the reference curve presented in figure 4.3. This also indicates that the presence of these interfering ions will impact the ISE readings in a positive way, and that the presence of these interfering ions may lead to the electrode overestimating concentrations of chloride in solution. Here all graphs show OK linearity, judging from the determination coefficients, where none are <0.990. These graphs also indicate that nitrate has significant impact as an interfering ion. This is evident by the slope in figure 4.5, which deviates from the reference in figure 4.3 by $+7.2\%$. However the largest deviation is shown in figure 4.7, resulting from sulphate. Here the slope increases by 11.5% compared to the reference recorded in figure 4.3. This indicates that these ions may have the largest impact as interfering ions, and their presence can lead to the electrode measured concentration of chloride being an overestimation of the actual chloride concentration in analyte solution.

Sodium calibration curves

A sodium calibration curve was recorded and used as a reference for the sodium electrode. This is presented in figure 4.8. The calibration curve was recorded using 10 mg/L and 1000 mg/L sodium standards, as well as a 100 mg/L chloride standard.

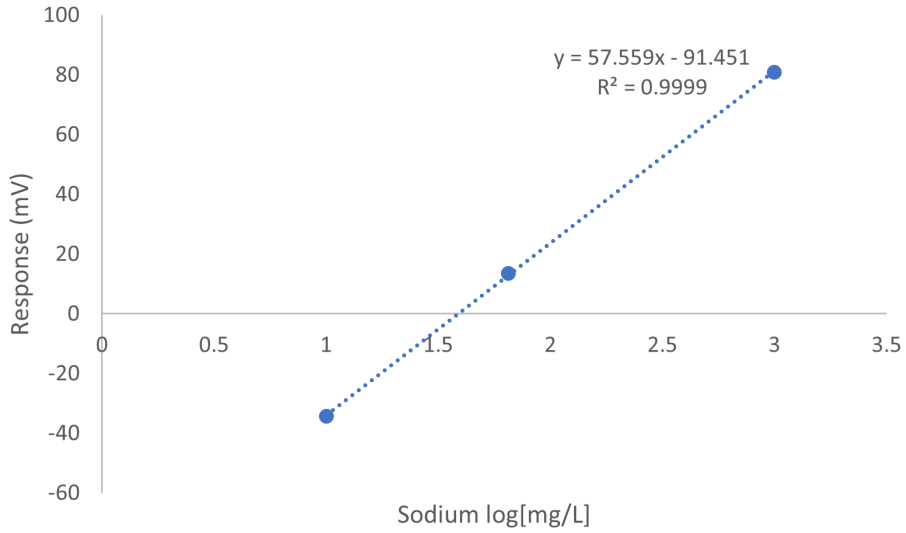

Figure 4.8: Calibration curve recorded using the sodium electrode, in 10 and 1000 mg/L sodium standards, as well as a 100 mg/L chloride standard.

The figure shows a sodium electrode calibration curve, used as a reference curve. The curve has a slope of 57.779 mV per decade, and a determination coefficient of R^2=0.9999. Calibration curves recorded at constant interfering ion concentrations would ideally have the same slope as presented in figure 4.8, assuming the present ion is non-interfering. Figure 4.8 was also recorded using a 100 mg/L chloride standard, which explains the medium concentration point in the graph not being at log[Sodium mg/L] = 2. Ammonium was not tested here due to aqueous ammonia being used for pH adjustments, which would impact the recording of calibration curves.

Interference calibration curves were also recorded for the sodium ISE, to evaluate the impact of positively charged nutrients as interfering ions. The pH of each measured solution was adjusted to > 9, using 0.5 mL 25% aqueous ammonia. Micronutrients were evaluated as one, due to low individual concentrations, and ease of work. Micronutrient concentrations were based on the CHS1 standards. A curve with 0.1x, 1x and 10x micronutrient concentrations present in CHS1 nutrient solution, and 50 mg/L of sodium was prepared. CHS1 micronutrient concentrations were based on the data presented in table 2.2. A calibration curve using 5, 50 and 500 mg/L standards of sodium, with 1x CHS1 micronutrient concentrations was also recorded. The calibration curves are presented in figure 4.9.

As shown in the figure, the curve recorded with constant sodium concentrations and varying micronutrient concentrations (curve A, Fig. 4.9) has a non-zero slope of 3.0872 mV per decade, indicating a deviation from the ideal. The calibration curve recorded with varying analyte concentrations and constant micronutrient concentrations (curve B, Fig. 4.9) has a lower slope than the reference presented in figure 4.8, with a slope of 47.01 mV per decade, a decrease of 18.3%.

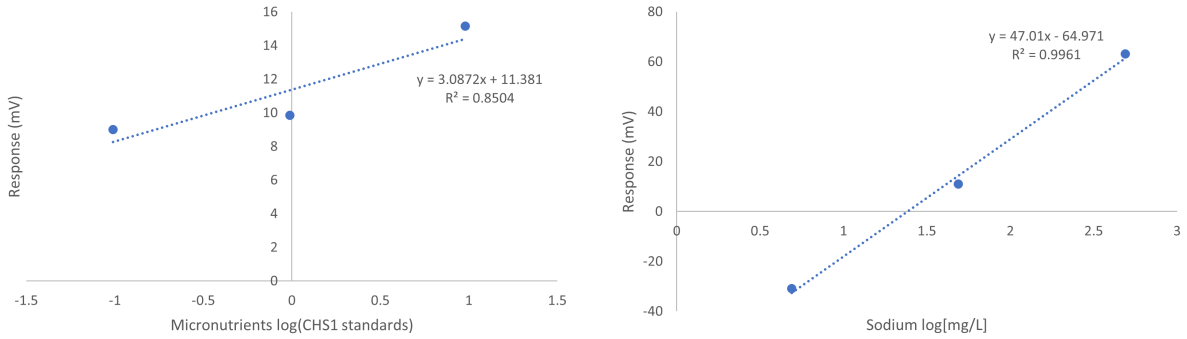

A B

Figure 4.9: Sodium electrode calibration curves recorded in the presence of CHS1 micronutrients. Curve A was recorded using 0.1x, 1x and 10x micronutrient concentrations proportioned by the CHS1 nutrient solution, with 50 mg/L sodium. Curve B was recorded using 1xCHS1 micronutrient concentration, and sodium concentrations of 5, 50 and 500 mg/L.

Positively charged macronutrient ions were evaluated individually. Calcium was evaluated as a possible interfering ion. Calibration curves are presented in figure 4.10. A curve with varying calcium concentrations of 5, 50 and 500 mg/L and constant sodium concentration of 50 mg/L was recorded (Curve A, figure 4.10). A separate curve with varying sodium concentrations of 5, 50 and 500 mg/L, and constant calcium concentration of 50 mg/L was also prepared (Curve B, figure 4.10).

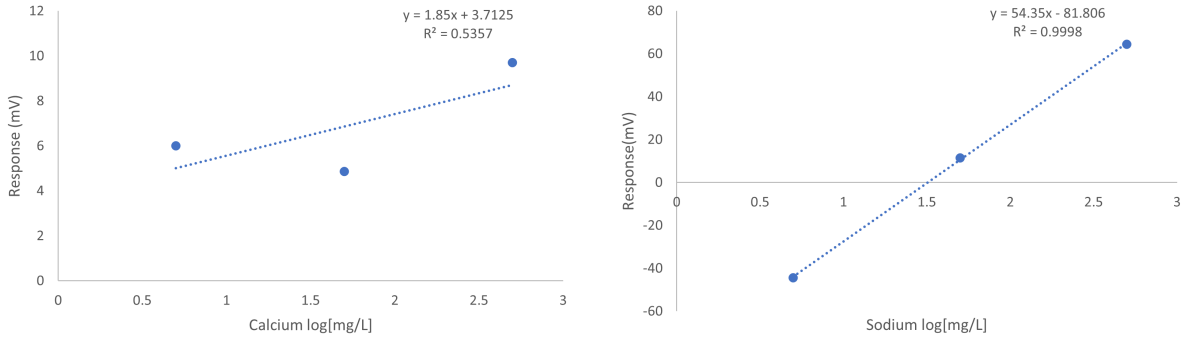

A B

Figure 4.10: Calibration curves recorded in the presence of the interfering ion calcium. Curve A was recorded using 5, 50 and 500 mg/L standards of calcium, with 50 mg/L of sodium. Curve B was recorded using 5, 50 and 500 mg/L standards of sodium, with 50 mg/L of calcium.

Figure 4.10, curve A, shows the curve recorded at varying calcium concentrations, and constant sodium concentrations. The curve presented has a non-zero slope, as the regression curve has a slope of 1.85 mV per decade. Curve B, same figure, shows the calibration curve recorded with varying sodium concentrations and constant calcium concentrations. Here the slope has a 5.6% decrease compared to the reference presented in figure 4.8.

Magnesium was also evaluated as an interfering ion. Magnesium sulphate was used to prepare standards used to record a calibration curve with 5, 50 and 500 mg/L of magnesium and constant sodium concentration of 50 mg/L(Curve A, figure 4.11). A second calibration curve was also recorded, with varying sodium concentrations of 5, 50 and 500 mg/L and constant magnesium concentration of 50 mg/L

(Curve B, figure 4.11). White precipitation was observed in solutions with high magnesium sulphate concentrations. The results are presented in figure 4.11.

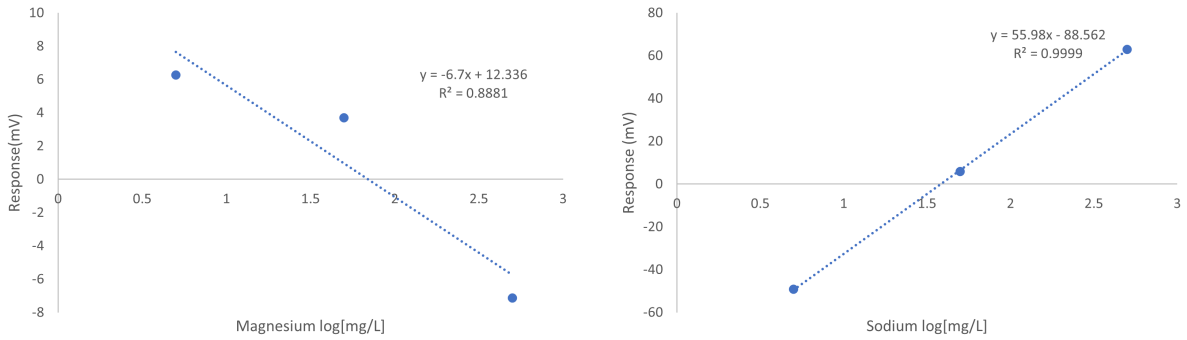

A B

Figure 4.11: Calibration curves recorded in the presence of the interfering ion magnesium. Curve A was recorded using 5, 50 and 500 mg/L standards of magnesium, with 50 mg/L of sodium. Curve B was recorded using 5, 50 and 500 mg/L standards of sodium, with 50 mg/L of magnesium.

In figure 4.11, curve A shows the curve recorded with constant sodium concentration, and varying magnesium concentration. This curve has a slope of -6.7 mV per decade. Curve B shows the varying sodium concentration calibration curve, and has a slope of 55.98 mV per decade, a decrease of 2.7% from the reference slope in figure 4.8.

Finally, potassium was evaluated as an interfering ion for the sodium ISE. A calibration curve with varying potassium concentrations of 5, 50 and 500 mg/L, and constant sodium concentration of 50 mg/L was prepared(Curve A, figure 4.12). A calibration curve with varying sodium concentrations of 5, 50 and 500 mg/L, and constant potassium concentration of 50 mg/L was also prepared(Curve B, figure 4.12). The resulting curves are presented in figure 4.12.

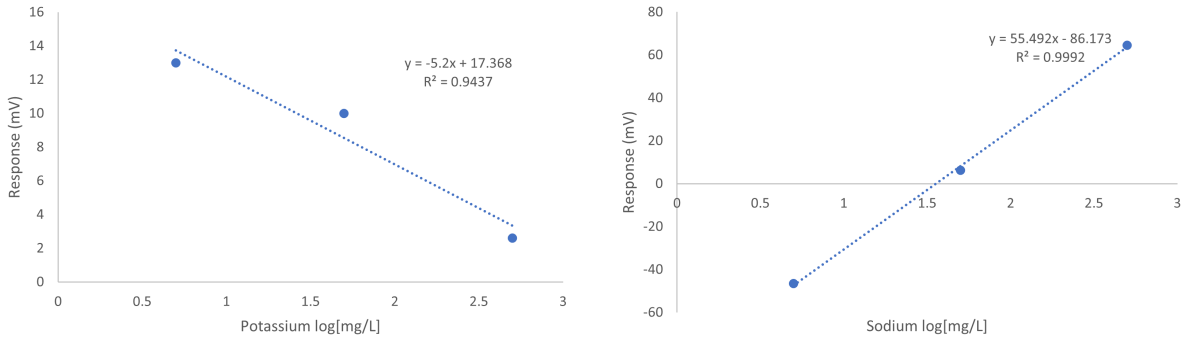

A B

Figure 4.12: Calibration curves recorded in the presence of the interfering ion potassium. Curve A was recorded using 5, 50 and 500 mg/L standards of potassium, with 50 mg/L of sodium. Curve B was recorded using 5, 50 and 500 mg/L standards of sodium, with 50 mg/L of potassium.

Curve A, figure 4.12, is the curve recorded at constant sodium concentrations, and with varying potassium concentrations. The slope here is -5.2 mV per decade. Curve B figure 4.12, was recorded using varying sodium concentrations, and shows a lower slope compared to the reference in figure 4.8, decreasing by 3.6% to 55.492 mV per decade.

The constant analyte ion concentration curves (presented as curve A in figures 4.9, 4.10, 4.11 and 4.12) show varying results. The expected result would be an increase in electrode response with increasing interfering ion concentrations. The results for the micronutrients (curve A, figure 4.9) and calcium (curve A, figure 4.10) show this, with positive slopes in both curves. The calcium curve shows an increase per decade of 1.85 mV, which indicates less impact. The micronutrients curve, curve A in figure 4.9, shows a larger slope of 3.0872 mV per decade, but seems to be largely impacted by the high concentration point, which is much higher than what is expected to be found in hydroponic solutions at 10x normal nutrient solution (CHS1) concentrations. Both these results indicate an increase in measured sodium concentrations using the ISE with an increase in micronutrient and calcium concentrations. The results for magnesium and potassium however deviate from the expected results, as both graphs A in figure 4.11 and figure 4.12 have negative slopes(-6.7 mV per decade for magnesium, -5.2 mV per decade for potassium). Especially magnesium seems to have a large negative impact with increase in concentration, with the 500 mg/L magnesium concentration point eliciting an electrode response of -8 mV, whereas the electrode response for all other interfering ion concentrations are positive values. The magnesium curve, curve A fig 4.11, also has a determination coefficient of R^2=0.8881, which is significantly less of the accepted 0.990. The results for varying concentrations of potassium and magnesium both indicate an interfering effect, but in a way that would lead to the electrode underestimating the sodium concentration in solution. Also here all curves show a low determination coefficient, R^2<0.990, indicating that any correlation may be non-linear in nature.

The calibration curves recorded with constant interfering ion concentration (curves B in 4.9, 4.10, 4.11 and 4.12) all slopes deviate from the reference presented in figure 4.8. All show lower slopes and intercepts than the reference. A suppression of the curve like this would indicate that the sodium electrode would measure a lower concentration of sodium in the presence of interfering ions, as compared to solutions without interfering ions. The largest deviation from ideal is shown in curve B, figure 4.9 for micronutrients, where the slope decreases by 18.3% compared to the reference in figure 4.8. This result deviates from the result presented by the graph with varying interfering ions, curve A in the same figure, and its reliability can be questioned. The same can be said for calcium, curve B figure 4.10, where the slope with constant interference (decrease from reference by 5.6%) indicates that the sodium electrode will underestimate the sodium concentration, while the graph with varying interfering ions (curve A, positive slope of 1.85 mV per decade) indicate an overestimation. The results for both magnesium shown in figure 4.11 and potassium in figure 4.12 show a slight suppression of the calibration curve compared to the reference shown in figure 4.8. In the presence of magnesium the slope decreases by 2.7% compared to the reference, while in the presence of potassium the slope decreases by 3.6% The suppression here are however smaller than would be expected, when compared to the varying interfering ion concentrations curves (Curves A) presented in the same figures.

ISA was not used in these experiments, in order to have no influence from the possible interfering nature of the ISA solution. This is however not advisable, and might have resulted in erroneous measurements. This could possibly explain the deviating measurements for magnesium, shown in curve A figure 4.11.

The results here indicate that all tested ions will have an interfering effect, both for the chloride and sodium electrodes. The chloride results indicate an interference in the positive way, where the largest contributions to overestimations of chloride concentrations measured using the electrode are nitrate and sulphate. All tested ions are however shown to contribute and interfere. For the sodium electrode, all ions are shown to interfere, and they are shown to possibly interfere by decreasing the electrode response. This could lead to an underestimation of sodium concentrations measured by the electrode, where potassium

and magnesium are suspected to have the largest impact, as the results for micronutrients and calcium are unsatisfactory.

4.2 Interference Spiking

Interference impact on ISEs was also evaluated using interference spiking. Here, electrode response was measured in a 117 mg/L sodium chloride concentration (2 mM, 46 mg/L sodium, 71 mg/L chloride) with ISA, before spiking to adjust interfering ion concentrations in solution to the same level as would be present in nutrient solution (CHS1). The same was performed to adjust concentrations to half the levels present in nutrient solution. Concentrations the solutions were spiked to are described in table 3.4. Spiking was performed by addition of 100 µL of 200x or 100x CHS1 standards into 20 mL of 117 mg/L sodium chloride with ISA. The experiment was performed with possible interfering ions per electrode, meaning negative ions were tested for the chloride electrode, while positive ions were tested for the sodium electrode.

Conditions were chosen to indicate realistic electrode behavior in the presence of realistic interference concentrations. A 117 mg/L sodium chloride solution was chosen as a realistic baseline, for areas and conditions with relatively high salt concentrations. The electrode behavior was tested with 1x and 0.5x CHS1 concentrations to give an indication of electrode behavior in hydroponics, where the concentrations of nutrient ions can be halved over the growth period. ISA was also used to keep the ionic strength of solutions as stable as possible before and after spiking. In this experiment a deviation of more than 10% is assumed to show that interfering ions have a large impact.

The results of the interference spiking experiment vary per interference and per ISE. This experiment gives a much more intuitive look at the interference behavior of nutrients in solutions than the calibration curves. The results presented can only be used as an indication of behavior, however, and not a quantitative way of measuring and accurately predicting ISE behavior in the presence of interferences.

The results from the interference spiking experiment with the chloride electrode are shown in table 4.1.

Table 4.1: Results of interference spiking in solutions measured by the chloride electrode. The table shows measured chloride concentration before and after spiking to adjust interfering ion concentrations to 1x or 0.5x nutrient solution (CHS1) levels. The difference between the two values is presented as the relative deviation.

Interfrence	Pre-add[mg/L]	Post-add[mg/L]	Deviation[%]
KNO_3, 1x	52.2	58.7	12.5
KNO_3, 0.5x	57.1	61.4	7.5
KH_2PO_4, 1x	54.5	57.4	5.3
KH_2PO_4, 0.5x	54.5	55.7	2.2
NH_4NO_3, 1x	58.4	58.4	0
NH_4NO_3, 0.5x	55.4	56.6	2.2
$MgSO_4$, 1x	66.7	73.9	10.8
$MgSO_4$, 0.5x	67.1	69.5	3.6
Micronutrients, 1x	57.1	58.7	2.8
Micronutrients, 0.5x	58.7	59.7	1.7
CHS1, 1x	64.6	77.2	19.5
CHS1, 0.5x	65.7	72.1	9.7

The results shown in table 4.1 for the chloride electrode. The results presented here indicate a general trend of low interference, with most possible interferences resulting in a less than 10% change in the

measured chloride concentrations. The exceptions to this are however KNO_3, $MgSO_4$ and CHS1 nutrient solution.

The results for KNO_3 and $MgSO_4$ reinforce the findings from the calibration curve experiment, that nitrate and sulphate are the interfering ions with the largest impact on the chloride electrode. Nitrate gives the largest deviation with an increase of 12.5% at 1x CHS1 standards of KNO_3, and 7.5% at 0.5x standards of potassium nitrate. Sulphate increases the measured chloride concentration by 10.8% after spiking to the same concentration of magnesium sulphate as found in the nutrient solution. This was the second highest of individual nutrients, and indicates that sulphate will interfere with the measurement of chloride concentrations using the electrode. CHS1 solution gives a change 19.5% for 1x concentrations and 9.7% for 0.5x concentrations, the highest in the experiment for each spiking levels, indicating that all interfering ions contribute to the overestimation of chloride in solution.

All deviations in table 4.1 are positive, indicating that the chloride electrode will overestimate the concentrations of chloride in the presence of nutrients present in CHS1.

Spiking was also performed using the sodium ISE. Here the pH was adjusted using 25% aqueous ammonia before spiking, and the pH was measured using pH papers before and after. No appreciable difference in pH was observed after spiking the concentrations described in table 3.4, using 100 µL of solution. The results from interference spiking with the sodium ISE are presented in table 4.2 below.

Table 4.2: Results of interference spiking in solutions measured by the sodium electrode. The table shows measured sodium concentration before and after spiking to adjust interfering ion concentrations to 1x or 0.5x nutrient solution (CHS1) levels. The difference between the two values is presented as the relative deviation.

Interfrence	Pre-add[mg/L]	Post-add[mg/L]	Deviation[%]
KNO_3, 1x	43.9	34.5	-21.4
KNO_3, 0.5x	37.3	33.3	-10.7
KH_2PO_4, 1x	33.9	30.0	-11.5
KH_2PO_4, 0.5x	48.7	41.0	-15.8
NH_4NO_3, 1x	59	47	-20.3
NH_4NO_4, 0.5x	57.3	51.5	-10.1
$MgSO_4$, 1x	45.4	37.3	-17.8
$MgSO_4$, 0.5x	44.2	40.3	-8.8
$Ca(NO_3)_2$, 1x	42.1	38.0	-9.7
$Ca(NO_3)_2$, 0.5x	38.3	35.7	-6.8
Micronutrients, 1x	62.1	62.6	0.8
Micronutrients, 0.5x	59	57.4	-2.7
CHS1, 1x	52.6	41.5	-21.1
CHS1, 0.5x	49.4	43.1	-12.8

Table 4.2 showing the results for the sodium electrode indicate much larger deviations than the ones shown for the chloride electrode. Here multiple nutrients give deviations of >10%, such as potassium, ammonium and magnesium. The findings in table 4.2 indicates that potassium and ammonium will have the largest individual impacts on the sodium concentrations measured by the sodium ISE. This is indicated by the large deviations for KNO_3, where spiking to 1x CHS1 concentrations gave a decrease

in measured sodium concentrations of -21.4%, and spiking to 0.5x nutrient solution concentrations gave a deviation of -10.7%. Spiking with KH_2PO_4 caused a deviation of -11.5% and -15.8% for spiking to 1x and 0.5x CHS1 concentrations respectively. Ammonium is also shown to impact the sodium electrode, as spiking to 1x CHS1 concentrations gave a deviation of -20.3%, while spiking to 0.5x CHS1 concentrations gave a deviation of -10.1%. The results for ammonium are unexpected, as the HACH ISENa381 manual recommends ammonium hydroxide (aqueous ammonia) to adjust pH for samples[31].

Magnesium is also shown to have a large impact, as spiking to 1x magnesium sulphate concentrations gives a deviation of -17.8%. This along with the results for potassium support the results from the calibration curve experiment, where potassium and magnesium were found to have the largest impact on the sodium electrode.

The results for micronutrients deviates from the calibration curve experiment. Micronutrient spiking caused an increase in measured sodium concentration of 0.8% at 1x CHS1 concentration and a decrease in measured concentration of -2.7% at 0.5x CHS1 concentrations, having the lowest deviations in table 4.2. However the findings from the calibration curve experiment indicate that these should give a large deviation. Near all deviations in table 4.2 are negative, which indicates that all interfering ions in CHS1 nutrient solutions will have a negative impact on measured sodium concentrations, and that the sodium electrode will underestimate sodium concentrations in the presence of interfering ions.

The pH was not observed to decrease to an unacceptable level (< 9) after spiking for any samples in this experiment, but the possibility of a pH decrease impacting the results for the sodium electrode is still appreciable. An example could be for ammonium, which is shown to have a large impact in table 4.2, while manufacturer documentation indicates that it should not[31]. The result could be skewed as a result of buffering occurring with addition of NH_4NO_3, which could lead to a lower pH, and an increase in concentration of protons in solution. Table 3.2, of the selectivity coefficients provided in manufacturer documentation, indicates that hydrogen ions will have a large impact on sodium electrode measurements (K=20 at pH<9), which could explain the ammonium results presented here. This could have been quantified and established with the use of a pH meter in this experiment.

The results for both the chloride and sodium electrodes deviates from the selectivity coefficients provided in the manufacturer documentation. The given selectivity coefficients, provided in table 3.2, only indicate potassium as a possible interference in hydroponic solutions, while the results presented here, and in the calibration curve experiment, indicate that most nutrient ions will interfere with the measurements by the electrodes. ISA has also been used in all spiking experiments, in an attempt to maintain the same ionic strength across all samples, and as such changes in ionic strength are not assumed to cause the differences presented in the spiking experiment.

The method used here is a fast and efficient way of indicating which species and ions will have an effect on electrode behavior. The results presented here were quickly and easily compiled, and covered the range of interferences of interests in short time, especially compared to the recording of calibration curves for each interference. However, their use as other than an indication of interference in ISE measurements is dubious. These results show ISE behavior when interferences are spiked into synthetic solutions of sodium chloride with ISA, but not much can be extrapolated out of these conditions. More comprehensive, labor, and time-consuming methods must be used for results which can have a direct impact on quantitative measurements made later. An example of this would be to experimentally determine the selectivity coefficients of interfering ions in realistic conditions. This would however be more time and labor intensive, and would have to be repeated for ISE applications, as selectivity coefficients often are

condition dependent[33]. The spiking method employed here can however be used as a screening tool, indicating which ions can give the largest contribution to ISE interference.

4.3 Electrode behavior over a 12-day span of time

The electrode behavior over time was evaluated. This was done by measuring the electrode response, as relative concentration over time. A synthetic, lab prepared, nutrient solution (CHS1) containing 117 mg/L of sodium chloride was chosen as a preferred medium for testing over longer time. Before the experiment, two calibration curves were recorded for each electrode. At first a two point-calibration curve using 10 and 100 mg/L chloride standards was recorded. The resulting calibration curve for both the chloride (graph A) and sodium (graph B) electrodes are presented in figure 4.13 below.

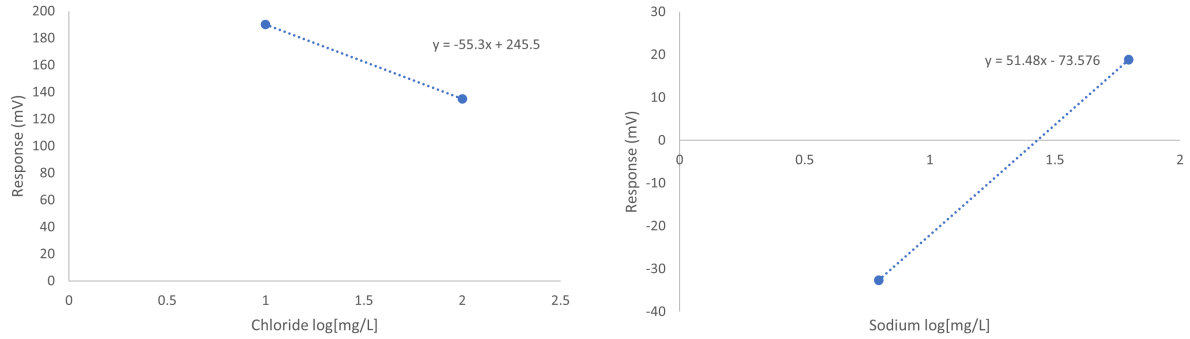

A B

Figure 4.13: Calibration curves recorded using 10 and 100 mg/L chloride standards with ISA, for the chloride electrode (A) and sodium electrode (B).

The calibration curves presented in figure 4.13 are used as a reference for the other calibration curves recorded during this experiment, both in nutrient solution and after end of the 12-day experimental period.

A second calibration curve was also recorded before the over time experiment. Here calibration curves using 10 and 100 mg/L chloride in CHS1 nutrient solution were used as standards. The resulting curves are presented in figure 4.14 below.

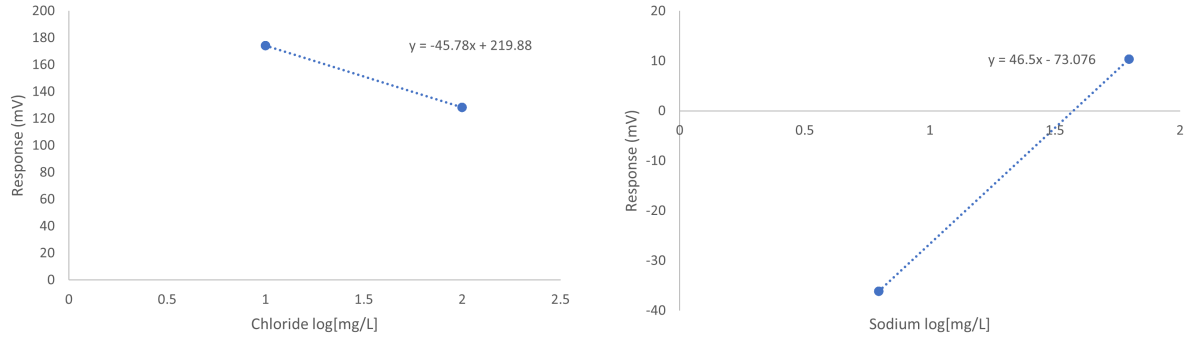

A B

Figure 4.14: Calibration curves recorded using 10 and 100 mg/L chloride standards in CHS1 nutrient solution, for the chloride electrode (A) and sodium electrode (B).

Figure 4.13 show the calibration curve of standards with ISA, while figure 4.14 shows the calibration curve of 10 and 100 mg/L chloride in CHS1 nutrient solution. This was a continuation of the experiments with interferences, to give a comparable idea to the results presented and discussed for the interference calibration curves and interference spiking experiments. The changes in the calibration curve slopes and

intercepts follow the same trends presented for the earlier experiments. For the chloride electrode, the slope increases while the intercept increases, as can be seen by comparing the graphs in figures 4.13 and 4.14. This is consistent with the previously discussed results, and shows that interferences present in CHS1 solution will interfere and compete with chloride on the electrode sensor surface, leading to a higher measured concentration, than actual concentration in solution. The slope increases by 17.8% from standards to nutrient solution, going from -55.3 to -45.78 mV per decade, which indicates that ions present in the CHS1 nutrient solution will have a rather large impact on the measurement of chloride concentration. This reinforces the findings in table 4.1, where the total CHS1 solution has the highest impact on the chloride electrode, with a 19.5% change.

The same can be said for the sodium electrode, where the same trend as previously observed continues. Both the slope and intercept decreases in CHS1 compared to the standards with ISA, as can be seen in figure 4.14, compared to figure 4.13. The intercept decrease is small (0.7% decrease), while the slope decreases from 51.48 to 46.5 mV per decade, a decrease of 9.7%. This also supports the findings in table 4.2, where CHS1 has the highest impact on the measured sodium concentration, with a change of -21.1% in measured concentration. The same is indicated here. The fact that the slope and intercept decreases also indicates that the measured sodium concentration will be lower than the actual concentration, further indicating that interferences lead to a decrease in measured sodium concentrations for the sodium electrode.

Immediately after the recording of the second calibration curves, the electrodes were cleaned and introduced to the Erlenmeyer flasks containing nutrient solutions (CHS1) with 117 mg/L sodium chloride. Both electrodes were left to record for 12 days. For the first two hours, measurements were made every minute, while for the rest of the experiment measurements were made every half hour. The recorded measurements were relative, and were collected directly from the internal measurements made by the logger(HACH HQ40d).

The aim of this experiment was to observe any drift in electrode measurements, and the reliability of electrode measurements over time. Synthetic (lab prepared) nutrient solution was used, in order to gain insight into electrode behavior in controlled realistic conditions of interfering ions, with no major outside influences to change concentrations in solution, like plant growth would in a hydroponic setup. The flasks were also closed with parafilm, to avoid evaporation and outside contamination. Over the time of the experiment no changes in volume were observed.

The relative concentrations were graphed as a function of time, along with the temperature of solution measured by the respective electrodes. The results presented here for the over time behavior only serve to indicate the behavior of electrodes, not present accurate measurements of the concentration in solution. The data graphed in figures 4.15, 4.16, 4.17 and 4.18 are the relative concentration measurement data from the electrodes, and are not accurate. The graphs still indicate how the behaviors behave in these conditions, and are as such valuable.

The experiment was observed several times over the 12-day time frame. One of the most important observations made was the presence of precipitation in the flask used for the sodium electrode after pH adjustments. The precipitation settled on the electrode after several days, and the electrode was shaken to remove buildup. Air bubbles were also observed on the chloride electrode early in the experiment. These were removed by gentle movement of the electrode, and were not re-observed over the 12 day period. Near the end of the experiment the light in the fume hood the setup was contained in was left on overnight and the following, due to an oversight. This happened on day 9, and was rectified by turning

off the lights on day 11.

Results for the chloride electrode are presented first. Figure 4.15 shows the relative concentration measured by the chloride ISE over the first two hours of the experiment. Measurements were made every minute. The blue line represents the recorded chloride concentration, while the orange line is the temperature measured by the electrode.

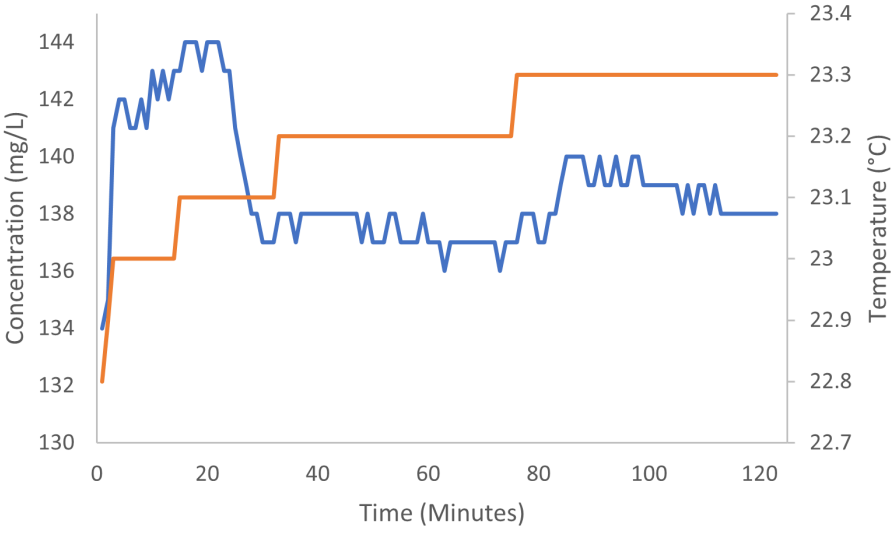

Figure 4.15: Relative chloride concentration(blue) and temperature(orange) measured over a two hour period, using the chloride electrode, presented as a function of time.

Over the two hour period, presented in figure 4.15, the chloride electrode recorded chloride concentrations with rather high precision. Over the two hour period, from the first to the final measurement, the recorded concentration increases by 3%. However, a clear stabilization period can be observed in the graph. Over the first 30 minutes the recorded chloride concentration increases rapidly, before stabilizing. In the first 30 minutes the recorded concentration remains at a level about 7.5% higher than after stabilization. The graph also shows many peaks, indicating changes from minute to minute of about 1 mg/L in measured concentrations. This indicates that the measurements are a little sporadic, over the entire period. This should however not have a significant impact on the measured concentration.

Figure 4.16 shows the ISE measured concentration and temperatures over the 12 day period. Measured temperatures are shown in orange, while recorded concentrations are shown in blue. Measurements were made every 30 minutes.

Over the 12-day period the chloride electrode shows significant drift. The recorded concentration stably increases after about 14 hours, and goes from about 135-140 mg/L in the first 12 hours, to around 260 mg/L at the end of the experiment. This represents an increase of about 86%. This indicates that the chloride electrode exhibits severe drift over a 12-day period, when left in the same solution. The drift also increases over time, as can be seen by the slope of the graph increasing over time, with the recorded concentration increasing faster after the 150 hour mark than before. The reason for this is unknown. The graph also shows that the electrode is seemingly impacted by the temperature of solution, with the recorded concentration decreasing with increasing temperature. This is evident in the region from 50 to 150 hours, and from 200 hours until the end of the experiment. Peaks in the measured temperature, indicating temporary increase in the solution temperature, have corresponding valleys in the recorded concentrations. This indicates that the electrode is susceptible to temperature changes.

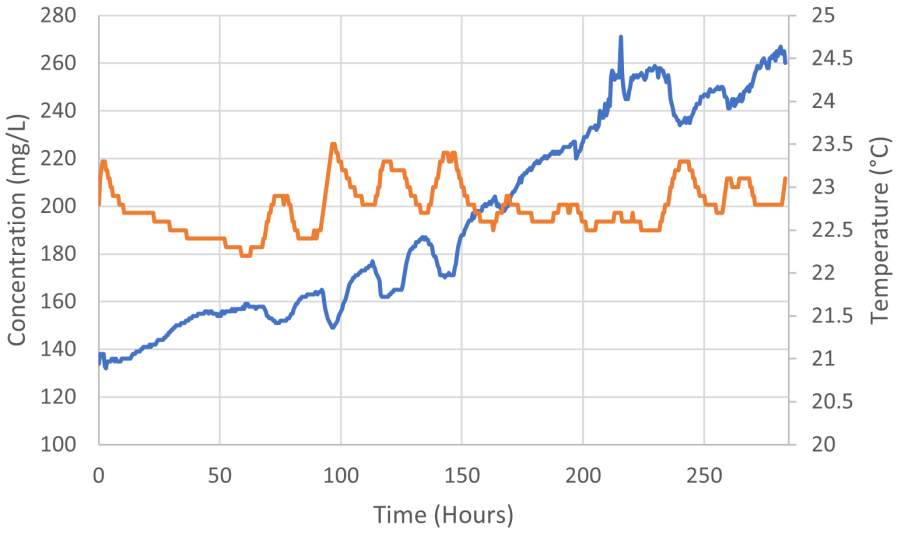

Figure 4.16: Recorded relative chloride concentration(blue) and measured temperature(orange) by the chloride electrode over a 12-day period.

The results for the sodium electrode are presented in figures 4.17 and 4.18. The measured concentration and temperature for the two first hours are presented in figure 4.17 below, where the relative measured concentration is represented in blue, and the measured temperature is represented in orange.

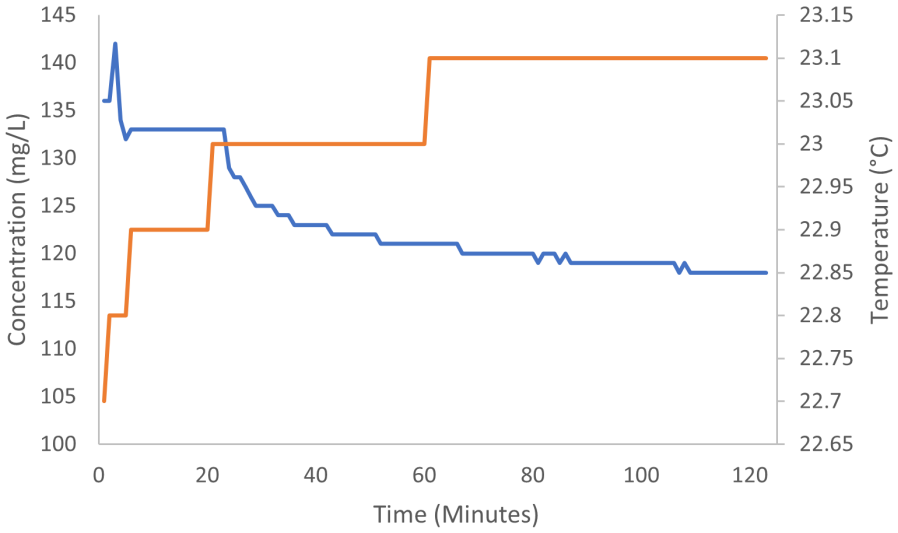

Figure 4.17: Relative sodium concentration(blue) and temperature(orange) measured over a two hour period, using the sodium electrode, presented as a function of time.

The sodium electrode shows larger measurement deviations over the two hour period than the chloride electrode, as can be seen in figure 4.17. From the first to the final measurement, the recorded concentration decreases by 13.2%. Over the experimental period a plateau in the recorded concentration is reached between 7 and 24 minutes, before it decreases until end.

The results for the entire 12-day period are presented in figure 4.18. Measured temperatures are shown in orange, while recorded concentrations are shown in blue. Measurements were made every 30 minutes.

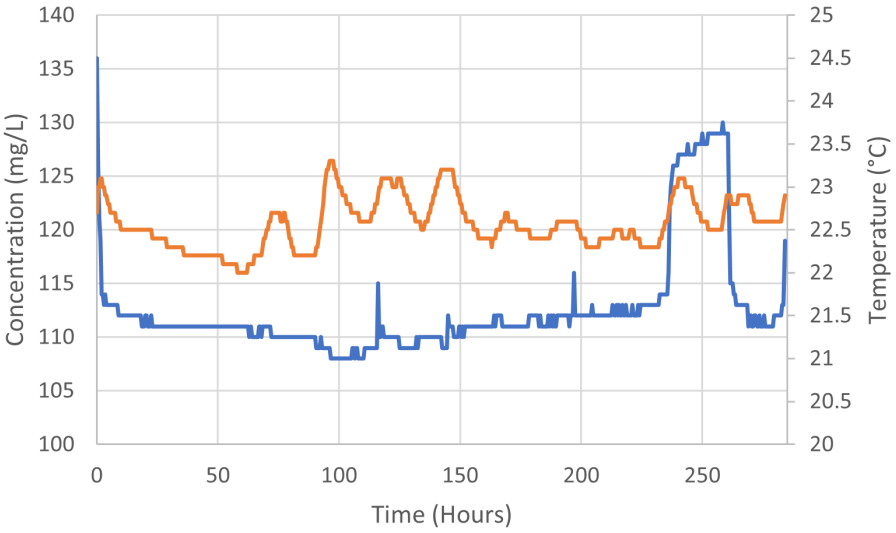

Figure 4.18: Recorded relative sodium concentration(blue) and measured temperature(orange) by the sodium electrode over a 12-day period.

As can be seen from the 12-day graph in figure 4.18, the sodium concentration recorded by the sodium electrode stabilizes at a lower level than initially recorded, and remains stable over the entire period. There are a few exceptions to this, but these can be explained by external factors. Sharp peaks are observed at 116 and 197 hours, which are the same times at which the electrode was gently rocked to remove precipitation settling on the electrode head. A temporary increase in recorded sodium concentration is also observed from 232 to 262 hours. This coincides with the time where the fume hood lights were accidentally left on. This could indicate that the electrode is impacted by light from external sources. The same can be the reason for the increase in the final measurement of the series, with the lights being turned on in the fume hood before the experiment was concluded. The sodium electrode shows no signs of being influenced by the changes in solution temperature observed, nor to have very large drift over a 12 day period. Drift is observed in the sodium electrode over the 12-day period, but to an appreciably lower extent than in the chloride electrode measurements. From the first to the last measurement the recorded sodium concentration decreases by 12.5%, but as can be seen from figure 4.18 these end point measurements are appreciably higher than most measurements over the period.

The electrical conductivity (EC) of the used CHS1 solution with 117 mg/L of sodium chloride was measured at the end of the experiment, using a WTW Multi 350i meter, with an EC electrode. Prepared, unused, solution was used as a standard, and measured to 1.352 mS/cm, while the solution used for the chloride electrode measurements measured to 1.464 mS/cm after the 12-day period. This represents an increase of about 8%. This means that the observed drift in the chloride electrode is not a result of concentration by evaporation.

After conclusion of the 12-day time period, new calibration curves were recorded, in order to check for drift. Two-point calibration curves using respective chloride and sodium standards were recorded. The calibration curves are presented in figure 4.19. Curve A shows the chloride calibration curve, while curve B shows the sodium calibration curve.

The post-experiment calibration curve was recorded in an effort to observe electrode drift. These are presented in figure 4.19, and compared to the pre-experiment calibration curves presented in figure 4.13.

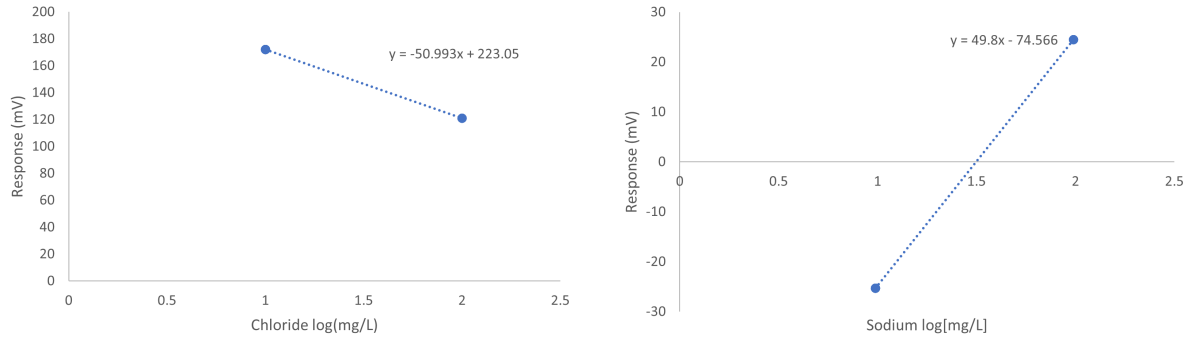

A B

Figure 4.19: Two-point calibration curves recorded after the 12-day period. 10 and 100 mg/L standards were used, with ISA. Curve A shows the chloride electrode calibration curve, while curve B shows the sodium electrode calibration curve.

The slope for the chloride electrode (Curve A, figures 4.13 and 4.19) increases by 7.8%, while the slope for the sodium electrode (Curve B, figures 4.13 and 4.19) decreases by 3.3%. This further reinforces the discussed results, with the chloride electrode showing an appreciable slope increase of 7.8%, indicating that the electrode experiences appreciable drift when kept in the same solution over a 12-day period. The sodium electrode shows a lower deviation between slopes at a decrease of 3.3%, indicating that it experiences little drift over a 12 day period in one solution.

4.4 Hydroponic samples

Two batches of samples from an experiment at NTNU Social Research CIRiS were analyzed using the sodium and chloride electrodes, and validated using IC (negatively charged ions) and ICP-MS (positively charged ions). These results are presented in this section.

The CIRiS experiment consisted of eight separate growth systems, where lettuce was grown in eight different nutrient solutions. Four of these nutrient solutions, experimental units 3, 4, 5 and 8, had increased sodium and chloride levels. Sodium and chloride stock solutions were added to these solutions to adjust the sodium and chloride concentrations to theoretical starting values of 115 mg/L of sodium and 135 mg/L of chloride. No additional sodium or chloride was added to nutrient solution from experimental units 1, 2, 6 and 7. Samples collected from nutrient solutions with elevated levels of sodium and chloride will be discussed as "high level" samples, while samples from solutions with unaltered sodium and chloride will be discussed as "low level" samples.

The first batch of samples were collected at the start of the hydroponic experiment at CIRiS, in November of 2021. ICP-MS samples were prepared at CIRiS, and about a liter of sample material was collected for ISE analysis. Sample material was collected from experimental units (EU) 2 through 8, with two individual samples collected for EU7, referred to as 7_1 and 7_2. IC samples were also collected from this sample material. The samples were analyzed in chronological order, working from the EU nomenclature used in the CIRiS experiment. The results of the chloride ISE analysis, and the concentrations of chloride in the sample determined by IC, with percentage deviations, are presented in table 4.3 below.

Table 4.3: Chloride concentrations determined using the chloride electrode and IC on the first batch of hydroponic samples collected in November 2021. The deviations of the ISE values from the IC values are also shown.

Sample	2	3	4	5	6	7_1	7_2	8
ISE [mg/L]	11.9	138.7	126.7	137.4	12.6	10.3	11	169.7
IC [mg/L]	22.2	124.4	125.7	129.6	22.4	22.1	22.7	127.7
Deviation [%]	-46.4	11.5	0.8	6	-43.6	-53.4	-51.5	32.9

Table 4.3 shows the results from the chloride analysis of the first batch of samples. Here the chloride ISE gives good results for most of the high level chloride samples, where sample 4 deviates <1%, while samples 5 and 3 are higher but still acceptable. The exception here is sample 8, which shows a deviation 32.9%. Here the chloride electrode overestimates the chloride concentration, compared to the IC determined concentration. The low level chloride samples however show a different trend. Here the electrode underestimates the concentration determined by IC by at least 40%, which is a significant underestimation. For the first batch the chloride electrode underestimates chloride concentrations at low levels, and overestimates it at high levels.

The same sample material from batch 1 was also used for sodium ISE analysis. The pH of these samples was adjusted to >9 using 0.5 mL 25% aqueous ammonia. As previously described precipitation was observed in all samples after addition of aqueous ammonia. The results of the sodium electrode analysis, and elemental sodium concentrations determined using ICP-MS, of the first batch of hydroponic samples are presented in table 4.4.

Table 4.4: Sodium concentrations determined using the sodium electrode and ICP-MS on the first batch of hydroponic samples collected in November 2021. The deviations of the ISE values from the ICP-MS values are also shown.

Sample	2	3	4	5	6	7_1	7_2	8
ISE [mg/L]	3.8	80.3	84	75.2	3.8	3.5	3.5	69.9
ICP-MS [mg/L]	9.4	134.9	134.2	134.7	9.1	9.4	9.4	134.7
Deviation [%]	-59.8	-40.5	-37.4	-44.2	-58.3	-62.7	-62.7	-48.1

The results for batch 1, presented in table 4.4, show a general trend of the sodium ISE underestimating the concentrations of sodium present in solution, compared to the levels determined using ICP-MS. The ISE measures concentrations of 37.4 to 62.7% less than the concentrations determined by ICP-MS. The results discussed for interferences earlier would indicate an underestimation, but these are much larger than expected, and much higher than reflected in the interference spiking experiment.

The results presented in tables 4.3 and 4.4 are also presented graphically in figure 4.20. In these graphs the concentrations determined by the ISEs are represented by the y-axis, and the results determined by the alternative methods are represented on the x-axis. Linear regression was also performed on the data, and a y=x curve was added for clarity.

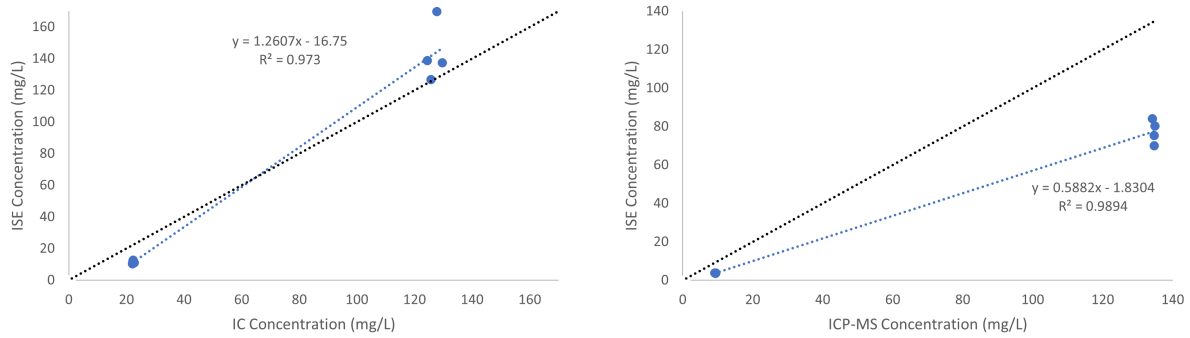

A B

Figure 4.20: Graphic representations of the ISE determined concentrations compared to the alternative methods on the first batch of hydroponic samples. Graph A shows chloride concentrations as determined by ISE and IC, while graph B shows sodium concentrations as determined by ISE and ICP-MS. Linear regression has been performed on both data sets, shown in blue with calculated slopes and intercepts, and the line y=x is graphed in black.

The graphs in figure 4.20 reinforces the results discussed for batch 1. Ideally the linear regression should coincide with the black line present in the graphs, at y=x. If the linear regression yielded a slope at the same point as the black line plotted, the electrodes and alternative methods would measure the same concentrations at 1:1. This would here be interpreted to indicate that the ISEs measured the correct concentrations. The chloride graph, curve A in figure 4.20, shows that the electrode underestimates the chloride concentration in low level samples, and overestimates in high level samples. The sodium graph (curve B, figure 4.20) shows that the electrode underestimates sodium concentrations in all samples, with the slope indicating that the electrode measures about half the concentration measured by ICP-MS. Determination coefficients can here indicate the precision of the ISE measurements. Here the chloride

graph shows less than ideal linearity at R^2=0.973. This reflects the relatively large spread in the chloride ISE concentrations.

A second batch of samples were collected at the end of the experiment, approximately 5 weeks after the start. This sample material was collected in December 2021, and frozen until January 2022. As previously mentioned the glass bottles used for sample material cracked during freezing. ICP-MS samples were collected before freezing and are as such unaffected. ISE and IC analysis was performed on frozen and thawed sample material, and could as such be affected, although there are no apparent indication of this being the case.

Samples analyzed using the electrodes, from the second batch of sample materials collected were not filtered or pre-treated, other than freezing and thawing before analysis.

Sample material was collected from all eight experimental units, EU 1 through 8, and were analyzed in the order described in section 3.5. The results of the chloride ISE analysis compared to the concentrations of chloride determined using IC is presented in table 4.5.

Table 4.5: Chloride concentrations determined using the chloride electrode and IC on the second batch of hydroponic samples collected in December 2021. The deviations of the ISE values from the IC values are also shown.

Sample	1	2	3	4	5	6	7	8
ISE [mg/L]	6	3.4	136.2	135.6	118.9	4.3	5.5	113.6
IC [mg/L]	11.6	9.7	85.7	98.7	88.2	10.7	9.9	84.3
Deviation [%]	-48.3	-64.9	58.9	37.4	34.8	-57.7	-44.3	34.8

The chloride ISE results for the second batch, presented in table 4.5, reflects the same trend as that for the first batch, but to a higher degree. The deviations in the high level chloride samples increase to at least 34.8%, where they reached a max level of 32.9% for the first batch. The Deviations reached as high as 58.9% for these chloride samples. The deviations for low level chloride samples also increase, with deviations between electrode and IC measurements, with a maximum deviation of -54% in table 4.3 to -65% in table 4.5. One of the factors that might impact these results are the potential presence of more contamination in these later samples, as a result of growth of algae, plant matter, debris etc. "dirtying" the water from the growing process. This would also explain why the deviations for the sodium electrode also increase, as will be discussed.

The sample material from batch 2 was also analyzed using the sodium electrode. As described earlier the pH was adjusted using 0.5 mL 25% aqueous ammonia, and precipitation was observed. The results of sodium ISE analysis, compared to the concentration of sodium determined using ICP-MS is presented in table 4.6.

The trend from the first batch carries over to the second batch for the sodium electrode as well. The results from the analysis of the second batch, presented in table 4.6, also shows that the sodium ISE underestimates the sodium concentrations in solution at all levels, compared to concentrations determined by ICP-MS. The deviations here are assumed to be because of the presence of high concentrations of interfering ions. As demonstrated in the interference calibration curve and spiking experiments, the presence of interfering ions leads to the sodium electrode underestimating the actual sodium concentration in solution. The results here show a significantly higher deviation than indicated by the spiking

Table 4.6: Sodium concentrations determined using the sodium electrode and ICP-MS on the second batch of hydroponic samples collected in December 2021. The deviations of the ISE values from the ICP-MS values are also shown.

Sample	1	2	3	4	5	6	7	8
ISE [mg/L]	5.7	3.9	66.4	71.5	62.8	4.7	3.7	68.8
ICP-MS [mg/L]	9.8	9.7	122.6	121.4	123.9	9.9	10.4	129.2
Deviation [%]	-41.5	-59.9	-45.9	-41.1	-49.3	-52.6	-64.5	-46.8

experiment, where the results from the spiking of CHS1 nutrient solution give a decrease in measured sodium concentration by 21.1%, whereas the lowest deviation recorded in real life hydroponic samples showed an underestimation of 37.4% compared to concentrations measured by ICP-MS. This shows that the interfering ions have a large impact on this electrode, as the nutrient solutions measured in the real life hydroponic samples are more concentrated than the CHS1 nutrient solution, as can be seen in the table presented in Appendix A.1.

As described with the first batch, the results from tables 4.5 and 4.6 are also presented graphically. Linear regression was also performed on both data sets. The results are shown in figure 4.21.

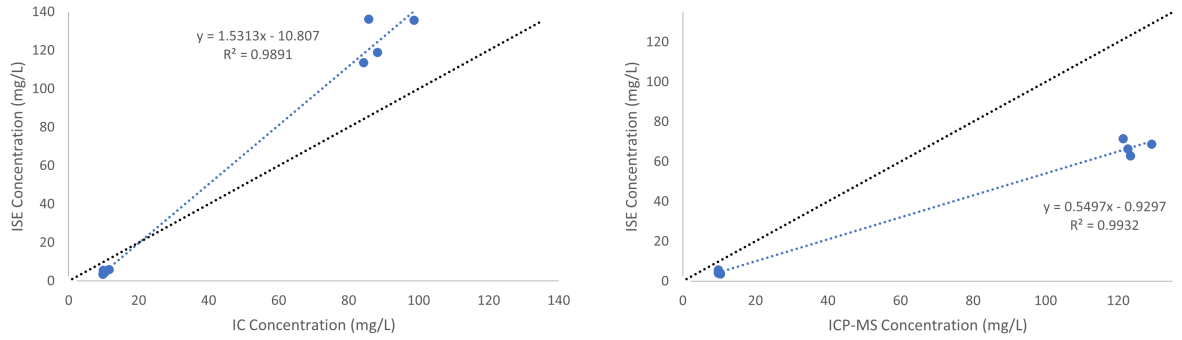

A B

Figure 4.21: Graphic representations of the ISE determined concentrations compared to the alternative methods on the second batch of hydroponic samples. Graph A shows chloride concentrations as determined by ISE and IC, graph B shows sodium concentrations as determined by ISE and ICP-MS. Linear regression has been performed on both data sets, shown in blue with calculated slopes and intercepts, and the line y=x is graphed in black.

The analysis of the second batch of hydroponic samples shows the same trends as the first batch, but to a larger degree. This is also reflected in figure 4.21. The slope of the chloride ISE-IC graph (curve A in figures 4.20 and 4.21) has increased from 1.2607 to 1.5313 mg/L measured by the electrode per mg/L measured by IC, with an increase in the deviations in the higher level chloride samples. the precision increased, as evident by the increasing slope coefficient from R^2=0.973 in curve A, figure 4.20 to R^2=0.9891 in curve A, figure 4.21. The slope for the sodium ISE-ICP-MS graph (curve B in figures 4.20 and 4.21) decreased from 0.5582 to 0.5497 mg/L measured by the electrode per mg/L measured by ICP-MS. The precision however increased, as can be seen by the determination coefficient increasing from R^2=0.9894 in curve B, figure 4.20 to R^2=0.9932 in curve B, figure 4.21.

The results here are also highly dependent on the calibration curve used. The results discussed here are

dependent on calibration curves recorded before measurements were made. However, for the second batch of hydroponic samples, a second calibration curve was also recorded at the end of the laboratory day, which gave a different curve than that recorded at the start. These results can be seen in Appendix A.3. Briefly summarized, the results using the second calibration curve, give lower deviations for the sodium ISE, ranging from -12.8 to -46.2%, which is better than the results presented in table 4.6. This is due to the second calibration curve for the sodium ISE being closer to the ideal of 59.2 mV per decade than the first calibration curve, which indicates that the sodium electrode is both impacted by the presence of interfering ions, but also indicates that the electrode is susceptible to drift or further conditioning during use, despite being conditioned overnight. Using the second calibration curve, the chloride ISE further underestimates concentrations in low level chloride samples, measuring down to -70%. This indicates that the second calibration curve is the result drift.

4.5 Flow cell experiment

4.5.1 Pump testing

The electrodes were tested in a real life hydroponic system, using an at-line solution consisting of two separate flow cells connected in series. Two cells were chosen due to the pH adjustments needed for the sodium electrode, and the effect this had on the chloride electrode, as shown earlier. Two flow cells were designed in cooperation with the NTNU Faculty of Science workshop, and were employed in a hydroponic system at NTNU Social Research CIRiS over a period of 4 weeks and 5 days. Issues related to drift, accuracy and biofouling were investigated.

Polyoxymethylene (POM) was chosen as the material for the flow cell structure due to it being structurally rigid and solid, while also remaining relatively easy to work with. The material is also chemically inert to several acids and bases, including ammonia. It is however not UV resistant[75]. The glue used on the cells did, however, not provide sufficient friction and several times the glued spigots were loosened or detached from the cell, and had to be re-glued before further use. This was especially a problem during flow cell setup and testing, and had to be remedied by further work at the workshop, where spigots and tubing were fused together and O-rings were fitted to ensure a tight fit

The time used for the Verdeflex pumps to exchange the solution in the two cells coupled in series was tested. The cells were filled with deionized water, before 100 mg/L potassium hydrogen phthalate (KHP) solution was pumped into the cells at one minute intervals. Stirring was induced in both cells using magnet stirrers. The content of each cell was analyzed using a Shimadzu UV Mini 1240 spectrophotometer at wavelength 254 nm after each minute interval, and compared to a 100 mg/L KHP sample. The results are presented in figure 4.22. The absorbance of solution in the first cell is presented in blue, while the second cell is presented in orange.

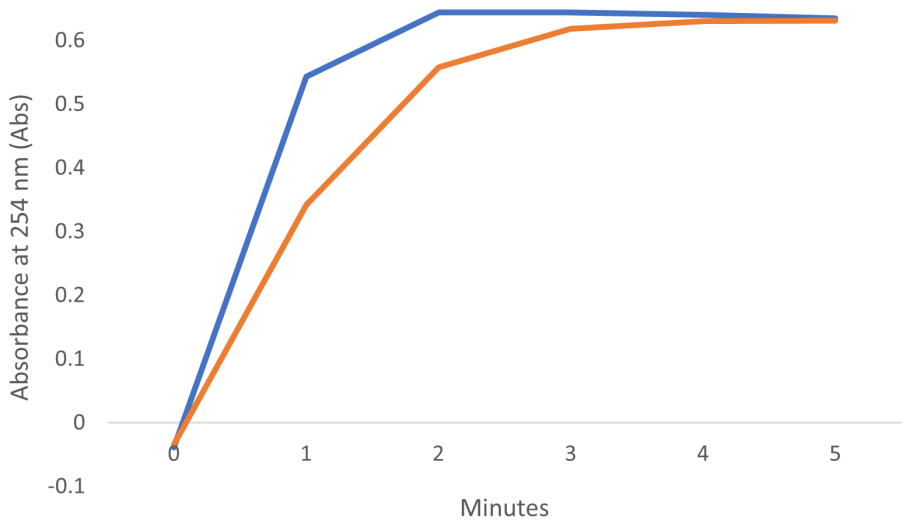

Figure 4.22: Graph of the measured absorbance, at 254 nm, of solution pipetted from cell 1 (blue) and cell 2 (orange) over five one minute intervals of pumping to exchange cell solution.

The spectrophotometer absorbance was set to zero using a deionized water sample before analysis. The absorbance of a 100 mg/L KHP standard sample was also measured, and found to be 0.641 Abs. After the duration of the experiment another sample of deionized water was measured, and found to have an absorbance of -0.036 Abs.

The time used for the pumps to exchange solution in both cells was important to the experiment, and was investigated, and are presented in figure 4.22. Only minute intervals were tested due to limitations with the digital plug through timers used, which could only be set to turn on and off at minute intervals. After two minutes the absorbance of solution collected from the first cell deviated by less than 0.5% from the absorbance of the KHP standard. After 4 minutes the absorbance of solution from cell 1 deviated by 0.2%, while the absorbance of solution from cell 2 deviated by 1.7% from the KHP standard. Complete exchange of solution was as such expected to occur after 4 minutes. Measurements were also made after five minutes, where the deviation for the first cell increased to 0.9%, while the deviation for the second cell decreased to 1.6%. The increase in deviation in the first cell is expected to be due to instrumental deviation in the Shimadzu UV Mini 1240 spectrophotometer used. The spectrophotometer was left to heat up for 15 minutes before use, but this could have been insufficient. This could also explain the discrepancy between the measurements performed on DI water samples. The absorbance of DI water was set to zero, but when the absorbance of a DI water sample was recorded after the experiment it was found to have -0.039 ABS.

4.5.2 Experiment results

The two flow cells were transported and set up with the chloride and sodium electrode as described in Materials and Methods, section 3.6.2. The Verdeflex pumps were used to introduce the "waiting solution" (10 mg/L sodium, 17 mg/L chloride standard with ISA) and hydroponic nutrient solution at desired timings. Nutrient solution was set to be introduced to the cells at two times per week, Mondays at 07:00 a.m. and Thursdays at 07:00 a.m., while the waiting solution was introduced to the cells on Mondays and Thursdays at 11:00 a.m. The pumps were set to run for four minutes at each introduction of solution, to ensure complete exchange in both cells. The described process of introduction of nutrient solution into cells for electrode analysis will be referred to as electrode sampling, or ISE sampling, from now on.

The sampling process occurred as described for most of the experimental period, with three exceptions. On the second day of the experiment, Friday the 22nd of April, electrode sampling was started at 07:00 a.m. and concluded at 11:00 a.m. Sampling was not induced on the first day of the experiment, Thursday the 21st, due to an error with the timer used for the nutrient solution pump. The experimental setup was also altered from the first to the second day of experiment, as described in Materials and Methods, section 3.6.2. With the change in the setup the pumps were set to run for one minute extra at each exchange of solution. The second deviation from the described process occurred on Thursday the 19th of May. On this day significant growth was observed on the chloride electrode after the electrode sampling and analysis from 7 a.m. till 11 a.m. The electrode was cleaned, and new sampling and analysis was initiated from 2 p.m. till 6 p.m. on the same day. These two samples are referred to as sample 9 and 10. Only one IC and ICP-MS sample was collected this day. On the final day of the experiment, Monday the 23rd of May, sampling occurred from 7 till 11 a.m. A little growth was however observed on the chloride electrode, and as such new sampling was performed. The electrode was cleaned, and one liter of hydroponic nutrient solution was reserved, and introduced into the cells by pumping. New measurements were repeated from 12 p.m. till 2 p.m.

The flow cell experiment was set up and conducted in a climate-controlled room at NTNU Social Research CIRiS, from the 20th of April until the 23rd of May. Over this period salad was grown in a hydroponic system, using nutrient solution. For the first five days of the experiment, spanning samplings 1 and 2, no nutrients were added to hydroponic solution, and only tap water was used. As the planted seeds sprouted nutrients were added on the fifth day, and the nutrient concentrations in solution was adjusted to the levels described in figure 2.2. After a week, spanning samplings 2 and 4, the sodium chloride concentration of the nutrient solution was adjusted to 292 mg/L (5 mM; 115 mg/L sodium, 117 mg/L chloride). After another week, spanning samplings 5 and 6, he sodium chloride concentration was increased, and adjusted to 877 mg/L (15 mM, 345 mg/L sodium, 532 mg/L chloride). After this the nutrient solution was not adjusted for the remainder of the experiment. Samples 1 and 2 do as such provide an indication of electrode behavior with low sodium and chloride levels, as well as low levels of interfering ions. 3 and 4 were recorded after addition of nutrients, and provide information on electrode behavior in conditions with low analyte ions, and relatively high concentrations of interfering ions. Before samples 5 and 6, sodium chloride levels were adjusted to a "medium" level, and provide insight to electrode behavior where analyte concentrations are about the same as concentrations of interferences. After sample 6 the sodium chloride concentrations are adjusted to a high level, and provide information on the behavior of electrodes in a solution where analyte ion concentrations are higher than interfering ion concentrations.

In an effort to discourage growth of biofilms and biofouling of sensors in this experiment, the tubing

and cells carrying the hydroponic solution were either dark or darkened before use. This was also one of the reasons for POM being the material of choice for the flow cells used. The use of dark tubing can be regarded as successful, as no growth or biofilm formation was observed on the inside of the tubes used in the experiment. Both electrodes were inspected for growth and biofouling on a weekly basis. The electrodes were extracted from their cell, inspected visually and images were taken of each cell tip. This occurred on Thursdays after electrode sampling and measurements. In cases where growth on the electrodes was observed, the electrode was cleaned and sampling and measurements were repeated on the same day. The electrodes were also inspected, and images were taken, on the final day of the experiment.

Images of the chloride electrode are presented in figure 4.23. The images are labeled 1 through 5, and are presented in chronological order. 1 through 4 have been captured after 1, 2, 3 and 4 weeks have elapsed, respectively, while 5 has been captured at the conclusion of the experiment. Significant growth of biofilm can be seen in image 4, figure 4.23.

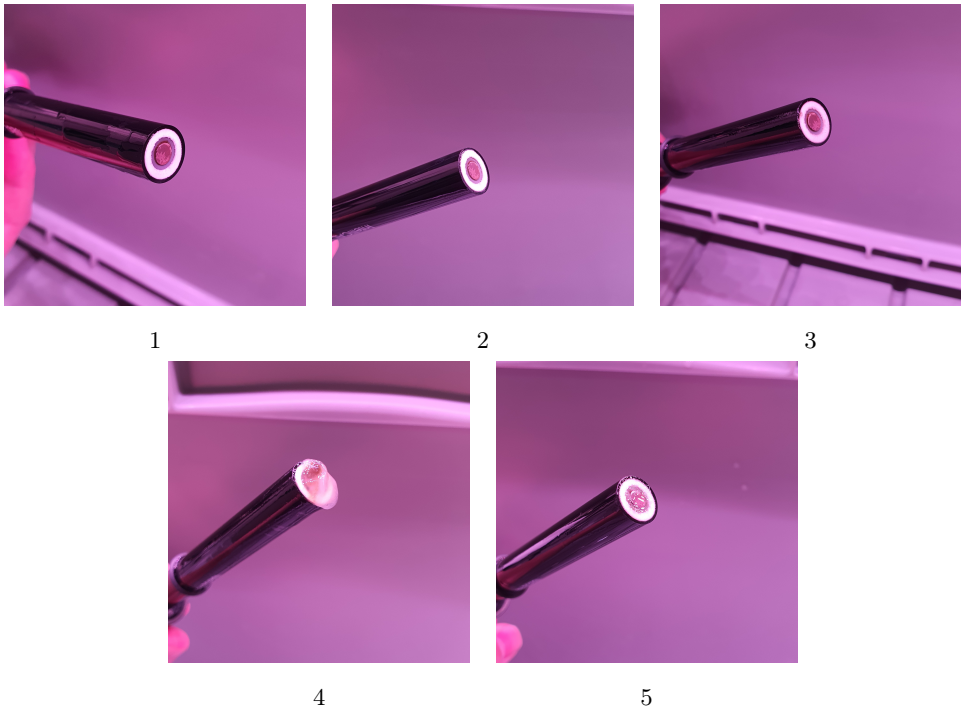

Figure 4.23: Images of the chloride electrode over the duration of the flow cell experiment. Images 1 through 4 have been captured after as many weeks had elapsed, while image 5 was captured at the experiment conclusion.

Using dark and opaque cells was as such not enough to discourage growth in the cells themselves. As can be seen in image 4 figure 4.23, significant growth occurred in the primary cell housing the chloride electrode. Growth was observed on the electrode, but was also found in the cell itself at the conclusion of the experiment.

Images captured of the sodium electrode are presented in figure 4.24. Images are labeled as described for figure 4.23. No growth was observed on the sodium electrode over the experiment duration.

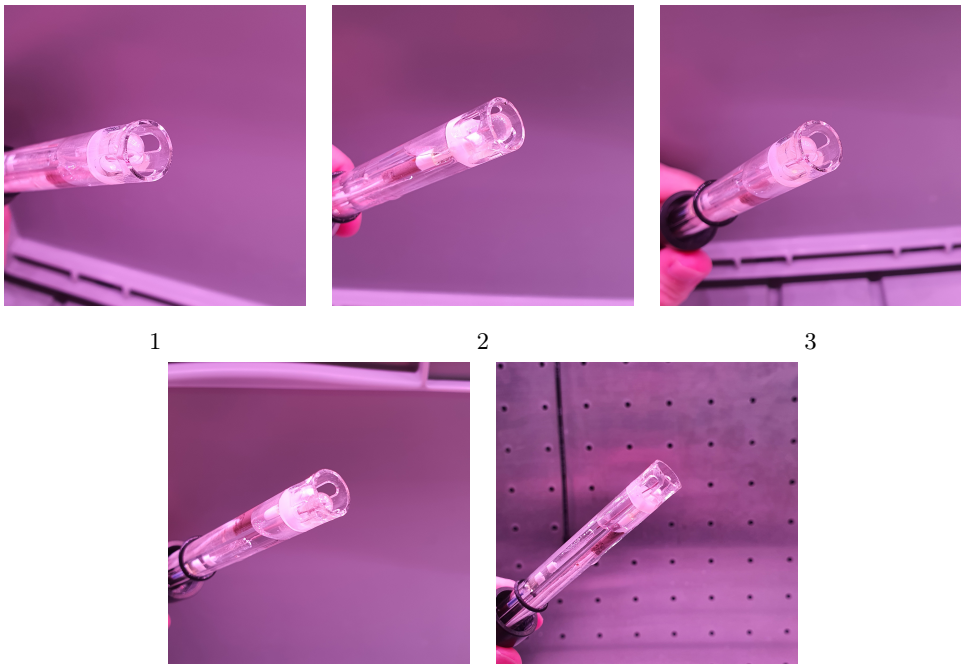

Figure 4.24: Images of the sodium electrode over the duration of the flow cell experiment. Images 1 through 4 have been captured after as many weeks had elapsed, while image 5 was captured at the experiment conclusion.

As can be seen in figure 4.24, no growth was observed on the sodium electrode. No growth was observed in the second cell either. This is likely due to the addition of 10 mL 2.5% aqueous ammonia, which adjusted the pH in cell >9, which would create a hostile and inhospitable environment, discouraging biofilm formation. Precipitate was however observed in the collected waste from the experiment. The second cell was not inspected for precipitate during the experiment duration, and precipitate was not observed in the cell after the experiment.

The concentrations of chloride and sodium measured by the electrodes was recorded and graphed for the entire experiment period. Figure 4.25 shows the concentration of chloride(blue) and temperature of solution(orange) measured by the chloride electrode over the experimental period.

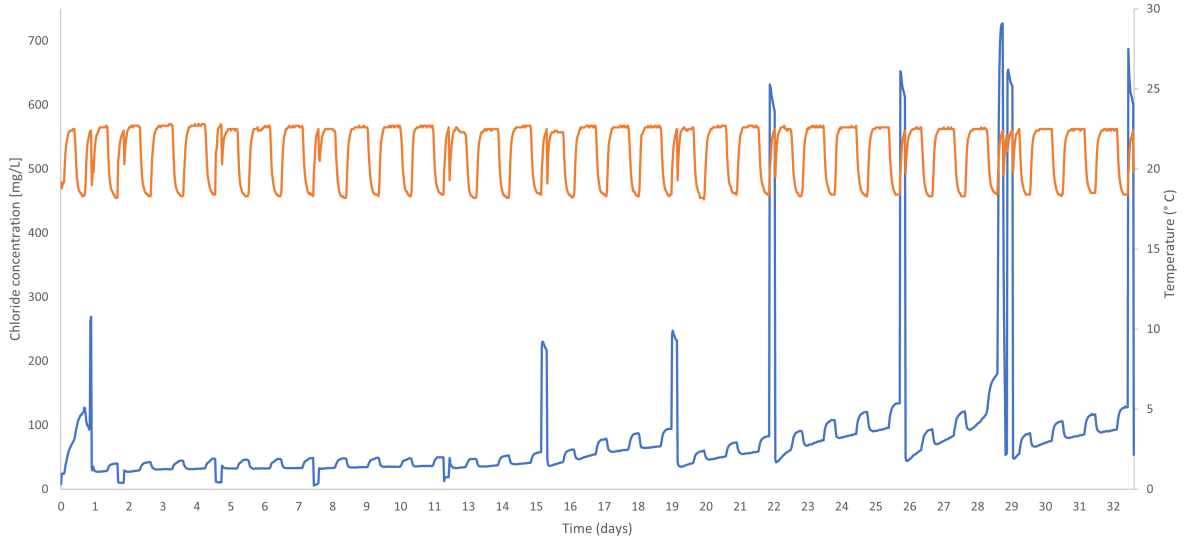

Figure 4.25: Graph of the chloride concentration(blue) and temperature(orange) measured by the chloride electrode in the flow cell experiment.

The results for the chloride electrode over the duration of the experiment are presented in figure 4.25. On the first day of the experiment an error in the setup was discovered. No sampling was done, and it was discovered that pH adjusted sample flowed back from the second cell with the sodium electrode, into the first cell containing the chloride electrode. This can be seen in graph 4.25, where the readings from day 0 to day 1 are elevated and erratic. This was remedied by elevating the first flow cell, and implementing a new joint in the tubing between the cells, as can be seen in figure 3.3. The inclusion of a new joint would also cause a loss of pressure between over the connection between cells, which was remedied by increasing the interval of pumping to exchange cell solutions from four to five minutes. This was kept for the duration of the experiment, and was not shown to have a negative impact on the exchange of solution in either cell.

Over the experimental period the chloride electrode drifts, as can be seen between samplings in figure 4.25. Between samplings and sample measurements the measured chloride concentration in waiting solution increases. This is especially evident after adjustments of sodium chloride levels in the nutrient solution, and can be seen after day 15 in figure 4.25. Whether this drift is a result of electrode use over time, or the result of impact from measurement of high concentrations samples is not known. The shown drift is however appreciably higher than observed in the 12 day experiment, with the measured chloride concentration in the prepared "waiting" solution increasing by 158% from day 29 until day 32.

The results in figure 4.25 also indicate that the chloride electrode is affected by fluctuations in temperature, as can be seen by the spikes in measured chloride concentrations between samplings. These reflect the drops in temperatures measured at the same time.

The measured concentrations of chloride in the hydroponic solution are presented in table 4.7. The concentrations measured using ion chromatography on samples collected the same day are also presented in the table, and the relative deviation between IC and electrode determined concentrations are shown.

Table 4.7: Concentrations of chloride in hydroponic solution determined by the chloride electrode and IC at each sampling during the flow cell experiment.

Sample	1	2	3	4	5	6	7	8	9	10	11	12
ISE [mg/L]	10.1	11	7.3	17.7	224	238.6	609.4	630.3	686.8	641.7	629.4	611.8
RSD_{ISE}[%]	4.1	4.1	15.9	11.3	2	2.2	2.3	2.2	8.2	1.4	4.3	1.4
IC [mg/L]	6.5	6.5	11.2	12.2	161.8	160	446.5	459	465.7	465.7	477.4	477.4
ISE/IC Deviation [%]	55.4	69.2	-34.8	45.1	38.6	49.1	36.5	37.3	47.5	37.8	31.8	28.2

Samples 1 and 2 in table 4.7 provide an indication of the chloride electrode behavior in samples of low ionic strength, and with relatively low concentrations of interfering ions. The electrode measures inaccurate concentrations, and with higher than ideal RSD. After addition of nutrients the chloride electrode accuracy declines, while the RSD of measurements skyrocket, as can be seen in samples 3 and 4 in the same table. This further underlines that the chloride electrode is impacted by interfering ions, especially when chloride concentration $<$ interfering ion concentrations. After adjustments to higher chloride concentrations (samples 5 through 12, table 4.7) the electrode generally overestimates the chloride concentration in solution compared to IC, but the RSD of the measurements remains rather stable and low, at $<$2.5% for almost all samples 5 through 12, except for samples 9 and 11, which will be discussed separately. The deviations between chloride concentrations measured by the electrode, and those determined by ion chromatography are substantial over the entire experiment duration. Even in conditions which should favor electrode accuracy, with higher concentrations of analyte than interfering ions (samples 7 through 12) the deviations are between 28 and 47%. Deviations here are lower than for low chloride concentrations (samples 1 through 6), as nutrient concentrations are expected to decrease over time, as the lettuce absorb nutrients to grow. Samples 6 and 7 deviates from this however. While the chloride concentration more than doubles, the deviation between ISE and IC measurements decrease by 13%. This is not to be expected according to interferences behaving as described by the Nichloskii-Eisenmann equation, where interference influence is assumed to be linear with concentration of interference and analyte. Assuming constant interference concentration between samples 6 and 7, the deviations should decrease by more than 13% as chloride concentrations increase. In real life the concentration of interferences decreased between these two sample points, rather than remaining constant. This indicates that the deviation between IC and ISE measurements can not only be explained by interfering ions, but other factors must also be contributing.

As discussed earlier significant growth was observed on the chloride electrode after four weeks had elapsed. This was observed after sample 9 had been collected and measured by the electrode. Sample 9 in table 4.7 was measured to the highest chloride concentration in the experiment, at 686.8 mg/L (7% higher than sample 10, measured on the same day). Sample 9 also had the highest RSD (8.2%) and deviation from IC measurement (47.5%) of samples measured after the final sodium chloride adjustment (samples 7 through 12). Both the elevated chloride measurement, RSD, and deviation between ISE and IC measurements, can be due to biofouling of the electrode sensor surface. A second measurement was initiated using the same conditions on the same day, sample 10 in table 4.7, which measured lower ISE concentrations, RSD and deviations from the IC measured concentration (ISE/IC deviation decrease of 10%). The same is the case between measurements 11 and 12 in the same table, where a little growth was observed after sample 11 measurements. Cleaning of the electrode gives higher accuracy and precision, and illustrates the need for successful anti-biofouling measures before ion selective electrodes can be implemented in

hydroponic systems.

The results of the IC analysis of samples of hydroponic nutrient solution are also presented in table 4.7. The results indicate that the concentration of chloride increases over time, from sample 7 to 12. This is unexpected, as the concentration of chloride in solution is expected to drop over the experiment duration, as chloride is absorbed by plant roots as nutrients. An expected drop in chloride concentration over time in hydroponic solution is reflected in the results from the IC analysis of hydroponic samples collected from CIRiS in November and December 2021, as presented in tables 4.3 and 4.5. The reason for deviations between the two experiments are unknown.

As established earlier the sodium electrode is susceptible to influence from hydrogen ions. As such the pH of samples for sodium analysis had to be adjusted to pH>9. During the flow cell experiment this was achieved by addition of approximately 10 mL of 2.5% aqueous ammonia to the approximately 100 mL of sample analyzed by the sodium ISE. This introduced problems for the overall setup, as ammonia, both in gaseous and aqueous form, can be detrimental to plant health. Due to this the container with the ammonia solution had to be kept in a separate room, and the solution used for sampling could not be reintroduced into the hydroponic system. Over the duration of the experiment this meant a volume of approximately 10 L hydroponic solution had to be discarded, and the hydroponic system had to be refilled several times. In real life applications this process should be reconsidered, especially in systems where the circular nature of hydroponics is of value.

Figure 4.26 shows the concentration of Sodium(blue) and temperature of solution(orange) measured by the sodium electrode over the experimental period.

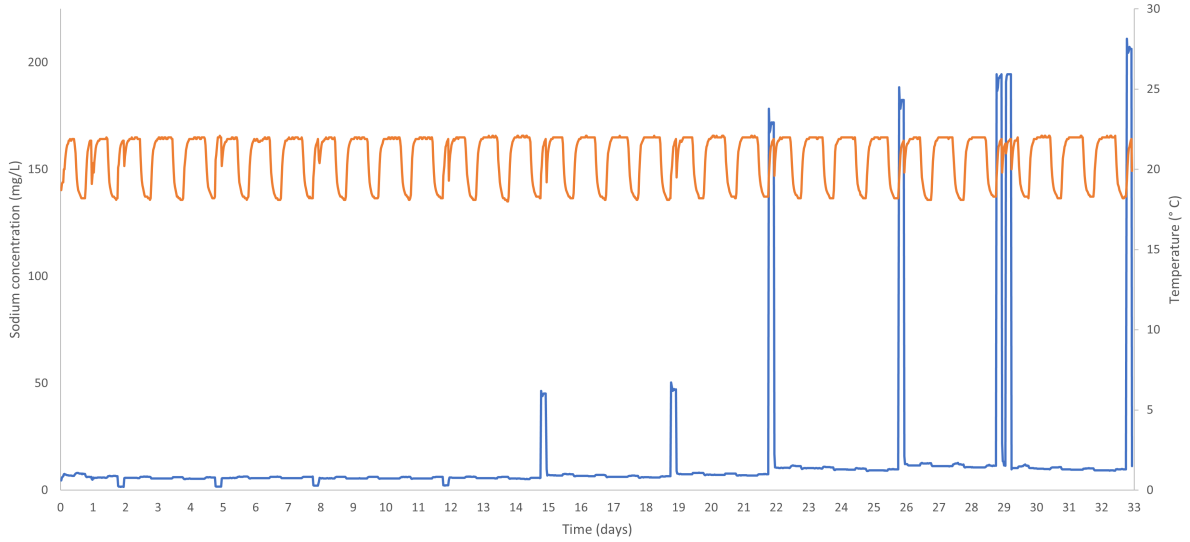

Figure 4.26: Graph of the sodium concentration(blue) and temperature(orange) measured by the sodium electrode in the flow cell experiment.

The sodium electrode also exhibited drift over the experiment duration, as shown in figure 4.26. The baseline readings from the 10 mg/L sodium standard increase after day 15, and especially after each sampling after sample 5. The increase in measured concentration over this period can be contributed to electrode drift, but could also be the result of incomplete exchange of solution in the second cell.

The measured concentrations of sodium in the hydroponic solution are presented in table 4.8 below. The concentrations measured using ICP-MS on samples collected the same day are also presented in the

table, and the relative deviation between ICP-MS and electrode determined concentrations are shown.

Table 4.8: Concentrations of sodium in hydroponic solution determined by the sodium electrode and ICP-MS at each sampling during the flow cell experiment.

Sample	1	2	3	4	5	6	7	8	9	10	11	12
ISE [mg/L]	1.8	1.8	2.3	2.4	50.1	52.7	190.4	202.4	214	215.5	229.4	230.4
RSD_{ISE}[%]	7.1	3.9	1.6	2.3	1.5	2.5	1.8	1.5	1.4	0.6	1.0	1.3
ICP-MS [mg/L]	3.8	3.8	6.9	7.0	107.8	111.3	323.2	343.5	349.4	349.4	351.1	351.1
ISE/ICP-MS Deviation [%]	-53.1	-53.1	-66.6	-65.9	-53.5	-52.7	-41.1	-41.1	-38.7	-38.3	-34.7	-34.4

Table 4.8 show the sodium concentrations in hydroponic nutrient solution measured by the sodium ion selective electrode over the duration of the flow cell experiment. Samples 1 and 2 show a baseline of electrode behavior in low sodium, low interference environments. The electrode measures low sodium concentrations, compared to ICP-MS, and high RSD for both samples. This could indicate that the sodium electrode needs adjustment of the ionic strength to measure accurate analyte concentrations in solution. No ISA was added for samples in this experiment, which could be a possible source of error in measurements. The deviations from the ICP-MS measurements also indicate this, as the sodium electrode measures 53.1% less sodium in solution than ICP-MS. Sampling for samples 3 and 4 occurred after addition of nutrients to solution, and provide insight into the accuracy of the sodium electrode in solutions with low analyte concentrations, and, relatively, high concentrations of interfering ions. The sodium electrode measures 66% less sodium in solution compared to ICP-MS for both sample 3 and 4, which indicate underestimation of the sodium concentration due to the presence of interfering ions, compared to the baseline tap water measurements in samples 1 & 2. Samples 5 and 6, where sodium chloride concentrations were adjusted to 292 mg/L show deviations of -53.5% and -52.7% respectively, between the concentrations determined by ISE and ICP-MS. This is possibly due to the presence of interfering ions, where the concentration of analyte is about the same as interferences. The deviations are lower than those for samples 3 and 4, which is as expected, as the sodium concentrations are higher compared to the interfering ion concentration in these samples. For samples 7 to 12 the deviations are even lower compared to samples 5 & 6. The deviations for samples 7 through 12 are less than -40%, decreasing over the sample series, from -38.7% for sample 7 to -34.4% for sample 12. This is as expected as sodium concentrations here are higher than the concentrations of interfering ions, meaning the impact of interferences are lower than for samples 5 and 6. With the exception of samples 1 and 2 the RSD values presented in table 4.8 are low, and indicates that the sodium electrode makes precise measurements, while exhibiting low accuracy.

The concentration of sodium and chloride increases over time, after the final adjustment before sample 7, as confirmed by ICP-MS and IC results in tables 4.8 and 4.7 respectively. Both concentrations are expected to decrease over the experimental period, but the increasing concentration can be a result of accumulation, and concentration by evaporation.

The calibration curves used for the flow cell experiment can be found in appendix A.4, figure A.6. The electrodes behavior over a 4 hour period in 100 mg/L respective sodium and chloride standards was also recorded, and can be found in figure A.7. The findings from figure A.7 indicted that the electrodes would measure a stable level of analyte after about 45 minutes, and for the 4 hour duration. This was used to determine the time of hydroponic nutrient sampling in the flow cell experiment. Data recorded at the first 45 minutes was discarded when calculating the mean concentrations found in tables 4.7 and

4.8, but are present in figures 4.25 and 4.26. Both the calibration curves and electrode behavior was recorded two days before experiment start at CIRiS. This could possibly introduce an error, as 50 hours elapsed between the recording of calibration curves and the continued use of electrodes. Alternatively calibration should be performed on-site, and in-situ, when possible for future implementations of ISEs in hydroponic systems.

5 Further Work

ISE applications in hydroponics show promise of possibly being a way to monitor and regulate nutrient solutions, both in terrestrial and extraterrestrial applications. For that, however, further research into the material presented in this thesis, as well as the refinement of it's ideas would be in order.

Before successful integration into existing systems, the sodium and chloride electrodes must be investigated further. Both show signs of being susceptible to interferences, and the influence of interfering ions to a larger degree than suggested by the manufacturer. Determination of the selectivity coefficients for the interferences with the largest impact would be recommenced, such as potassium and magnesium for the sodium electrode, and nitrate and sulphate for the chloride electrode. Experimentally determining the selectivity coefficient, rather than relying on manufacturer information, would give better understanding of the electrodes, their behavior in the presence of interferences, and enable more accurate measurements.

Another area of interest before ISEs can be fully implemented in hydroponic systems would be the lifetime of electrodes. Thorough investigation of the lifetime of sensors should be considered, in order to evaluate whether replacements would be needed after use over longer periods of time.

Biofouling of electrodes would also need to be combated before their use can be guaranteed. Investigations into anti-biofouling measures that would have negligible or zero impact on the plants grown in hydroponic systems are needed. A possible solution would be the implementation of UV-sanitization of hydroponic solution before introduction to cells for measurements. At-line UV-sanitization, hypothetically situated between the hydroponic system and electrodes, could kill algae and bacteria which would lead to biofouling and form biofilms, and could have negligible impact on either measurements or plants. Other methods should also be evaluated.

pH adjustment in the sodium electrode cell negated biofouling here, but the use of an electrode requiring adjustments of solution should be evaluated. Such adjustments would increase the amount of "moving parts" in a total implementation, and would possibly require more maintenance. The ability of such a system to be truly "closed-loop" would also have to be evaluated. In this experiment the addition of aqueous ammonia to adjust pH meant that nutrient solution used for analysis had to be discarded, instead of being reused. In applications where the possible circular nature of hydroponics is important, alternative electrodes that do not require pH adjustments should possibly be considered.

Further refinement of the cell design and implementation used is also of interest. Reduction of cell volumes, and the introduction of inter-cell pumps to move solutions could be considered. This would streamline the cell sampling, and lead to a lower total volume used, which could in turn lead to sampling frequency being increased. An implementation of calibration in the at-line sampling setup would also be beneficial, to eliminate drift.

This system should also be applied "in total", for accurate measurements. Methods to monitor other nutrients could be use to increase accuracy in measurements for sodium and chloride, by reducing the impact of interfering ions.

The implementation of sodium and chloride electrodes as early warning systems should also be investigated, in order to combat accumulation of e.g. sodium, and avoid displacement of other, vital, nutrients in plant availability, which could have detrimental impact on plant health.

Sodium and chloride are important parameters in specialized hydroponic systems, such as aquaponics or

extraterrestrial applications, and methods for monitoring these should be considered an important area for further investigations.

6 Conclusion

The electrodes evaluated are impacted by interfering ions present in hydroponic solutions. For the chloride electrode, the main interfering ions were determined to be nitrate and sulphate, while potassium and magnesium were found to be the main interferences for the sodium electrode. Most ions present in hydroponic solutions were however shown to be interfering with measurements for both electrodes. Interferences were determined by recording calibration curves in the presence of possible interfering ions, and by an experiment where sodium chloride solutions were spiked with possible interferences. Results indicate that the chloride electrode would overestimate the concentration of chloride in solutions with interfering ions present, while the sodium electrode would underestimate the concentration of sodium in solutions with interfering ions. The electrode behavior over time was also evaluated, and the chloride electrode was found to drift significantly over a 12 day period, while the sodium electrode exhibited less drift.

The electrodes were also used to analyze the chloride and sodium concentrations in hydroponic nutrient solution samples. The sodium electrode underestimated sodium concentrations in all samples, compared to concentrations determined using ICP-MS. The chloride electrode underestimated low chloride concentrations, and overestimated high chloride concentrations in hydroponic samples, compared to concentrations determined using ion chromatography.

An experimental setup for sampling and analysis of nutrient solution in a hydroponic system was developed and tested. Over the experiment, both electrode exhibited drift. The chloride electrode overestimated chloride concentrations while the sodium electrode underestimated sodium concentrations, compared to concentrations determined using IC and ICP-MS respectively. Biofouling was observed on the chloride electrode after 4 weeks of the experiment had elapsed. No biofouling was observed on the sodium electrode, possibly due to pH adjustments made to the sodium electrode samples.

In order to increase the accuracy of measurements made by both electrodes a new approach must be devised and implemented. Experimentally determining the selectivity coefficients of interfering ions for both electrodes is recommended. Implementation in tandem with other monitoring methods for main interferences should also be considered, as it would enable the correction of measurements made by the sodium and chloride electrodes.

References

[1] Silje A. Wolff, Liz H. Coelho, Irene Karoliussen, and Ann-Iren Kittang Jost. Effects of the Extraterrestrial Environment on Plants: Recommendations for Future Space Experiments for the MELiSSA Higher Plant Compartment. *Life : Open Access Journal*, 4(2):189–204, May 2014. ISSN 2075-1729. doi:10.3390/life4020189. URL https://www.ncbi.nlm.nih.gov/pmc/articles/PMC4187168/.

[2] Ø.M. Jakobsen, M. Schiefloe, Ø. Mikkelsen, C. Paille, and A.I.K. Jost. Real-time monitoring of chemical water quality in closed-loop hydroponics. *Acta Horticulturae*, 1296(127):1005–1018, November 2020. ISSN 0567-7572, 2406-6168. doi:10.17660/ActaHortic.2020.1296.127. URL https://www.actahort.org/books/1296/1296_127.htm.

[3] Toyoki Kozai, Genhua Niu, and Michiko Takagaki, editors. *Plant Factory An Indoor Vertical Farming System for Efficient Quality Foor Production*. Academic Press, 1 edition, 2016. ISBN 978-0-12-801775-3.

[4] Saad Khan, Ankit Purohit, and Nikita Vadsaria. Hydroponics: current and future state of the art in farming. *Journal of Plant Nutrition*, 44(10):1515–1538, June 2021. ISSN 0190-4167. doi:10.1080/01904167.2020.1860217. URL https://doi.org/10.1080/01904167.2020.1860217. Publisher: Taylor & Francis.

[5] P. Bradley and C. Marulanda. Simplified hydroponics to reduce global hunger. *Acta Horticulturae*, 554(31):289–296, June 2001. ISSN 0567-7572, 2406-6168. doi:10.17660/ActaHortic.2001.554.31. URL https://www.actahort.org/books/554/554_31.htm.

[6] G. Carmassi, L. Incrocci, R. Maggini, F. Malorgio, F. Tognoni, and A. Pardossi. Modeling Salinity Build-Up in Recirculating Nutrient Solution Culture. *Journal of Plant Nutrition*, 28(3):431–445, March 2005. ISSN 0190-4167. doi:10.1081/PLN-200049163. URL https://doi.org/10.1081/PLN-200049163. Publisher: Taylor & Francis.

[7] Michael Raviv and J. Heinrich Lieth. *Soilless Culture Theory and Practice*. Elsevier, 1 edition, 2008. ISBN 978-0-444-52975-6.

[8] S.W. Burrage. Nutrient Film Teqchnique in protected cultivation. *Acta Horticulturae*, 323(1):23–38, February 1993. ISSN 0567-7572, 2406-6168. doi:10.17660/ActaHortic.1993.323.1. URL https://www.actahort.org/books/323/323_1.htm.

[9] Ø.M. Jakobsen, M. Schiefloe, G. Simonsen, K.J.K. Attramadal, and A.I.K. Jost. Utilization of runoff nutrients from recirculating aquaculture systems for hydroponic crop cultivation. *Acta Horticulturae*, 1321(29):221–228, September 2021. ISSN 0567-7572, 2406-6168. doi:10.17660/ActaHortic.2021.1321.29. URL https://www.actahort.org/books/1321/1321_29.htm.

[10] Ramasamy Rajesh Kumar and Jae Young Cho. Reuse of hydroponic waste solution. *Environmental Science and Pollution Research*, 21(16):9569–9577, August 2014. ISSN 1614-7499. doi:10.1007/s11356-014-3024-3. URL https://doi.org/10.1007/s11356-014-3024-3.

[11] Sam E. Wortman. Crop physiological response to nutrient solution electrical conductivity and pH in an ebb-and-flow hydroponic system. *Scientia Horticulturae*, 194:34–42, October 2015. ISSN 0304-4238. doi:10.1016/j.scienta.2015.07.045. URL https://www.sciencedirect.com/science/article/pii/S0304423815301199.

[12] Hardeep Singh and Dunn Bruce. Electrical Conductivity and pH Guide for Hydroponics, October 2016. URL https://shareok.org/bitstream/handle/11244/331022/oksa_HLA-6722_2016-10.pdf?sequence=1.

[13] Damianos Neocleous and Dimitrios Savvas. NaCl accumulation and macronutrient uptake by a melon crop in a closed hydroponic system in relation to water uptake. *Agricultural Water Management*, 165:22–32, February 2016. ISSN 0378-3774. doi:10.1016/j.agwat.2015.11.013. URL https://www.sciencedirect.com/science/article/pii/S0378377415301669.

[14] A Lauchli and Steve Grattan. Plant Responses to Saline and Sodic Conditions. In *Agricultural Salinity Assessment and Management*. American Society of Civil Engineers, second edition edition, 1990. ISBN 978-0-7844-1169-8. doi:10.1061/9780784411698.ch06.

[15] Nikos G. Tzortzakis. Influence of NaCl and Calcium Nitrate on Lettuce and Endive Growth Using Nutrient Film Technique. *International Journal of Vegetable Science*, 15(1):44–56, November 2008. ISSN 1931-5260. doi:10.1080/19315260802446419. URL https://doi.org/10.1080/19315260802446419. Publisher: Taylor & Francis.

[16] Csaba Bartha, Laszlo Fodorpataki, Maria Del Carmen Martinez-Ballesta, Octavian Popescu, and Micaela Carvajal. Sodium accumulation contributes to salt stress tolerance in lettuce cultivars. *Journal of Applied Botany and Food Quality*, Vol 88:p.4248, March 2015. doi:10.5073/JABFQ.2015.088.008. URL https://ojs.openagrar.de/index.php/JABFQ/article/view/3381. Publisher: Journal of Applied Botany and Food Quality.

[17] S Sattar, Tayyab Husnain, and Dr. Arshad Javaid. Effect of NACL salinity on cotton (Gossypium arboreum L.) grown on MS medium and in hydroponic cultures. *Journal of Animal and Plant Sciences*, 20:87–89, January 2010.

[18] Woo-Jae Cho, Hak-Jin Kim, Dae-Hyun Jung, Dong-Wook Kim, Tae In Ahn, and Jung-Eek Son. On-site ion monitoring system for precision hydroponic nutrient management. *Computers and Electronics in Agriculture*, 146:51–58, March 2018. ISSN 0168-1699. doi:10.1016/j.compag.2018.01.019. URL https://www.sciencedirect.com/science/article/pii/S0168169917309316.

[19] Raymond M. Wheeler. Agriculture for Space: People and Places Paving the Way. *Open Agriculture*, 2(1):14–32, February 2017. ISSN 2391-9531. doi:10.1515/opag-2017-0002. URL https://www.degruyter.com/document/doi/10.1515/opag-2017-0002/html. Publisher: De Gruyter Open Access.

[20] C. Lasseur, J. Brunet, H. de Weever, M. Dixon, G. Dussap, F. Godia, N. Leys, M. Mergeay, and D. Van Der Straeten. MELiSSA: the European project of closed life support system. *Gravitational and Space Biology*, 23(2):3–13, September 2010. ISSN 1089988X. URL https://go.gale.com/ps/i.do?p=AONE&sw=w&issn=1089988X&v=2.1&it=r&id=GALE%7CA348311298&sid=googleScholar&linkaccess=abs. Publisher: American Society for Gravitational and Space Biology.

[21] Raymond M. Wheeler. Plants for human life support in space: from Myers to Mars. *Gravitational and Space Research*, 23(2), 2010. ISSN 2332-7774. URL http://gravitationalandspaceresearch.org/index.php/journal/article/view/490. Number: 2.

[22] Raymond M. Wheeler. Roadmaps and Strategies or Crop Resarch for Bioregenative Life Support

Systems. Technical Report NASA/TM-2009-214768, NASA Biological Sciences Office, Kennedy Space Center, Florida, 2009.

[23] A. A. Tikhomirov, S. A. Ushakova, N. P. Kovaleva, B. Lamaze, M. Lobo, and Ch. Lasseur. Biological life support systems for a Mars mission planetary base: Problems and prospects. *Advances in Space Research*, 40(11):1741–1745, January 2007. ISSN 0273-1177. doi:10.1016/j.asr.2006.11.009. URL https://www.sciencedirect.com/science/article/pii/S0273117706007198.

[24] Matthew Bamsey, Thomas Graham, Cody Thompson, Alain Berinstain, Alan Scott, and Michael Dixon. Ion-Specific Nutrient Management in Closed Systems: The Necessity for Ion-Selective Sensors in Terrestrial and Space-Based Agriculture and Water Management Systems. *Sensors*, 12(10):13349–13392, October 2012. ISSN 1424-8220. doi:10.3390/s121013349. URL https://www.mdpi.com/1424-8220/12/10/13349. Number: 10 Publisher: Molecular Diversity Preservation International.

[25] Peter W. Dillingham, Tanja Radu, Dermot Diamond, Aleksandar Radu, and Christina M. McGraw. Bayesian Methods for Ion Selective Electrodes. *Electroanalysis*, 24(2):316–324, 2012. ISSN 1521-4109. doi:10.1002/elan.201100510. URL https://onlinelibrary.wiley.com/doi/abs/10.1002/elan.201100510. _eprint: https://onlinelibrary.wiley.com/doi/pdf/10.1002/elan.201100510.

[26] Joseph Wang. *Analytical Electrochemistry*. John Wiley & Sons, Ltd, 3 edition, 2006. ISBN 978-0-471-79030-3.

[27] Douglas A. Skoog, Donald M. West, F. James Holler, and Stanley R. Crouch. *Fundementals of Analytical Chemistry*. Brooks/Cole, 9 edition, 2014. ISBN 978-0-495-55828-6.

[28] Ernő Lindner and Bradford D. Pendley. A tutorial on the application of ion-selective electrode potentiometry: An analytical method with unique qualities, unexplored opportunities and potential pitfalls; Tutorial. *Analytica Chimica Acta*, 762:1–13, January 2013. ISSN 0003-2670. doi:10.1016/j.aca.2012.11.022. URL https://www.sciencedirect.com/science/article/pii/S0003267012016789.

[29] B. J. Bailey, B. G. D. Haggett, A. Hunter, W. J. Albery, and L. R. Svanberg. Monitoring nutrient film solutions using ion-selective electrodes. *Journal of Agricultural Engineering Research*, 40(2):129–142, June 1988. ISSN 0021-8634. doi:10.1016/0021-8634(88)90110-2. URL https://www.sciencedirect.com/science/article/pii/0021863488901102.

[30] HACH ISECl181 User Manual Edition 5. Manual DOC022.53.80030, HACH Company/HACH Lange, May 2021. URL https://www.hach.com/asset-get.download-en.jsa?id=7648131615.

[31] HACH ISENa381 User Manual Edition 5. Manual DOC022.53.80027, HACH Company/HACH Lange, May 2021. URL https://www.hach.com/asset-get.download-en.jsa?id=7648131612.

[32] Yoshio Umezawa, Philippe Bühlmann, Kayoko Umezawa, Koji Tohda, and Shigeru Amemiya. Potentiometric Selectivity Coefficients of Ion-Selective Electrodes. Part I. Inorganic Cations (Technical Report). *Pure and Applied Chemistry*, 72(10):1851–2082, October 2000. ISSN 1365-3075. doi:10.1351/pac200072101851. URL https://www.degruyter.com/document/doi/10.1351/pac200072101851/html. Publisher: De Gruyter.

[33] Y. Umezawa, K. Umezawa, and H. Sato. Selectivity coefficients for ion-selective electrodes: Recommended methods for reporting KA,Bpot values (Technical Report). *Pure and Applied Chemistry*, 67(3):507–518, January 1995. ISSN 1365-3075. doi:10.1351/pac199567030507. URL https://www.degruyter.com/document/doi/10.1351/pac199567030507/html. Publisher: De Gruyter.

[34] Hak-Jin Kim, Won-Kyung Kim, Mi-Young Roh, Chang-Ik Kang, Jong-Min Park, and Kenneth A. Sudduth. Automated sensing of hydroponic macronutrients using a computer-controlled system with an array of ion-selective electrodes. *Computers and Electronics in Agriculture*, 93:46–54, April 2013. ISSN 0168-1699. doi:10.1016/j.compag.2013.01.011. URL https://www.sciencedirect.com/science/article/pii/S0168169913000264.

[35] M. Gutiérrez, S. Alegret, R. Cáceres, J. Casadesús, O. Marfà, and M. del Valle. Application of a potentiometric electronic tongue to fertigation strategy in greenhouse cultivation. *Computers and Electronics in Agriculture*, 57(1):12–22, 2007. ISSN 0168-1699. doi:10.1016/j.compag.2007.01.012. URL https://www.sciencedirect.com/science/article/pii/S0168169907000324.

[36] Alexander I. Railkin. *Marine Biofouling: Colonization Processes and Defenses*. CRC Press, Boca Raton, December 2003. ISBN 978-0-429-21079-2. doi:10.1201/9780203503232.

[37] Diego Meseguer Yebra, Søren Kiil, and Kim Dam-Johansen. Antifouling technology-past, present and future steps towards efficient and environmentally friendly antifouling coatings. *Progress in Organic Coatings*, 50(2):75–104, July 2004. ISSN 0300-9440. doi:10.1016/j.porgcoat.2003.06.001.

[38] Malin Hultberg, Håkan Asp, Salla Marttila, Karl-Johan Bergstrand, and Susanne Gustafsson. Biofilm Formation by Chlorella vulgaris is Affected by Light Quality. *Current Microbiology*, 69(5):699–702, November 2014. ISSN 1432-0991. doi:10.1007/s00284-014-0645-1. URL https://doi.org/10.1007/s00284-014-0645-1.

[39] Seungjun Lee, Chongtao Ge, Zuzana Bohrerova, Parwinder S. Grewal, and Jiyoung Lee. Enhancing plant productivity while suppressing biofilm growth in a windowfarm system using beneficial bacteria and ultraviolet irradiation. *Canadian Journal of Microbiology*, 61(7):457–466, July 2015. ISSN 1480-3275. doi:10.1139/cjm-2015-0024.

[40] Longbin Qi, Rongning Liang, Tianjia Jiang, and Wei Qin. Anti-fouling polymeric membrane ion-selective electrodes. *TrAC Trends in Analytical Chemistry*, 150:116572, May 2022. ISSN 0165-9936. doi:10.1016/j.trac.2022.116572. URL https://www.sciencedirect.com/science/article/pii/S0165993622000553.

[41] Peranandam Revathi, Palanisamy Iyapparaj, Rajkumar A. Vasanthi, Natesan Munuswamy, and Arunachalam Palavesam. Bioaccumulation of TBT and Its Cellular Toxic Effects on the Freshwater Prawn Macrobrachium rosenbergii. *Bulletin of Environmental Contamination and Toxicology*, 103 (5):689–696, November 2019. ISSN 1432-0800. doi:10.1007/s00128-019-02711-0.

[42] Vinod Kumar, Shevita Pandita, Gagan Preet Singh Sidhu, Anket Sharma, Kanika Khanna, Parminder Kaur, Aditi Shreeya Bali, and Raj Setia. Copper bioavailability, uptake, toxicity and tolerance in plants: A comprehensive review. *Chemosphere*, 262:127810, January 2021. ISSN 0045-6535. doi:10.1016/j.chemosphere.2020.127810. URL https://www.sciencedirect.com/science/article/pii/S0045653520320051.

[43] María Eugenia Letelier, Sebastián Sánchez-Jofré, Liliana Peredo-Silva, Juan Cortés-Troncoso, and Paula Aracena-Parks. Mechanisms underlying iron and copper ions toxicity in biological systems: Pro-oxidant activity and protein-binding effects. *Chemico-Biological Interactions*, 188(1):220–227, October 2010. ISSN 1872-7786. doi:10.1016/j.cbi.2010.06.013.

[44] Claudia M. Grozea and Gilbert C. Walker. Approaches in designing non-toxic polymer surfaces to

deter marine biofouling. *Soft Matter*, 5(21):4088–4100, 2009. doi:10.1039/B910899H. URL https://pubs.rsc.org/en/content/articlelanding/2009/sm/b910899h. Publisher: Royal Society of Chemistry.

[45] Jinghao Kuang and Phillip B. Messersmith. Universal surface-initiated polymerization of antifouling zwitterionic brushes using a mussel-mimetic peptide initiator. *Langmuir: the ACS journal of surfaces and colloids*, 28(18):7258–7266, May 2012. ISSN 1520-5827. doi:10.1021/la300738e.

[46] L. M. Granhag, J. A. Finlay, P. R. Jonsson, J. A. Callow, and M. E. Callow. Roughness-dependent removal of settled spores of the green alga Ulva (syn. Enteromorpha) exposed to hydrodynamic forces from a water jet. *Biofouling*, 20(2):117–122, April 2004. ISSN 0892-7014. doi:10.1080/08927010410001715482.

[47] Claudio Zuliani and Dermot Diamond. Opportunities and challenges of using ion-selective electrodes in environmental monitoring and wearable sensors. *Electrochimica Acta*, 84:29–34, December 2012. ISSN 0013-4686. doi:10.1016/j.electacta.2012.04.147. URL https://www.sciencedirect.com/science/article/pii/S0013468612007761.

[48] M. O. Elasri and R. V. Miller. Study of the response of a biofilm bacterial community to UV radiation. *Applied and Environmental Microbiology*, 65(5):2025–2031, May 1999. ISSN 0099-2240. doi:10.1128/AEM.65.5.2025-2031.1999.

[49] Marcin Pawlak and Eric Bakker. Chemical Modification of Polymer Ion-Selective Membrane Electrode Surfaces. *Electroanalysis*, 26(6):1121–1131, 2014. ISSN 1521-4109. doi:10.1002/elan.201300449. URL https://onlinelibrary.wiley.com/doi/abs/10.1002/elan.201300449. _eprint: https://onlinelibrary.wiley.com/doi/pdf/10.1002/elan.201300449.

[50] Hak-Jin Kim, Dong-Wook Kim, Won Kyung Kim, Woo-Jae Cho, and Chang Ik Kang. PVC membrane-based portable ion analyzer for hydroponic and water monitoring. *Computers and Electronics in Agriculture*, 140:374–385, August 2017. ISSN 0168-1699. doi:10.1016/j.compag.2017.06.015. URL https://www.sciencedirect.com/science/article/pii/S0168169916311577.

[51] Roland De Marco, Graeme Clarke, and Bobby Pejcic. Ion-Selective Electrode Potentiometry in Environmental Analysis. *Electroanalysis*, 19(19-20):1987–2001, 2007. ISSN 1521-4109. doi:10.1002/elan.200703916. URL https://onlinelibrary.wiley.com/doi/abs/10.1002/elan.200703916. _eprint: https://onlinelibrary.wiley.com/doi/pdf/10.1002/elan.200703916.

[52] Hee-Jo Han, Hak-Jin Kim, Dae-Hyun Jung, Woo-Jae Cho, and Yeong-Yeol Cho and Gong-In Lee. Real-time Nutrient Monitoring of Hydroponic Solutions Using an Ion-selective Electrode-based Embedded System. *Protected Horticulture and Plant Factory*, 29(2):141–152, April 2020. doi:10.12791/KSBEC.2020.29.2.141. URL https://www.ksbec.org/articles/article/9RXb/www.ksbec.org/articles/article/9RXb/. Publisher: Journal of Bio-Environment Control.

[53] Colin F. Poole. *The Essence of Chromatography*. Elsevier Science B.V., Amsterdam, The Netherlands, first edition edition, 2003. ISBN 978-0-444-50198-1.

[54] Rajmund Michalski. Ion Chromatography as a Reference Method for Determination of Inorganic Ions in Water and Wastewater. *Critical Reviews in Analytical Chemistry*, 36(2):107–127, July 2006. ISSN 1040-8347. doi:10.1080/10408340600713678. URL https://doi.org/10.1080/10408340600713678. Publisher: Taylor & Francis _eprint: https://doi.org/10.1080/10408340600713678.

[55] Elsa Lundanes, Léon Reubaset, and Tyge Greibrokk. *Chromatogrpahy: Basic Principles, Sample Preparations and Related Methods*. Wiley-VCH Verlag Gmbh & Co. KGaA, Weinheim, Germany, first edition edition, 2013. ISBN 978-3-527-33620-3.

[56] Paul R. Haddad, Pavel N. Nesterenko, and Wolfgang Buchberger. Recent developments and emerging directions in ion chromatography. *Journal of Chromatography A*, 1184(1):456–473, March 2008. ISSN 0021-9673. doi:10.1016/j.chroma.2007.10.022. URL https://www.sciencedirect.com/science/article/pii/S0021967307017463.

[57] R. H. Worden. ANALYTICAL METHODS | Geochemical Analysis (Including X-ray). In Richard C. Selley, L. Robin M. Cocks, and Ian R. Plimer, editors, *Encyclopedia of Geology*, pages 54–76. Elsevier, Oxford, January 2005. ISBN 978-0-12-369396-9. doi:10.1016/B0-12-369396-9/00096-4. URL https://www.sciencedirect.com/science/article/pii/B0123693969000964.

[58] Peter E. Jackson. Ion Chromatography in Environmental Analysis. In *Encyclopedia of Analytical Chemistry*. John Wiley & Sons, Ltd, 2006. ISBN 978-0-470-02731-8. doi:10.1002/9780470027318.a0835. URL https://onlinelibrary.wiley.com/doi/abs/10.1002/9780470027318.a0835. _eprint: https://onlinelibrary.wiley.com/doi/pdf/10.1002/9780470027318.a0835.

[59] Raaidah Saari-Nordhaus, Lakshmy M. Nair, and James M. Anderson. Elimination of matrix interferences in ion chromatography by the use of solid-phase extraction disks. *Journal of Chromatography A*, 671(1):159–163, June 1994. ISSN 0021-9673. doi:10.1016/0021-9673(94)80234-3. URL https://www.sciencedirect.com/science/article/pii/0021967394802343.

[60] John D. Pfaff. Method 300.0 - Determination of Inorganic Anions by Ion Chromatography. In Environmental Monitoring Systems Laboratory, editor, *Methods for the Determination of Metals in Environmental Samples*, pages 388–417. William Andrew Publishing, Westwood, NJ, January 1996. ISBN 978-0-8155-1398-8. doi:10.1016/B978-0-8155-1398-8.50022-7. URL https://www.sciencedirect.com/science/article/pii/B9780815513988500227.

[61] M. Farooq Wahab, Jordan K. Anderson, Mohamed Abdelrady, and Charles A. Lucy. Peak Distortion Effects in Analytical Ion Chromatography. *Analytical Chemistry*, 86(1):559–566, January 2014. ISSN 0003-2700. doi:10.1021/ac402624a. URL https://doi.org/10.1021/ac402624a. Publisher: American Chemical Society.

[62] Robert Thomas. *Practical Guide to ICP-MS: A Tutorial for Beginners, Second Edition*. CRC Press, Boca Raton, 2 edition, June 2008. ISBN 978-0-429-14872-9. doi:10.1201/9781420067873.

[63] Adrian A. Ammann. Inductively coupled plasma mass spectrometry (ICP MS): a versatile tool. *Journal of Mass Spectrometry*, 42(4):419–427, 2007. ISSN 1096-9888. doi:10.1002/jms.1206. URL https://onlinelibrary.wiley.com/doi/abs/10.1002/jms.1206. _eprint: https://onlinelibrary.wiley.com/doi/pdf/10.1002/jms.1206.

[64] Scott C. Wilschefski and Matthew R. Baxter. Inductively Coupled Plasma Mass Spectrometry: Introduction to Analytical Aspects. *The Clinical Biochemist. Reviews*, 40(3):115–133, August 2019. ISSN 0159-8090. doi:10.33176/AACB-19-00024.

[65] Kathryn L. Linge and Kym E. Jarvis. Quadrupole ICP-MS: Introduction to Instrumentation, Measurement Techniques and Analytical Capabilities. *Geostandards and Geoanalytical Research*, 33(4):

445–467, 2009. ISSN 1751-908X. doi:10.1111/j.1751-908X.2009.00039.x. URL https://onlinelibrary.wiley.com/doi/abs/10.1111/j.1751-908X.2009.00039.x.

[66] Rob Morris. Spectrophotometry. *Current Protocols Essential Laboratory Techniques*, 11(1), November 2015. ISSN 1948-3430, 1948-3430. doi:10.1002/9780470089941.et0201s11. URL https://onlinelibrary.wiley.com/doi/10.1002/9780470089941.et0201s11.

[67] NS-ISO 15705:2002. Water quality - Determination of the chemical oxygen demand index (ST-COD) - Small-scale sealed-tube method. Standard, Standards Norway, 2012. URL https://www.standard.no/no/Nettbutikk/produktkatalogen/Produktpresentasjon/?ProductID=587877.

[68] G. E Batley. Quality Assurance in Environmental Monitoring. *Marine Pollution Bulletin*, 39(1): 23–31, January 1999. ISSN 0025-326X. doi:10.1016/S0025-326X(99)00016-8. URL https://www.sciencedirect.com/science/article/pii/S0025326X99000168.

[69] J. Udesky, R. Dodson, L. Perovich, and R. Rudel. Wrangling environmental exposure data: guidance for getting the best information from your laboratory measurements. *Environmental Health*, 2019. doi:10.1186/s12940-019-0537-8.

[70] F. W. Fifield and P. J. Haines, editors. *Environmental analytical chemistry*. Blackwell Science, Oxford ; Malden, MA, 2nd ed edition, 2000. ISBN 978-0-632-05383-4.

[71] A. G. Asuero, A. Sayago, and A. G. González. The Correlation Coefficient: An Overview. *Critical Reviews in Analytical Chemistry*, 36(1):41–59, January 2006. ISSN 1040-8347, 1547-6510. doi:10.1080/10408340500526766. URL https://www.tandfonline.com/doi/full/10.1080/10408340500526766.

[72] James N. Miller. Basic statistical methods for Analytical Chemistry. Part 2. Calibration and regression methods. A review. *Analyst*, 116(1):3–14, January 1991. ISSN 1364-5528. doi:10.1039/AN9911600003. URL https://pubs.rsc.org/en/content/articlelanding/1991/an/an9911600003. Publisher: The Royal Society of Chemistry.

[73] Francisco Raposo. Evaluation of analytical calibration based on least-squares linear regression for instrumental techniques: A tutorial review. *TrAC Trends in Analytical Chemistry*, 77:167–185, March 2016. ISSN 0165-9936. doi:10.1016/j.trac.2015.12.006. URL https://www.sciencedirect.com/science/article/pii/S0165993615301242.

[74] Joseph P. Albano and William B. Miller. Photodegradation of FeDTPA in Nutrient Solutions. I. Effects of Irradiance, Wavelength, and Temperature. *HortScience*, 36(2):313–316, April 2001. ISSN 0018-5345, 2327-9834. doi:10.21273/HORTSCI.36.2.313. URL https://journals.ashs.org/hortsci/view/journals/hortsci/36/2/article-p313.xml. Publisher: American Society for Horticultural Science Section: HortScience.

[75] Sigrid Lüftl, Visakh P.M., and Sarath Chandran, editors. *Polyoxymethylene Handbook: Structure, Properties, Applications and Their Nanocomposites*. John Wiley & Sons, Inc., Hoboken, NJ, USA, March 2014. ISBN 978-1-118-91445-8 978-1-118-38511-1. doi:10.1002/9781118914458. URL http://doi.wiley.com/10.1002/9781118914458.

A Appendices

A.1 Hydroponic samples - theoretical nutrient concentrations

The theoretical start concentrations of macronutrients present in the hydroponic nutrient solutions collected as Hydroponic samples, batch 1 and 2, are presented in table A.1 below.

Table A.1: Theoretical concentrations used to prepare the hydroponic nutrient solutions EU1-8, analyzed as hydroponic batches 1 & 2, samples 1 through 8. K* are concentrations of potassium present after KOH has been used to adjust the pH of solutions.

Composition		EU1	EU2	EU3	EU4	EU5	EU6	EU7	EU8
NO3	[mM]	12.2	9.2	9.2	10.5	6.6	12.2	15.3	12.2
NH4	[mM]	3.5	2.6	2.6	1.3	5.2	3.5	4.4	3.5
H2PO4	[mM]	1.5	1.1	1.1	1.1	1.1	1.5	1.9	1.5
K	[mM]	5	3.8	3.8	3.8	3.8	5	6.3	5
Ca	[mM]	3.6	2.7	2.7	2.7	2.7	3.6	4.5	3.6
Mg	[mM]	1	0.8	0.8	0.8	0.8	1	1.3	1
SO4	[mM]	2	1.5	2.1	0.8	4.6	2	2.5	2.6
Cl	[mM]	0	0	3.8	3.8	3.8	0	0	3.8
Na	[mM]	0	0	5	5	5	0	0	5
K*	[mM]	6.6	5	5	5	5	6.6	8.3	6.6

A.2 Hydroponics samples batch 1, calibration curves

In this section the calibration curves used for the calculation of concentrations of sodium and chloride in the hydroponic samples, batch 1 collected 11.11.21, presented in section 4.4, tables 4.3 and 4.4, and figure 4.20.

Two calibration curves were recorded for each electrode. one using 10 and 100 mg/L of respective standards, and one using 100 and 1000 mg/L of respective standards. The Second set of calibration curves was recorded as some samples contained $>$ 100 mg/L of analyte.

The chloride calibration curves are presented in figure A.1. The 10 to 100 mg/L calibration curve is presented as curve A, while the 100 to 1000 mg/L calibration curve is presented as curve B.

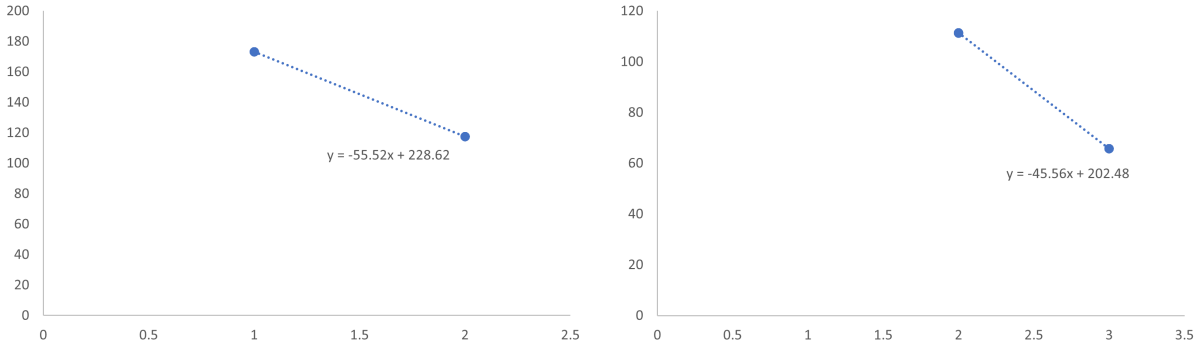

A B

Figure A.1: Calibration curve for the chloride electrode, used for calculations of concentrations in hydroponic samples, batch 1. Curve A was recorded using 10 and 100 mg/L standards, while curve B was recorded using 100 and 1000 mg/L standards.

The sodium calibration curves are presented in figure A.2. The 10 to 100 mg/L calibration curve is presented as curve A, while the 100 to 1000 mg/L calibration curve is presented as curve B.

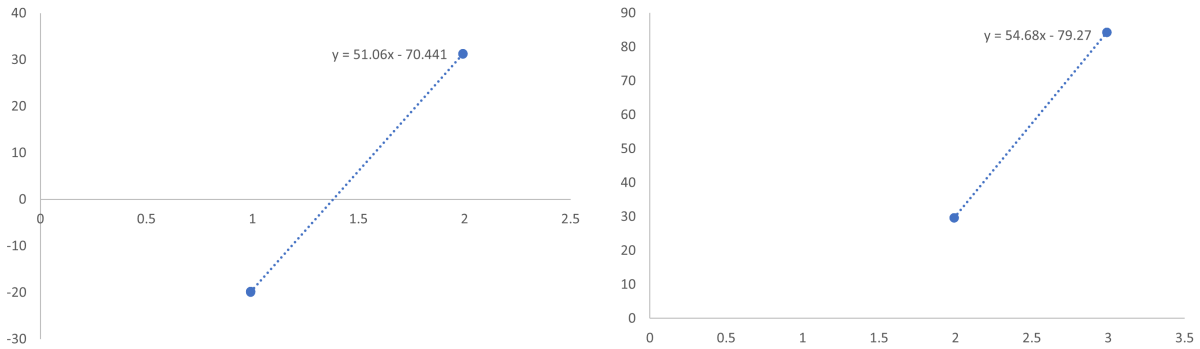

A B

Figure A.2: Calibration curve for the sodium electrode, used for calculations of concentrations in hydroponic samples, batch 1. Curve A was recorded using 10 and 100 mg/L standards, while curve B was recorded using 100 and 1000 mg/L standards.

Curve A were used to calculate concentrations in samples 2, 6, 7_1 and 7_2. Curves B were used to calculate concentrations in samples 3, 4, 5, and 8.

A.3 Hydroponic samples batch 2, calibration curves

This section presents the calibration curves used for the calculation of concentrations of sodium and chloride in hydroponic samples batch 2, collected 06.12.21, presented in section 4.4, tables 4.5 and 4.6, as well as figure 4.21.

The first set of calibration curves, recorded before the sample measurements were made are presented in figure A.3.

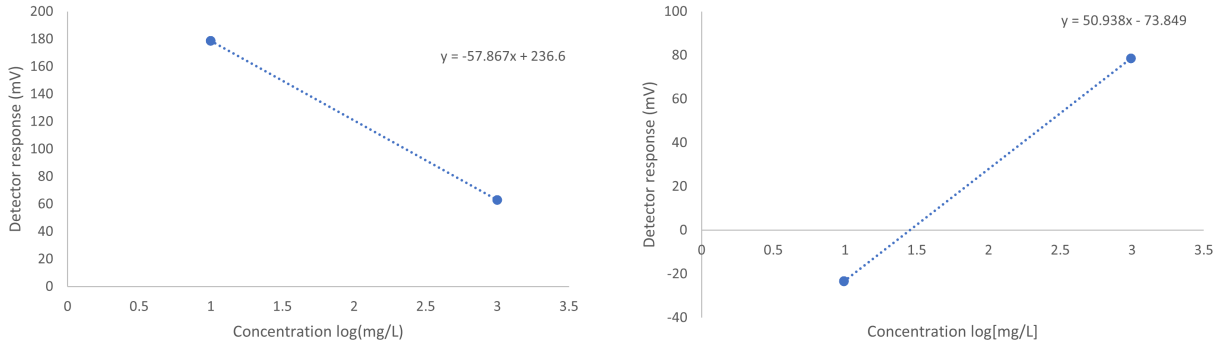

Figure A.3: Chloride and sodium calibration curves recorded before batch 2 analysis. Left hand graph shows chloride electrode calibration curve, right hand graph shows sodium calibration curve.

At the end of the day, a second calibration curve was recorded using the same conditions. These calibration curves are presented in figure A.4 below.

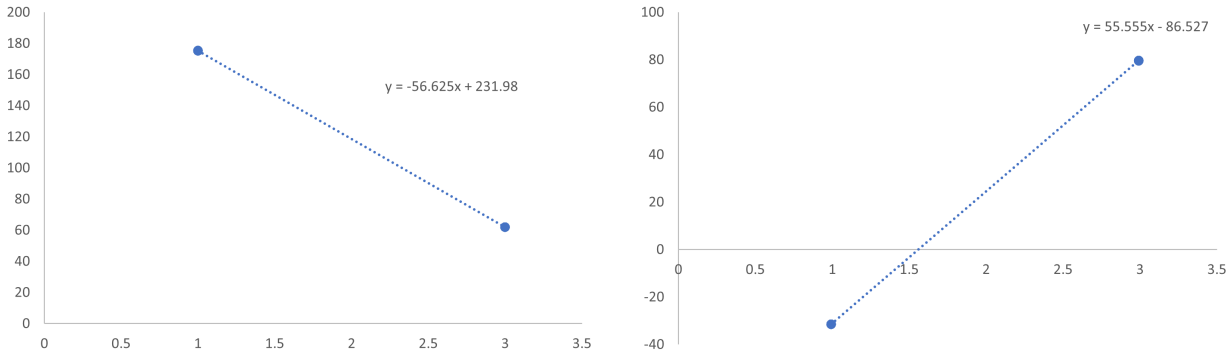

Figure A.4: Chloride and sodium calibration curves recorded after batch 2 analysis. Left hand graph shows chloride electrode calibration curve, right hand graph shows sodium calibration curve.

The resulting concentrations from the chloride electrode analysis using the second calibration curve are presented in table A.2. The results are also compared to the IC results for the batch.

Table A.2: Chloride concentrations determined using the HACH ISECl181 and IC on the second batch of hydroponic samples collected in December 2021, using the second calibration curve.

Sample	EU1	EU2	EU3	EU4	EU5	EU6	EU7	EU8
ISE [mg/L]	6	3.4	136.2	135.6	118.9	4.3	5.5	113.6
IC [mg/L]	11.6	9.7	85.7	98.7	88.2	10.7	9.9	84.3
Deviation [%]	-48.3	-64.9	58.9	37.4	34.8	-57.7	-44.3	34.8

The resulting concentrations from the sodium electrode analysis using the second calibration curve are

presented in table A.3. The results are also compared to the ICP-MS results for the batch.

Table A.3: Sodium concentrations determined using the HACH ISENa381 and ICP-MS on the second batch of hydroponic samples collected in December 2021, using the second calibration curve.

Sample	EU1	EU2	EU3	EU4	EU5	EU6	EU7	EU8
ISE [mg/L]	5.7	3.9	66.4	71.5	62.8	4.7	3.7	68.8
ICP-MS [mg/L]	9.750	9.732	122.646	121.412	123.895	9.919	10.415	129.257
Deviation [%]	-41.5	-59.9	-45.9	-41.1	-49.3	-52.6	-64.5	-46.8

A graphical representation of the data was also prepared, using the same method as for the results. The resulting graphs are presented in figure A.5

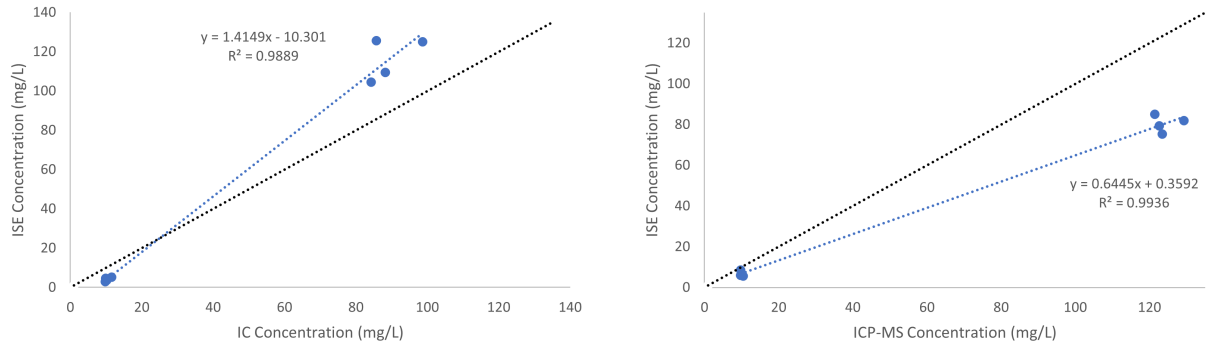

Figure A.5: The figure shows graphic representations of the ISE determined concentrations compared to the alternative methods on the second batch of hydroponic samples, using the second calibration curve The left graph shows chloride concentrations as determined by ISE and IC, while the right graph shows sodium concentrations as determined by ISE and ICP-MS. Linear regression has been performed on both data sets, shown in blue with calculated slopes and intercepts, and the line y=x is graphed in black.

A.4 Flow cell experiment, calibration curves

The calibration curves used for the chloride (curve A) and sodium (curve B) are shown in figure A.6 below.

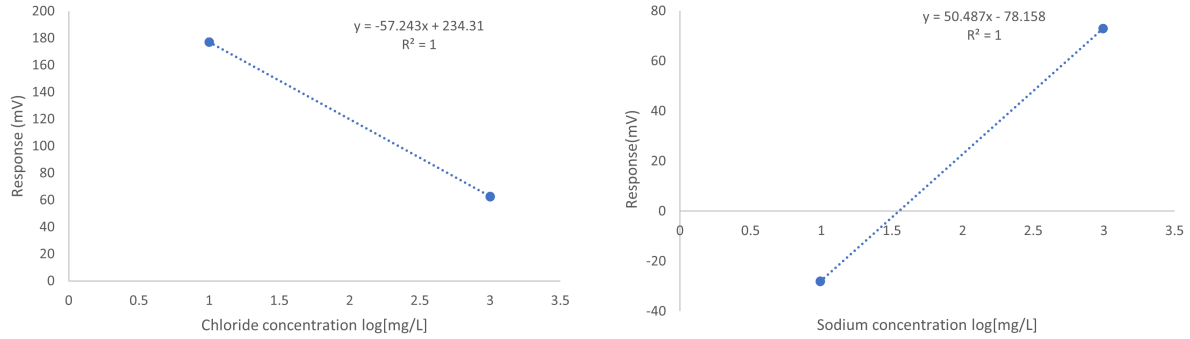

A B

Figure A.6: Calibration curve for the chloride(A) and sodium(B) electrodes used in the flow cell experiment.

The behavior of the chloride and sodium electrode in 100 mg/L chloride and sodium standards was also investigated. The electrodes were left in solution for 4 hours, with measurements every minute. The results are shown for the chloride electrode (Curve A) and the sodium electrode (Curve B) in figure A.7 below.

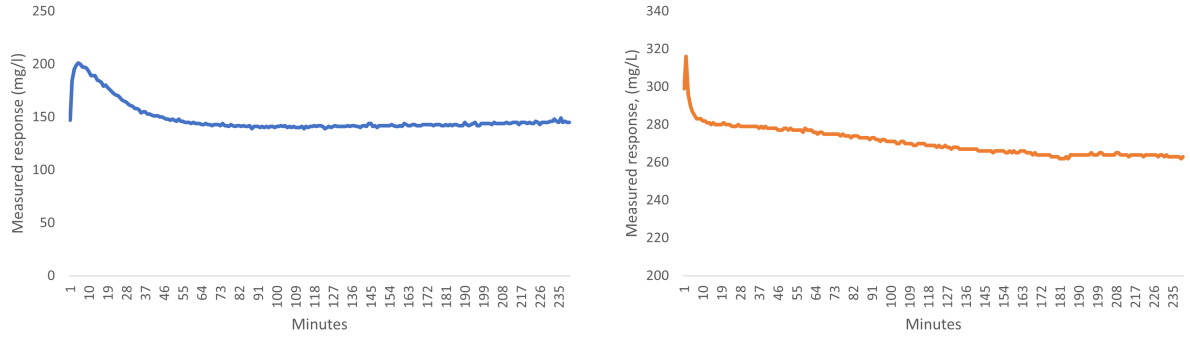

A B

Figure A.7: Behavior of the chloride (A) and sodium (B) electrode in 100 mg/L chloride and sodium standards over a 4 hour period.

The pH and electrical conductivity, EC, of the hydroponics nutrient solution used in the flow cell experiment was measured weekly after nutrients were added. This was to ensure plant health and growth. The pH was measured, and found to be withing acceptable limits (5.4-5.6) every week except for the final day of the experiment, where the pH had increased to 5.8. No action was taken to remedy this, as the experiment was ended. The electrical conductivity decreased over the experimental period, after final sodium chloride adjustment, as is expected. The results are presented in table A.4.

Table A.4: Weekly measured pH and EC of nutrient solution used in the flow cell experiment.

	pH	EC
1	5.42	1.200
2	5.52	1.566
3	5.52	2.596
4	5.49	2.475
5	5.85	2.414

Measurement 1 was made after adjustments to CHS1 nutrient concentrations, while measurement 2 was performed after sodium chloride concentrations were adjusted to 292 mg/L. Measurements 3, 4 and 5 were made after sodium chloride concentrations were adjusted to 877 mg/L. No adjustments were made to solution between measurements 3, 4 and 5.

A.5 Ion chromatography results

A.5.1 Hydroponic samples, Batch 1

The following pages show the results of the ion chromatography analysis of the first batch of hydroponic samples. The results are presented chronologically from 2 to 8, with 7_1 and 7_2.

Sample data

Ident	EU2
Sample type	Sample
Determination start	2021-11-18 17:01:47 UTC+1
Method	Logisk fortynning NTNU Kjemisk
Operator	

Anions

Data source	Conductivity detector 1 (940 Professional IC Vario 1)	
Channel	Conductivity	
Recording time	38,0	min
Integration	Manual	
Column type	Metrosep A Supp 7 - 250/4.0	
Eluent composition	Anion Eluent - 3,6 mM Na2CO3	
Flow	0,700	mL/min
Maximum flow monitored	yes	
Pressure	9,85	MPa
Maximum pressure monitored	yes	
Temperature	45,0	°C

Anions

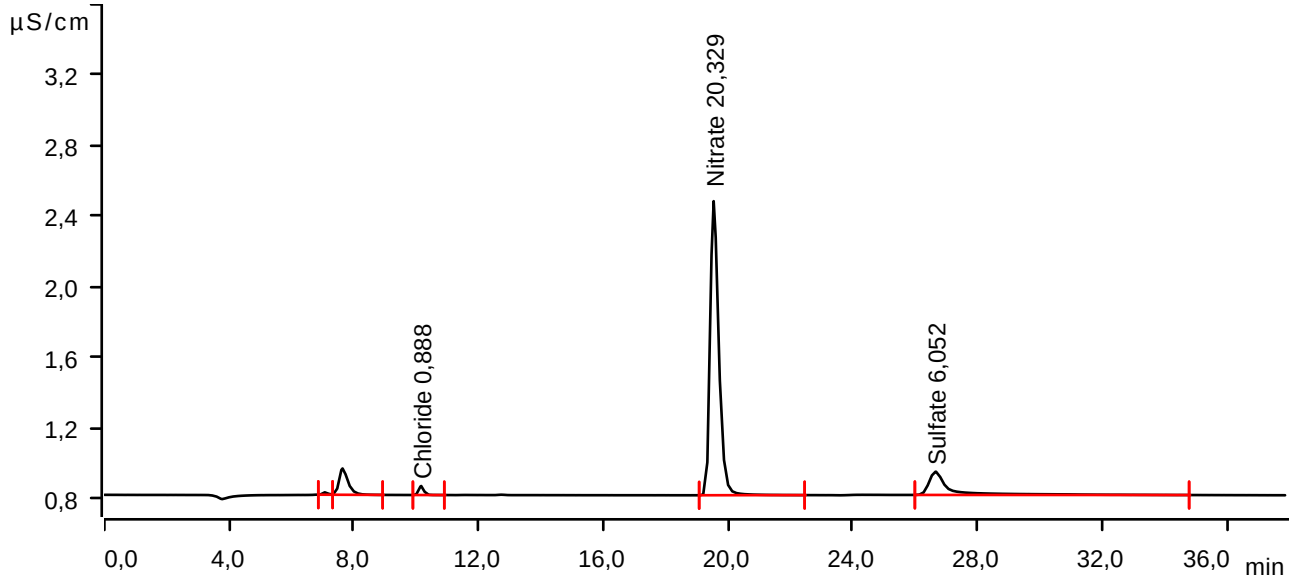

Peak number	Retention time min	Area (µS/cm) x min	Height µS/cm	Concentration mg/L	Component name
1	7,072	0,0028	0,013	invalid	
2	7,638	0,0500	0,149	invalid	
3	10,160	0,0096	0,051	0,888	Chloride
4	19,537	0,5314	1,665	20,329	Nitrate
5	26,650	0,1012	0,132	6,052	Sulfate

Sample data

Ident	EU3	
Sample type	Sample	
Determination start	2021-11-18 18:27:32 UTC+1	
Method	Logisk fortynning NTNU Kjemisk	
Operator		

Anions

Data source	Conductivity detector 1 (940 Professional IC Vario 1)	
Channel	Conductivity	
Recording time	38,0	min
Integration	Manual	
Column type	Metrosep A Supp 7 - 250/4.0	
Eluent composition	Anion Eluent - 3,6 mM Na2CO3	
Flow	0,700	mL/min
Maximum flow monitored	yes	
Pressure	9,85	MPa
Maximum pressure monitored	yes	
Temperature	45,0	°C

Anions

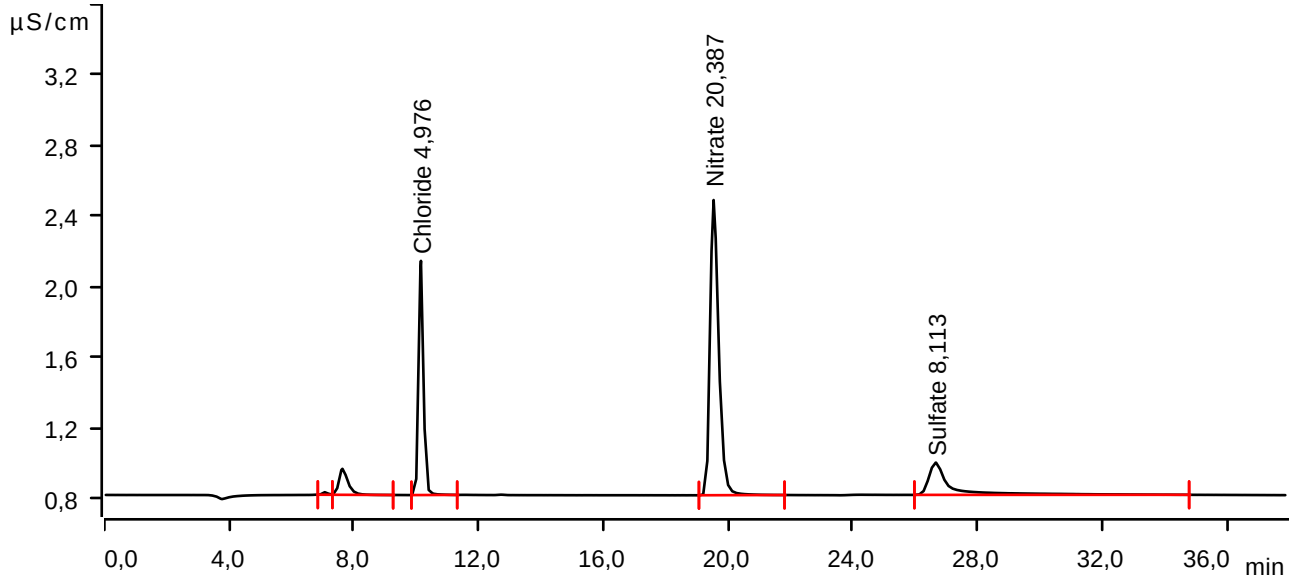

Peak number	Retention time min	Area (µS/cm) x min	Height µS/cm	Concentration mg/L	Component name
1	7,068	0,0030	0,014	invalid	
2	7,635	0,0498	0,147	invalid	
3	10,152	0,2357	1,326	4,976	Chloride
4	19,535	0,5330	1,671	20,387	Nitrate
5	26,657	0,1472	0,183	8,113	Sulfate

Sample data

Ident	EU4	
Sample type	Sample	
Determination start	2021-11-18 19:53:19 UTC+1	
Method	Logisk fortynning NTNU Kjemisk	
Operator		

Anions

Data source	Conductivity detector 1 (940 Professional IC Vario 1)	
Channel	Conductivity	
Recording time	38,0	min
Integration	Manual	
Column type	Metrosep A Supp 7 - 250/4.0	
Eluent composition	Anion Eluent - 3,6 mM Na2CO3	
Flow	0,700	mL/min
Maximum flow monitored	yes	
Pressure	9,91	MPa
Maximum pressure monitored	yes	
Temperature	45,0	°C

Anions

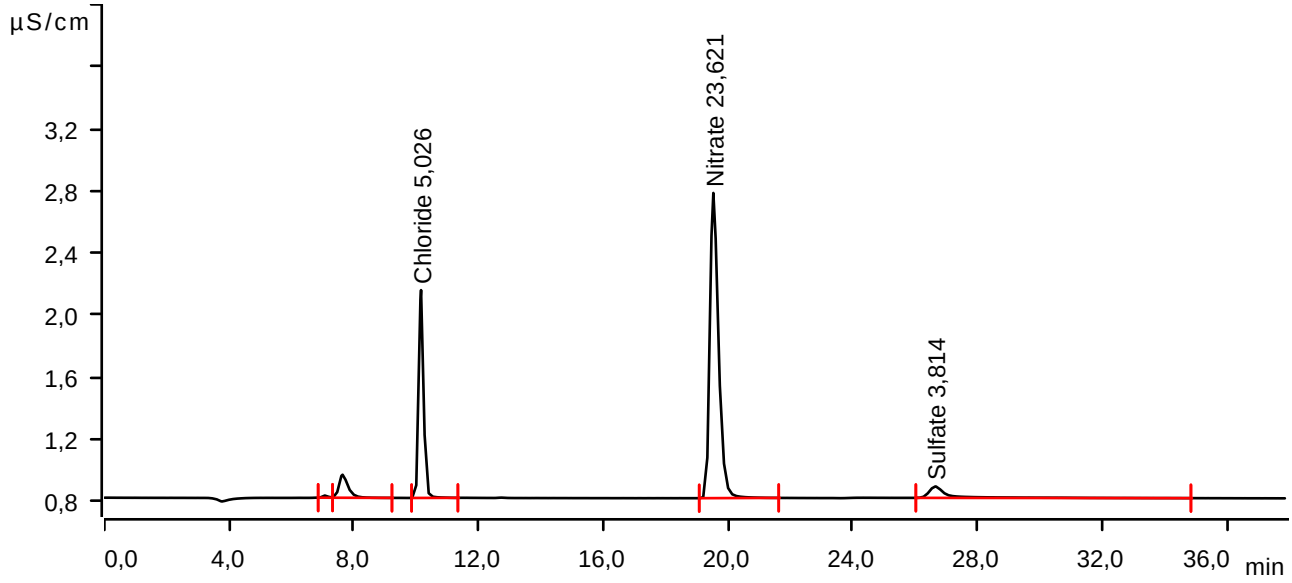

Peak number	Retention time min	Area (µS/cm) x min	Height µS/cm	Concentration mg/L	Component name
1	7,073	0,0029	0,014	invalid	
2	7,638	0,0504	0,148	invalid	
3	10,155	0,2385	1,339	5,026	Chloride
4	19,527	0,6276	1,966	23,621	Nitrate
5	26,642	0,0529	0,074	3,814	Sulfate

Sample data

Ident	EU5	
Sample type	Sample	
Determination start	2021-11-18 19:10:25 UTC+1	
Method	Logisk fortynning NTNU Kjemisk	
Operator		

Anions

Data source	Conductivity detector 1 (940 Professional IC Vario 1)	
Channel	Conductivity	
Recording time	38,0	min
Integration	Manual	
Column type	Metrosep A Supp 7 - 250/4.0	
Eluent composition	Anion Eluent - 3,6 mM Na2CO3	
Flow	0,700	mL/min
Maximum flow monitored	yes	
Pressure	9,91	MPa
Maximum pressure monitored	yes	
Temperature	45,0	°C

Anions

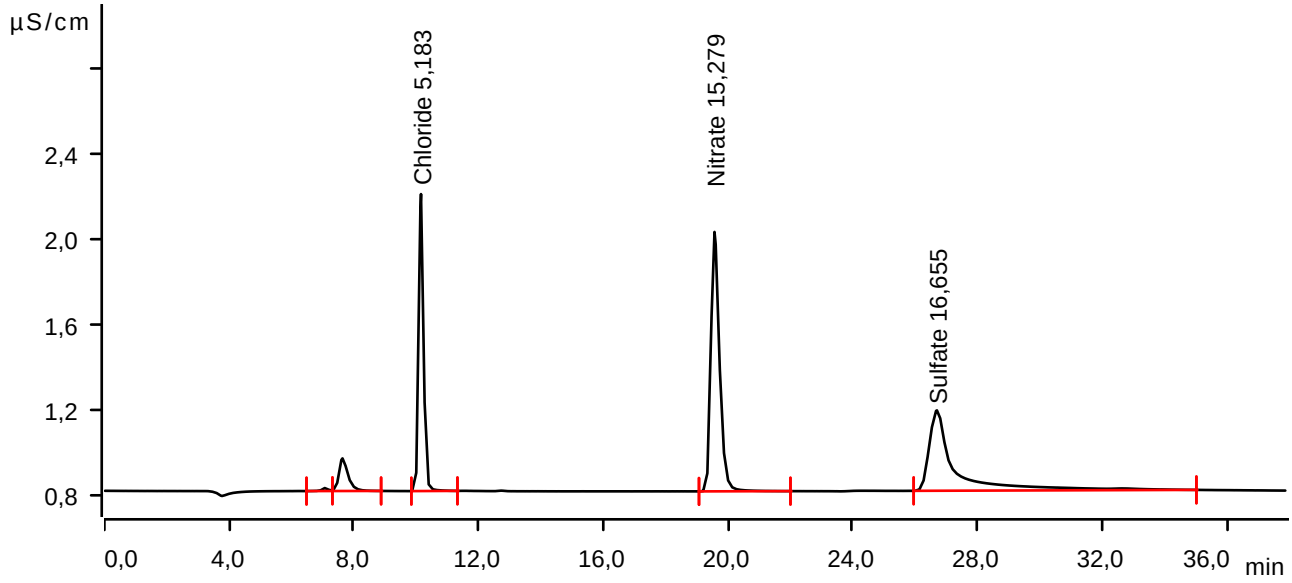

Peak number	Retention time min	Area (µS/cm) x min	Height µS/cm	Concentration mg/L	Component name
1	7,068	0,0033	0,014	invalid	
2	7,637	0,0519	0,153	invalid	
3	10,153	0,2473	1,391	5,183	Chloride
4	19,563	0,3879	1,215	15,279	Nitrate
5	26,695	0,3534	0,377	16,655	Sulfate

Sample data

Ident	EU6
Sample type	Sample
Determination start	2021-11-18 17:44:40 UTC+1
Method	Logisk fortynning NTNU Kjemisk
Operator	

Anions

Data source	Conductivity detector 1 (940 Professional IC Vario 1)	
Channel	Conductivity	
Recording time	38,0	min
Integration	Manual	
Column type	Metrosep A Supp 7 - 250/4.0	
Eluent composition	Anion Eluent - 3,6 mM Na2CO3	
Flow	0,700	mL/min
Maximum flow monitored	yes	
Pressure	9,85	MPa
Maximum pressure monitored	yes	
Temperature	45,0	°C

Anions

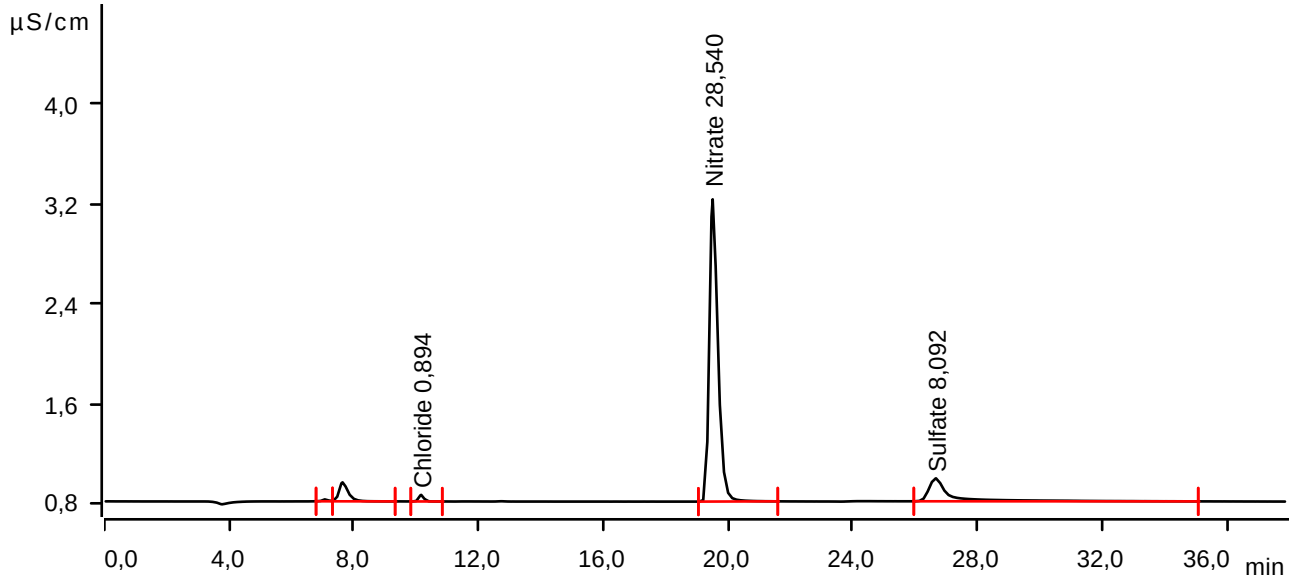

Peak number	Retention time min	Area (µS/cm) x min	Height µS/cm	Concentration mg/L	Component name
1	7,072	0,0033	0,015	invalid	
2	7,638	0,0519	0,152	invalid	
3	10,160	0,0099	0,053	0,894	Chloride
4	19,505	0,7754	2,419	28,540	Nitrate
5	26,657	0,1468	0,184	8,092	Sulfate

Sample data

Ident	EU7_1
Sample type	Sample
Determination start	2021-11-18 14:53:16 UTC+1
Method	Logisk fortynning NTNU Kjemisk
Operator	

Anions

Data source	Conductivity detector 1 (940 Professional IC Vario 1)	
Channel	Conductivity	
Recording time	38,0	min
Integration	Manual	
Column type	Metrosep A Supp 7 - 250/4.0	
Eluent composition	Anion Eluent - 3,6 mM Na2CO3	
Flow	0,700	mL/min
Maximum flow monitored	yes	
Pressure	9,85	MPa
Maximum pressure monitored	yes	
Temperature	45,0	°C

Anions

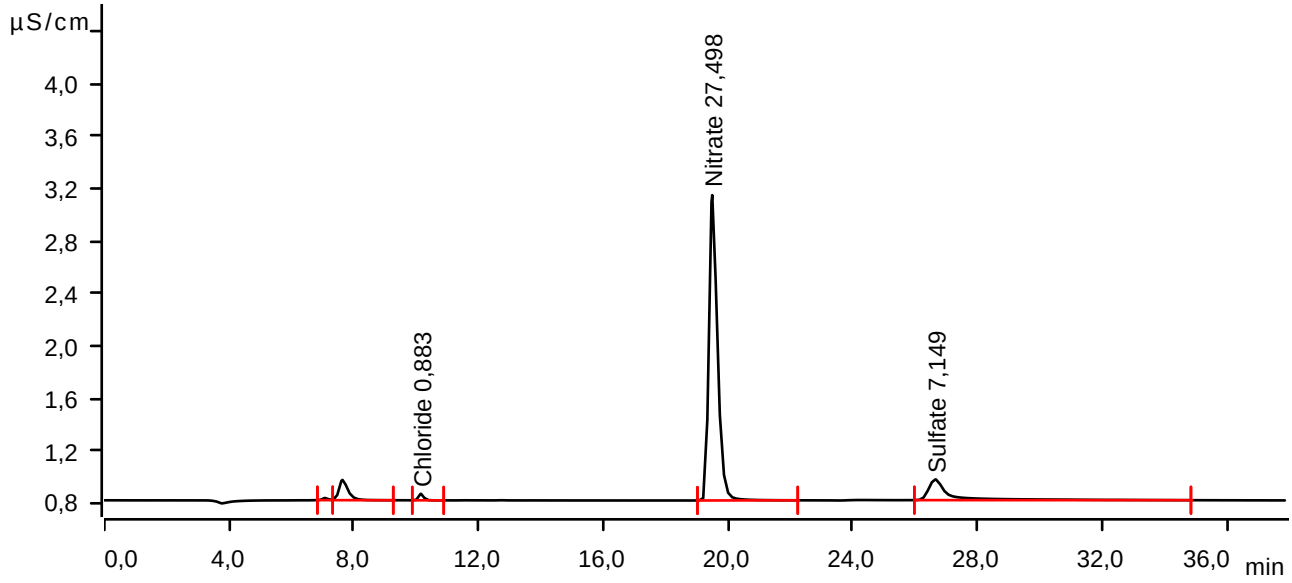

Peak number	Retention time min	Area (µS/cm) x min	Height µS/cm	Concentration mg/L	Component name
1	7,072	0,0036	0,016	invalid	
2	7,637	0,0526	0,154	invalid	
3	10,153	0,0093	0,050	0,883	Chloride
4	19,492	0,7437	2,325	27,498	Nitrate
5	26,643	0,1255	0,158	7,149	Sulfate

Sample data

Ident	EU7_2
Sample type	Sample
Determination start	2021-11-18 15:36:06 UTC+1
Method	Logisk fortynning NTNU Kjemisk
Operator	

Anions

Data source	Conductivity detector 1 (940 Professional IC Vario 1)	
Channel	Conductivity	
Recording time	38,0	min
Integration	Manual	
Column type	Metrosep A Supp 7 - 250/4.0	
Eluent composition	Anion Eluent - 3,6 mM Na2CO3	
Flow	0,700	mL/min
Maximum flow monitored	yes	
Pressure	9,91	MPa
Maximum pressure monitored	yes	
Temperature	45,0	°C

Anions

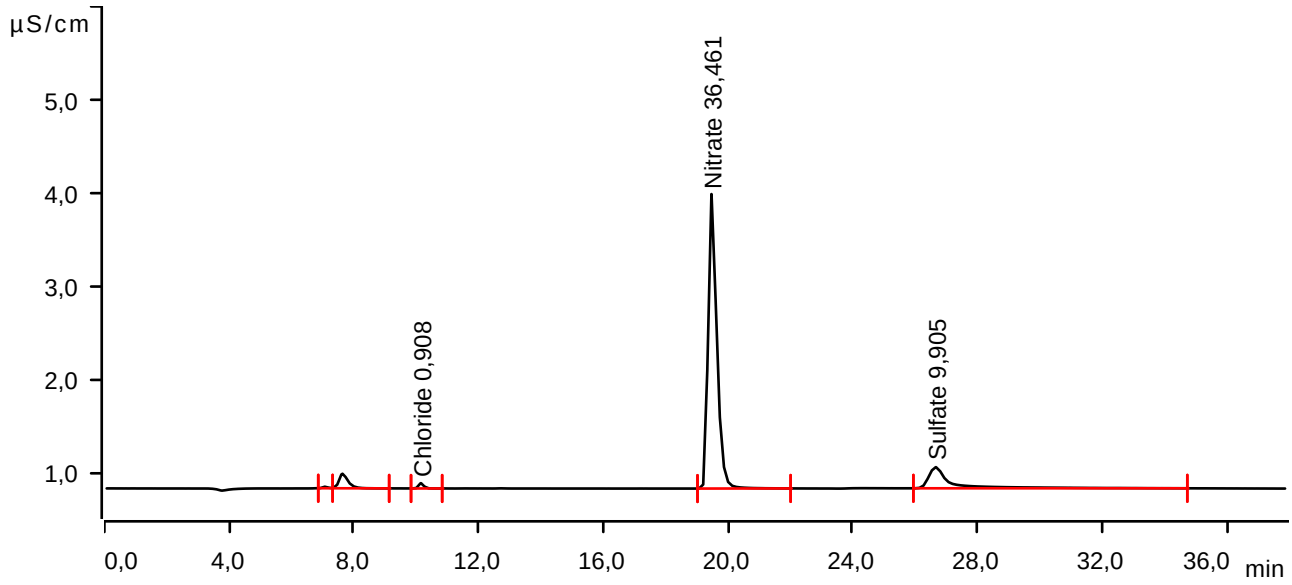

Peak number	Retention time min	Area (µS/cm) x min	Height µS/cm	Concentration mg/L	Component name
1	7,072	0,0035	0,016	invalid	
2	7,638	0,0530	0,156	invalid	
3	10,155	0,0107	0,057	0,908	Chloride
4	19,465	1,0234	3,162	36,461	Nitrate
5	26,657	0,1884	0,227	9,905	Sulfate

Sample data

Ident	EU8
Sample type	Sample
Determination start	2021-11-18 16:18:56 UTC+1
Method	Logisk fortynning NTNU Kjemisk
Operator	

Anions

Data source	Conductivity detector 1 (940 Professional IC Vario 1)	
Channel	Conductivity	
Recording time	38,0	min
Integration	Manual	
Column type	Metrosep A Supp 7 - 250/4.0	
Eluent composition	Anion Eluent - 3,6 mM Na2CO3	
Flow	0,700	mL/min
Maximum flow monitored	yes	
Pressure	9,85	MPa
Maximum pressure monitored	yes	
Temperature	45,0	°C

Anions

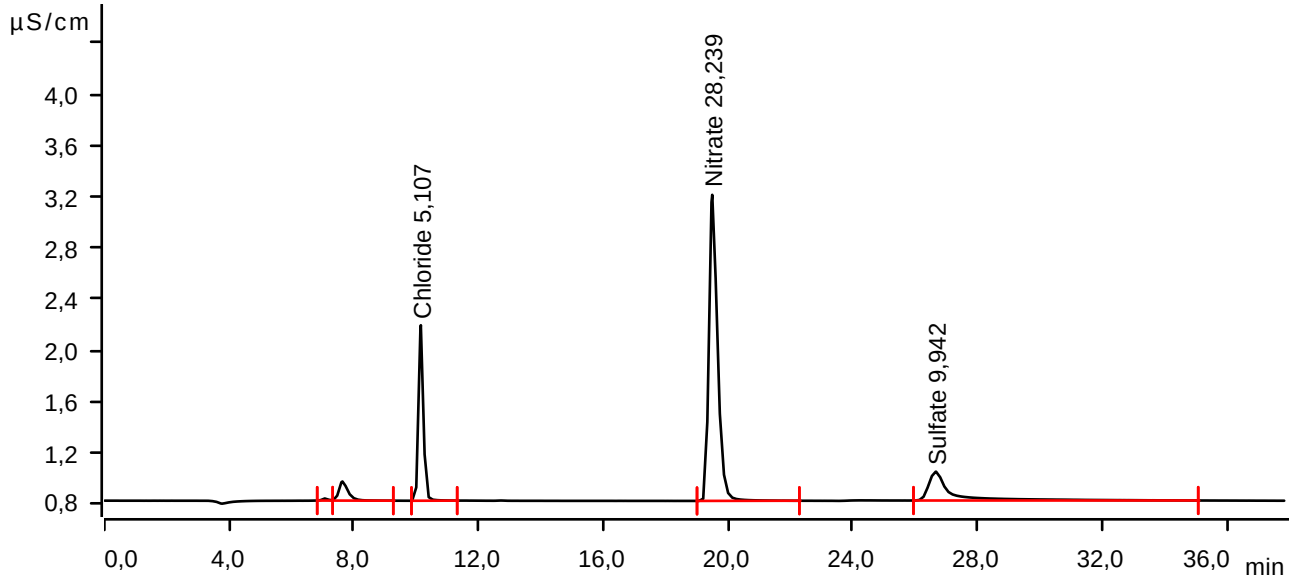

Peak number	Retention time min	Area (µS/cm) x min	Height µS/cm	Concentration mg/L	Component name
1	7,068	0,0035	0,016	invalid	
2	7,635	0,0509	0,149	invalid	
3	10,148	0,2430	1,370	5,107	Chloride
4	19,492	0,7662	2,390	28,239	Nitrate
5	26,657	0,1893	0,225	9,942	Sulfate

A.5.2 Hydroponic samples, Batch 2

The following pages show the results of the ion chromatography analysis of the second batch of hydroponic samples. The results are presented chronologically from 1 to 8.

Sample data

Ident	Jostein EU1
Sample type	Sample
Determination start	2022-03-31 15:30:32 UTC+2
Method	Logisk fortynning NTNU Kjemisk
Operator	

Anions

Data source	Conductivity detector 1 (940 Professional IC Vario 1)	
Channel	Conductivity	
Recording time	38,0	min
Integration	Manual	
Column type	Metrosep A Supp 7 - 250/4.0	
Eluent composition	Anion Eluent - 3,6 mM Na2CO3	
Flow	0,700	mL/min
Maximum flow monitored	yes	
Pressure	10,14	MPa
Maximum pressure monitored	yes	
Temperature	45,0	°C

Anions

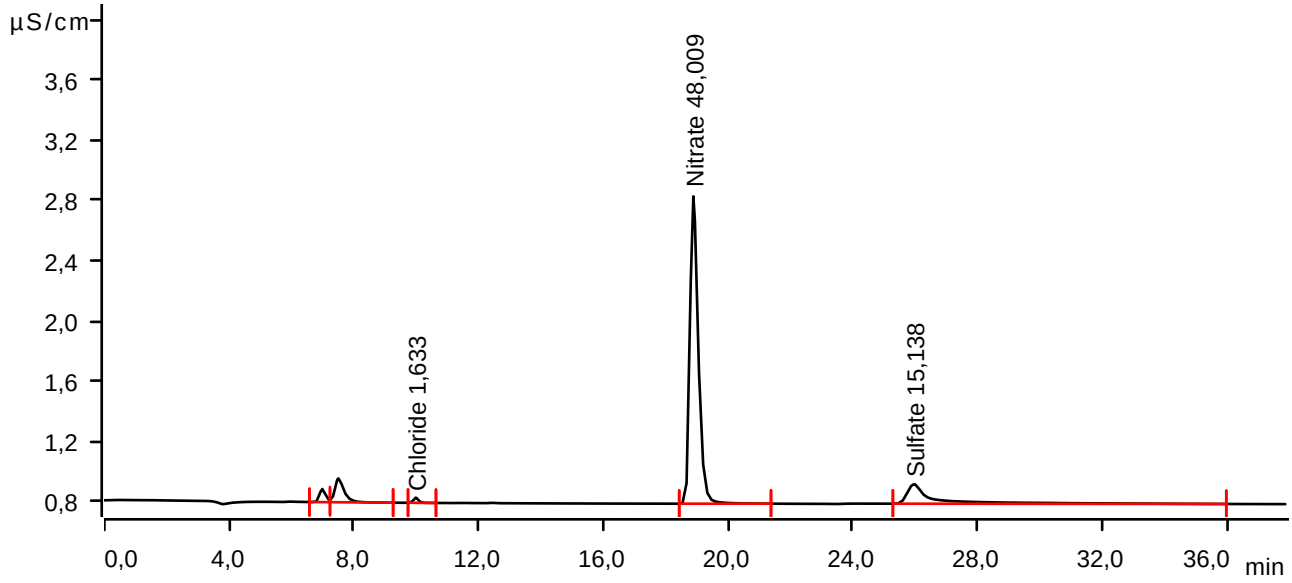

Peak number	Retention time min	Area (µS/cm) x min	Height µS/cm	Concentration mg/L	Component name
1	6,988	0,0194	0,087	invalid	
2	7,507	0,0553	0,158	invalid	
3	9,983	0,0064	0,034	1,633	Chloride
4	18,885	0,6342	2,040	48,009	Nitrate
5	25,960	0,1325	0,130	15,138	Sulfate

Sample data

Ident	Jostein EU2
Sample type	Sample
Determination start	2022-03-31 16:16:54 UTC+2
Method	Logisk fortynning NTNU Kjemisk
Operator	

Anions

Data source	Conductivity detector 1 (940 Professional IC Vario 1)	
Channel	Conductivity	
Recording time	38,0	min
Integration	Manual	
Column type	Metrosep A Supp 7 - 250/4.0	
Eluent composition	Anion Eluent - 3,6 mM Na2CO3	
Flow	0,700	mL/min
Maximum flow monitored	yes	
Pressure	9,97	MPa
Maximum pressure monitored	yes	
Temperature	45,0	°C

Anions

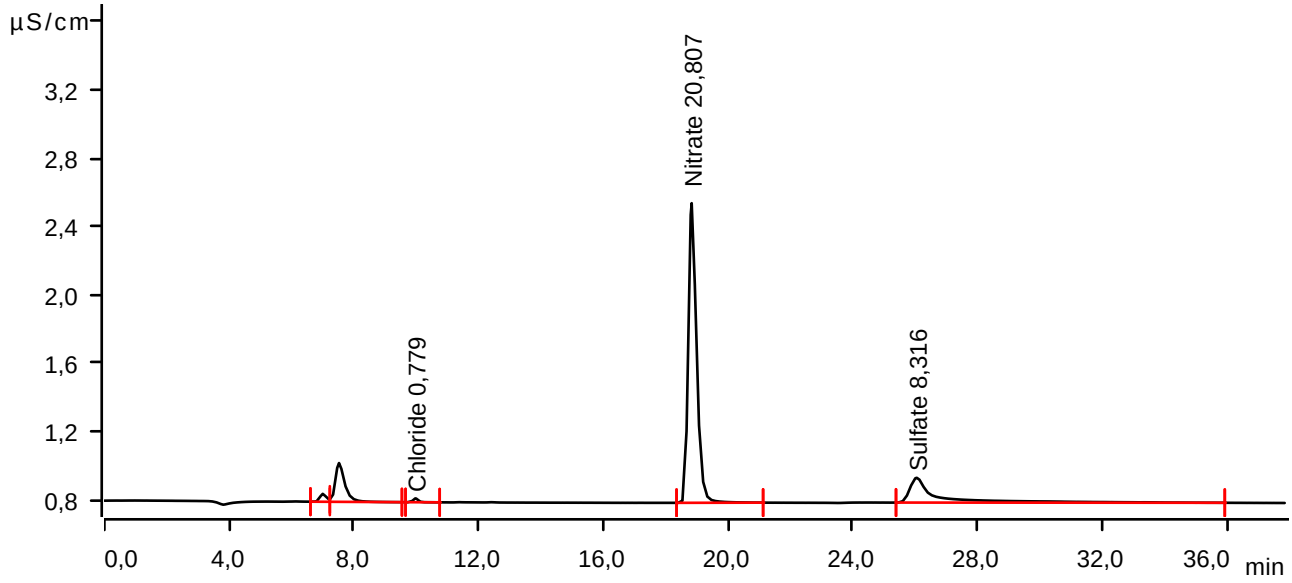

Peak number	Retention time min	Area (µS/cm) x min	Height µS/cm	Concentration mg/L	Component name
1	7,002	0,0109	0,046	invalid	
2	7,525	0,0801	0,227	invalid	
3	9,972	0,0043	0,023	0,779	Chloride
4	18,832	0,5420	1,755	20,807	Nitrate
5	26,048	0,1490	0,145	8,316	Sulfate

Sample data

Ident	Jostein EU3
Sample type	Sample
Determination start	2022-03-31 16:59:44 UTC+2
Method	Logisk fortynning NTNU Kjemisk
Operator	

Anions

Data source	Conductivity detector 1 (940 Professional IC Vario 1)	
Channel	Conductivity	
Recording time	38,0	min
Integration	Manual	
Column type	Metrosep A Supp 7 - 250/4.0	
Eluent composition	Anion Eluent - 3,6 mM Na2CO3	
Flow	0,700	mL/min
Maximum flow monitored	yes	
Pressure	9,91	MPa
Maximum pressure monitored	yes	
Temperature	45,0	°C

Anions

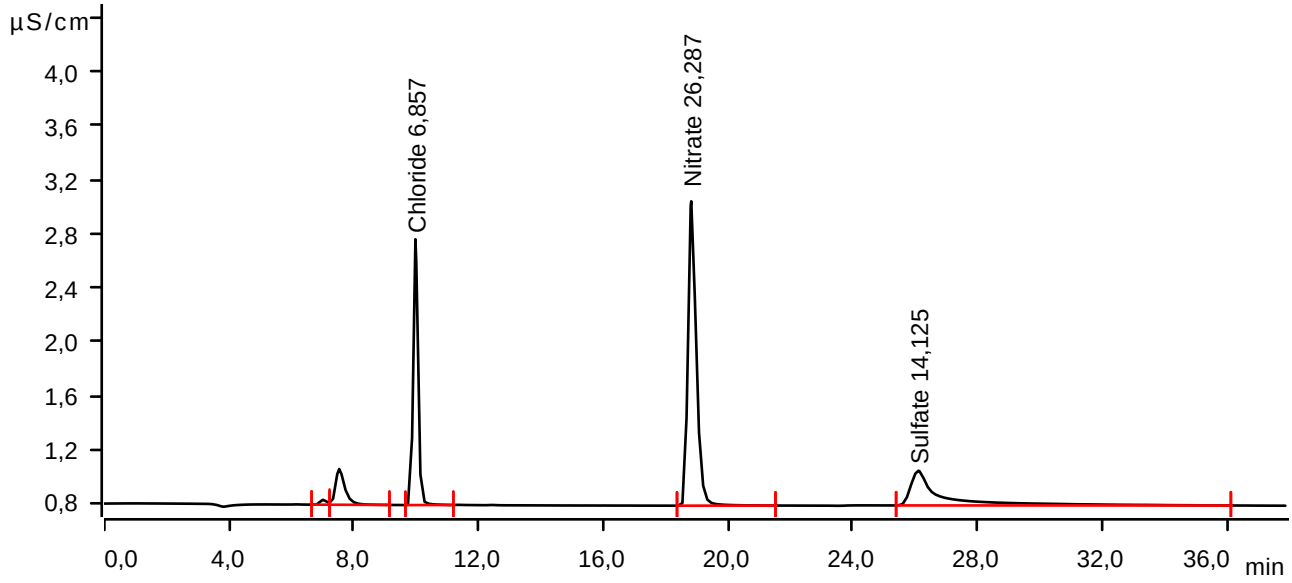

Peak number	Retention time min	Area (µS/cm) x min	Height µS/cm	Concentration mg/L	Component name
1	7,008	0,0087	0,036	invalid	
2	7,532	0,0931	0,265	invalid	
3	9,973	0,3482	1,972	6,857	Chloride
4	18,818	0,7011	2,258	26,287	Nitrate
5	26,098	0,2880	0,257	14,125	Sulfate

Sample data

Ident	Jostein EU4
Sample type	Sample
Determination start	2022-03-31 17:42:33 UTC+2
Method	Logisk fortynning NTNU Kjemisk
Operator	

Anions

Data source	Conductivity detector 1 (940 Professional IC Vario 1)	
Channel	Conductivity	
Recording time	38,0	min
Integration	Manual	
Column type	Metrosep A Supp 7 - 250/4.0	
Eluent composition	Anion Eluent - 3,6 mM Na2CO3	
Flow	0,700	mL/min
Maximum flow monitored	yes	
Pressure	9,85	MPa
Maximum pressure monitored	yes	
Temperature	45,0	°C

Anions

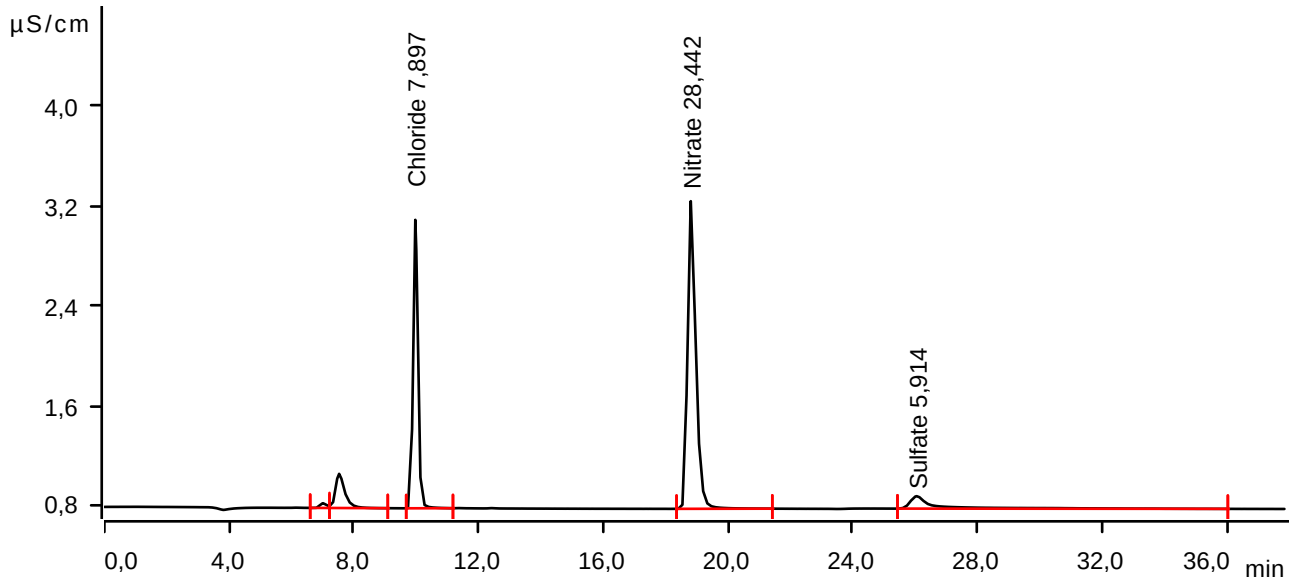

Peak number	Retention time min	Area (µS/cm) x min	Height µS/cm	Concentration mg/L	Component name
1	7,005	0,0090	0,038	invalid	
2	7,528	0,0955	0,273	invalid	
3	9,970	0,4075	2,309	7,897	Chloride
4	18,803	0,7651	2,462	28,442	Nitrate
5	26,047	0,0970	0,099	5,914	Sulfate

Sample data

Ident	Jostein EU5
Sample type	Sample
Determination start	2022-03-31 18:25:22 UTC+2
Method	Logisk fortynning NTNU Kjemisk
Operator	

Anions

Data source	Conductivity detector 1 (940 Professional IC Vario 1)	
Channel	Conductivity	
Recording time	38,0	min
Integration	Manual	
Column type	Metrosep A Supp 7 - 250/4.0	
Eluent composition	Anion Eluent - 3,6 mM Na2CO3	
Flow	0,700	mL/min
Maximum flow monitored	yes	
Pressure	9,85	MPa
Maximum pressure monitored	yes	
Temperature	45,0	°C

Anions

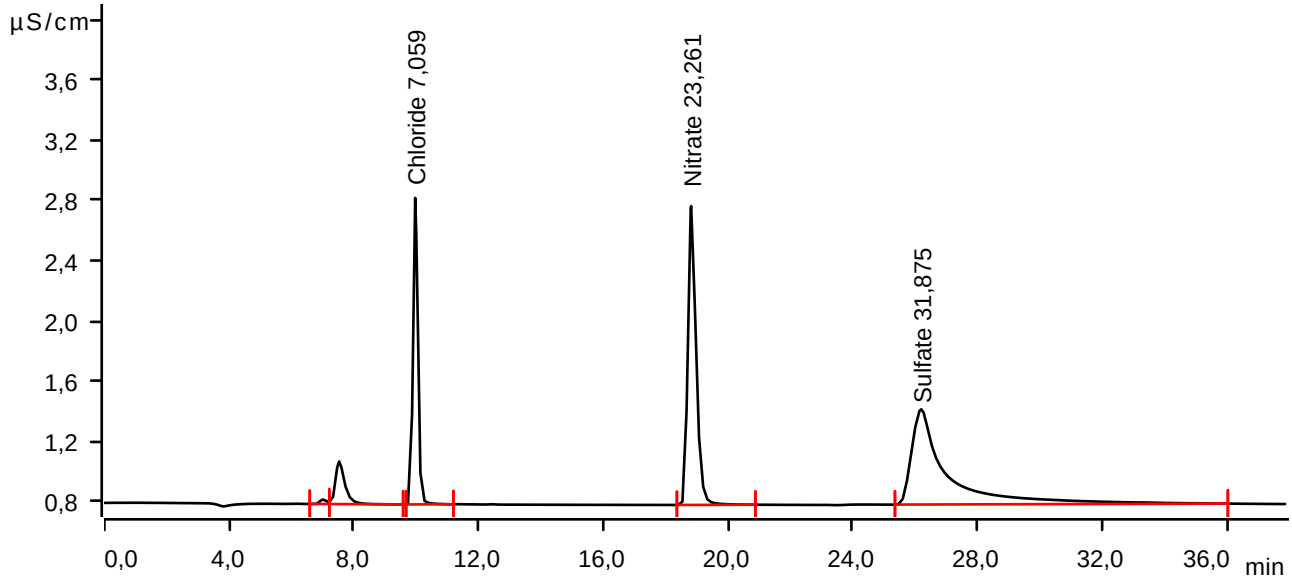

Peak number	Retention time min	Area (µS/cm) x min	Height µS/cm	Concentration mg/L	Component name
1	7,003	0,0073	0,030	invalid	
2	7,528	0,0999	0,283	invalid	
3	9,967	0,3597	2,034	7,059	Chloride
4	18,815	0,6126	1,983	23,261	Nitrate
5	26,193	0,8287	0,632	31,875	Sulfate

Sample data

Ident	Jostein EU6
Sample type	Sample
Determination start	2022-03-31 19:08:10 UTC+2
Method	Logisk fortynning NTNU Kjemisk
Operator	

Anions

Data source	Conductivity detector 1 (940 Professional IC Vario 1)	
Channel	Conductivity	
Recording time	38,0	min
Integration	Manual	
Column type	Metrosep A Supp 7 - 250/4.0	
Eluent composition	Anion Eluent - 3,6 mM Na2CO3	
Flow	0,700	mL/min
Maximum flow monitored	yes	
Pressure	9,91	MPa
Maximum pressure monitored	yes	
Temperature	45,0	°C

Anions

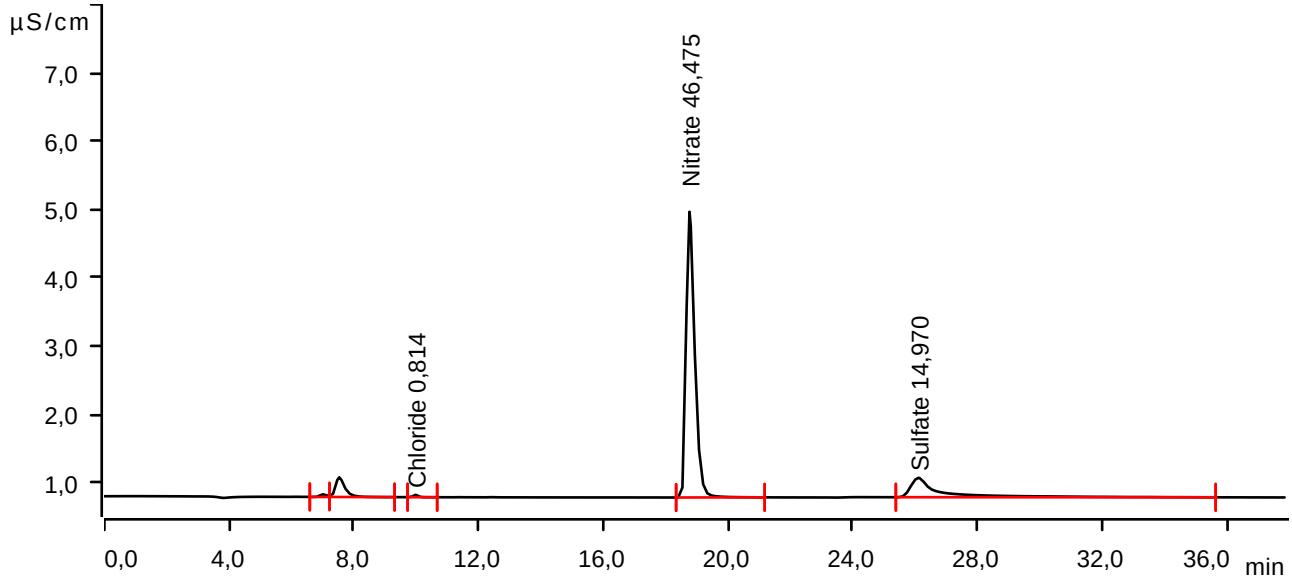

Peak number	Retention time min	Area (µS/cm) x min	Height µS/cm	Concentration mg/L	Component name
1	7,008	0,0090	0,038	invalid	
2	7,532	0,1012	0,288	invalid	
3	9,977	0,0063	0,034	0,814	Chloride
4	18,762	1,3306	4,183	46,475	Nitrate
5	26,105	0,3098	0,284	14,970	Sulfate

Sample data

Ident	Jostein EU7
Sample type	Sample
Determination start	2022-03-31 19:50:57 UTC+2
Method	Logisk fortynning NTNU Kjemisk
Operator	

Anions

Data source	Conductivity detector 1 (940 Professional IC Vario 1)	
Channel	Conductivity	
Recording time	38,0	min
Integration	Manual	
Column type	Metrosep A Supp 7 - 250/4.0	
Eluent composition	Anion Eluent - 3,6 mM Na2CO3	
Flow	0,700	mL/min
Maximum flow monitored	yes	
Pressure	9,91	MPa
Maximum pressure monitored	yes	
Temperature	45,0	°C

Anions

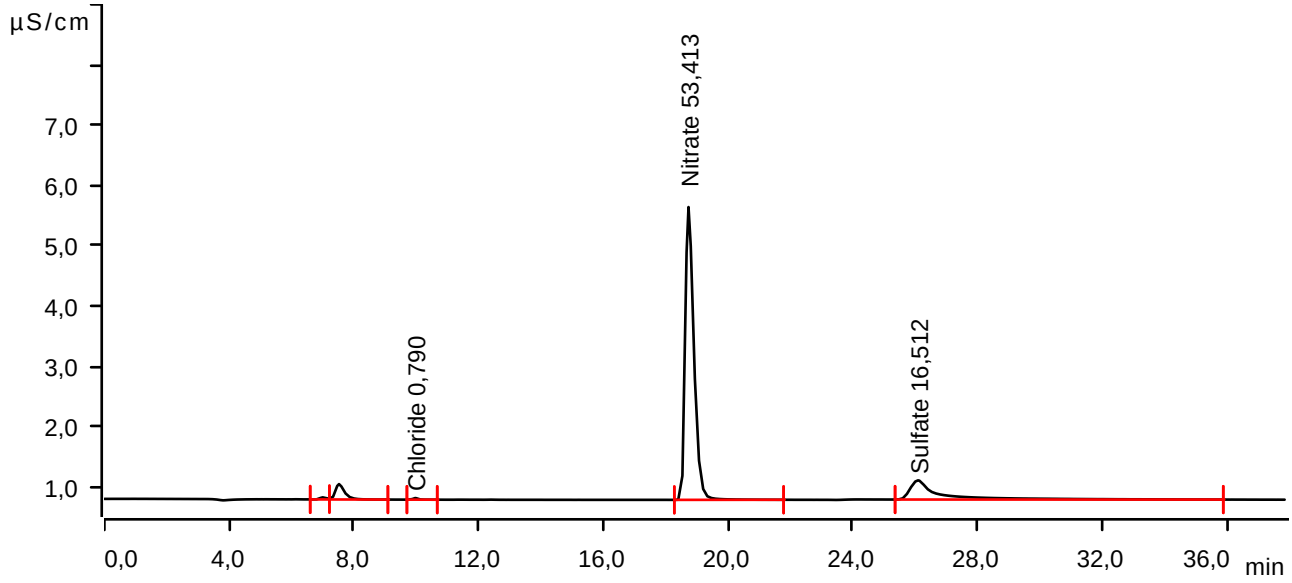

Peak number	Retention time min	Area (µS/cm) x min	Height µS/cm	Concentration mg/L	Component name
1	7,000	0,0081	0,034	invalid	
2	7,525	0,0886	0,255	invalid	
3	9,968	0,0049	0,026	0,790	Chloride
4	18,730	1,5626	4,859	53,413	Nitrate
5	26,090	0,3506	0,318	16,512	Sulfate

Sample data

Ident	Jostein EU8
Sample type	Sample
Determination start	2022-03-31 20:33:44 UTC+2
Method	Logisk fortynning NTNU Kjemisk
Operator	

Anions

Data source	Conductivity detector 1 (940 Professional IC Vario 1)	
Channel	Conductivity	
Recording time	38,0	min
Integration	Manual	
Column type	Metrosep A Supp 7 - 250/4.0	
Eluent composition	Anion Eluent - 3,6 mM Na2CO3	
Flow	0,700	mL/min
Maximum flow monitored	yes	
Pressure	9,85	MPa
Maximum pressure monitored	yes	
Temperature	45,0	°C

Anions

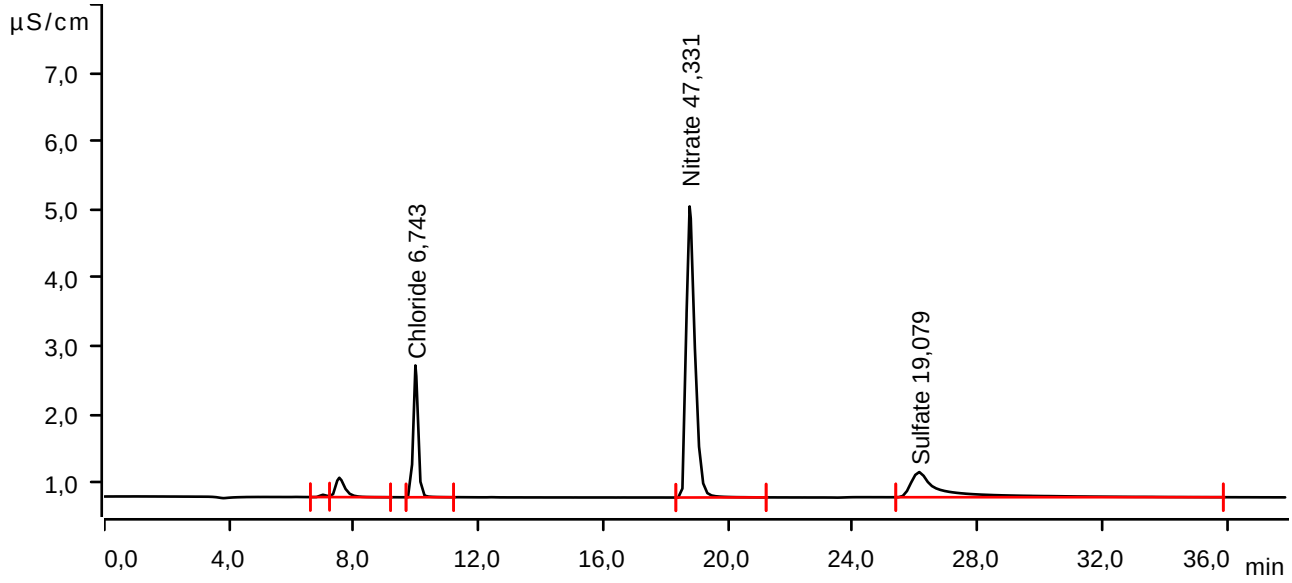

Peak number	Retention time min	Area (µS/cm) x min	Height µS/cm	Concentration mg/L	Component name
1	7,008	0,0080	0,034	invalid	
2	7,533	0,0998	0,284	invalid	
3	9,973	0,3417	1,930	6,743	Chloride
4	18,765	1,3588	4,262	47,331	Nitrate
5	26,125	0,4214	0,367	19,079	Sulfate

A.5.3 Flow cell experiment

The following pages show the results of ion chromatography analysis of samples collected from the flow cell experiment. Sample nomenclature is somewhat different than presented in table 4.7. Sample 1 and 2 was collected on the same day, and have been named W2D1 in the accompanying files. Sample numbering and naming are then as such: The following pages show the IC results in chronological order.

IC Sample name	Sample, table 4.7
W2D1	1 & 2
W2D2	3
W3D1	4
W3D2	5
W4D1	6
W4D2	7
W5D1	8
W5D2	9 & 10
W0D0	11 & 12

Sample data

Ident	W2D1
Sample type	Sample
Determination start	2022-05-12 14:54:15 UTC+2
Method	Logisk fortynning NTNU Kjemisk
Operator	

Anions

Data source	Conductivity detector 1 (940 Professional IC Vario 1)	
Channel	Conductivity	
Recording time	38,0	min
Integration	Automatically	
Column type	Metrosep A Supp 7 - 250/4.0	
Eluent composition	Anion Eluent - 3,6 mM Na2CO3	
Flow	0,700	mL/min
Maximum flow monitored	yes	
Pressure	9,80	MPa
Maximum pressure monitored	yes	
Temperature	45,0	°C

Anions

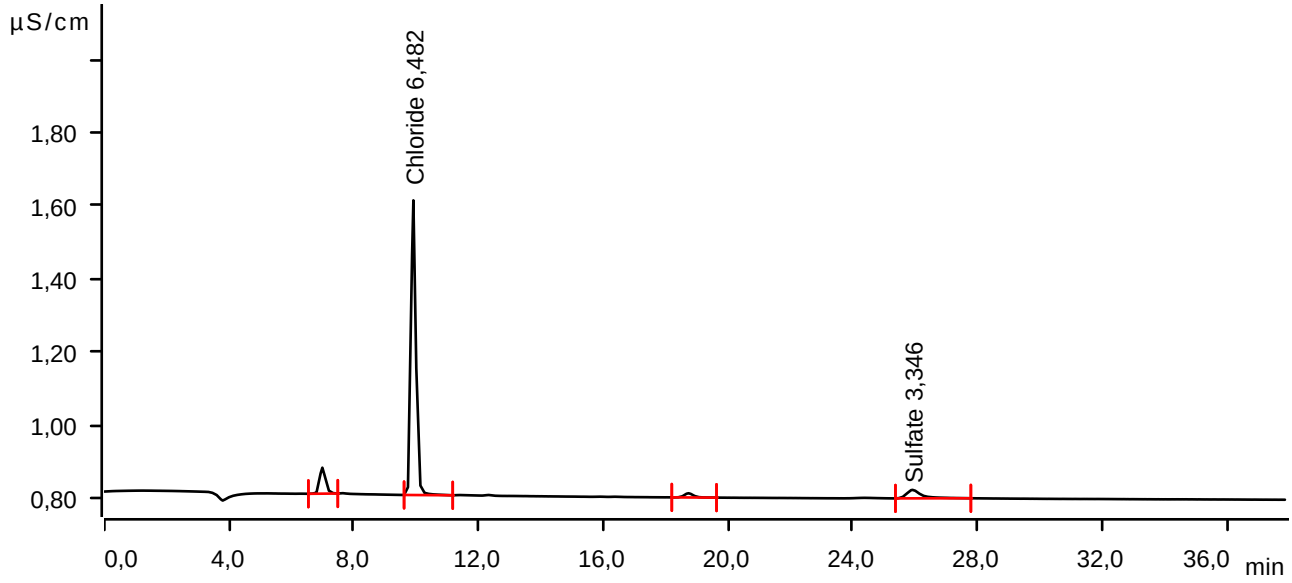

Peak number	Retention time min	Area (µS/cm) x min	Height µS/cm	Concentration mg/L	Component name
1	6,990	0,0155	0,071	invalid	
2	9,908	0,1431	0,805	6,482	Chloride
3	18,733	0,0039	0,012	invalid	
4	25,915	0,0129	0,023	3,346	Sulfate

Sample data

Ident	W2D2
Sample type	Sample
Determination start	2022-05-12 15:36:42 UTC+2
Method	Logisk fortynning NTNU Kjemisk
Operator	

Anions

Data source	Conductivity detector 1 (940 Professional IC Vario 1)	
Channel	Conductivity	
Recording time	38,0	min
Integration	Automatically	
Column type	Metrosep A Supp 7 - 250/4.0	
Eluent composition	Anion Eluent - 3,6 mM Na2CO3	
Flow	0,700	mL/min
Maximum flow monitored	yes	
Pressure	9,85	MPa
Maximum pressure monitored	yes	
Temperature	45,0	°C

Anions

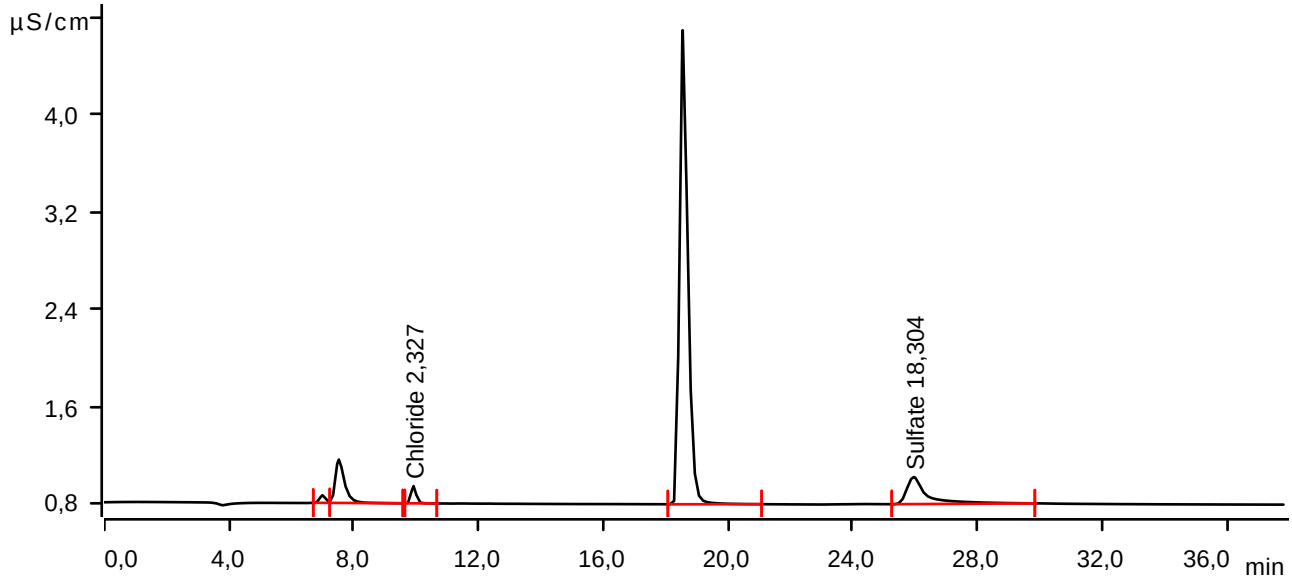

Peak number	Retention time min	Area (µS/cm) x min	Height µS/cm	Concentration mg/L	Component name
1	6,993	0,0131	0,062	invalid	
2	7,518	0,1231	0,356	invalid	
3	9,915	0,0259	0,142	2,327	Chloride
4	18,545	1,2103	3,887	invalid	
5	25,952	0,1678	0,222	18,304	Sulfate

Sample data

Ident	W3D1
Sample type	Sample
Determination start	2022-05-12 16:19:09 UTC+2
Method	Logisk fortynning NTNU Kjemisk
Operator	

Anions

Data source	Conductivity detector 1 (940 Professional IC Vario 1)	
Channel	Conductivity	
Recording time	38,0	min
Integration	Automatically	
Column type	Metrosep A Supp 7 - 250/4.0	
Eluent composition	Anion Eluent - 3,6 mM Na2CO3	
Flow	0,700	mL/min
Maximum flow monitored	yes	
Pressure	9,80	MPa
Maximum pressure monitored	yes	
Temperature	45,0	°C

Anions

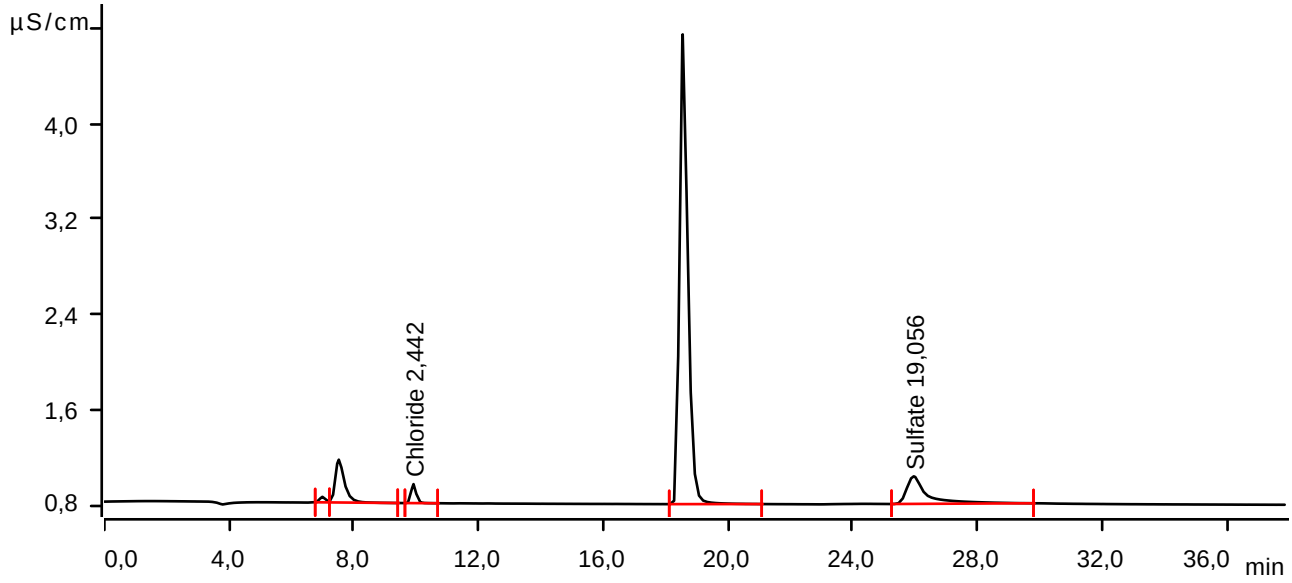

Peak number	Retention time min	Area (µS/cm) x min	Height µS/cm	Concentration mg/L	Component name
1	6,992	0,0094	0,046	invalid	
2	7,517	0,1231	0,359	invalid	
3	9,913	0,0292	0,160	2,442	Chloride
4	18,543	1,2282	3,943	invalid	
5	25,952	0,1765	0,231	19,056	Sulfate

Sample data

Ident	W3D2
Sample type	Sample
Determination start	2022-05-12 17:01:36 UTC+2
Method	Logisk fortynning NTNU Kjemisk
Operator	

Anions

Data source	Conductivity detector 1 (940 Professional IC Vario 1)	
Channel	Conductivity	
Recording time	38,0	min
Integration	Automatically	
Column type	Metrosep A Supp 7 - 250/4.0	
Eluent composition	Anion Eluent - 3,6 mM Na2CO3	
Flow	0,700	mL/min
Maximum flow monitored	yes	
Pressure	9,85	MPa
Maximum pressure monitored	yes	
Temperature	45,0	°C

Anions

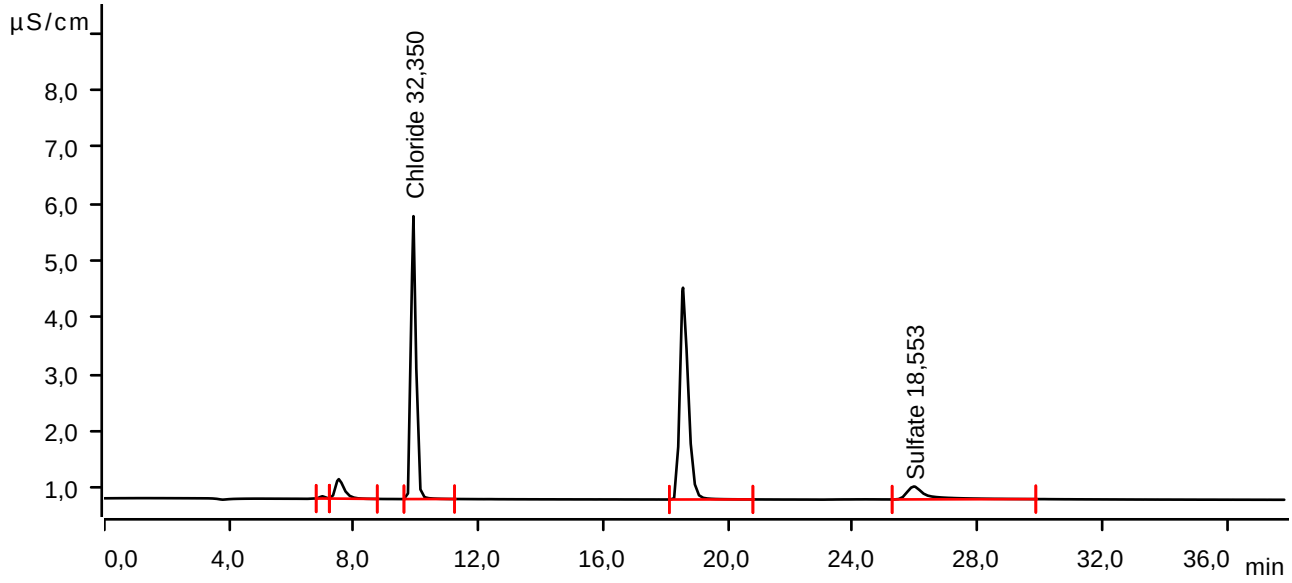

Peak number	Retention time min	Area (µS/cm) x min	Height µS/cm	Concentration mg/L	Component name
1	6,992	0,0076	0,040	invalid	
2	7,517	0,1143	0,343	invalid	
3	9,912	0,8844	4,971	32,350	Chloride
4	18,555	1,1558	3,721	invalid	
5	25,957	0,1707	0,226	18,553	Sulfate

Sample data

Ident	W4D1	
Sample type	Sample	
Determination start	2022-05-12 17:44:04 UTC+2	
Method	Logisk fortynning NTNU Kjemisk	
Operator		

Anions

Data source	Conductivity detector 1 (940 Professional IC Vario 1)	
Channel	Conductivity	
Recording time	38,0	min
Integration	Automatically	
Column type	Metrosep A Supp 7 - 250/4.0	
Eluent composition	Anion Eluent - 3,6 mM Na2CO3	
Flow	0,700	mL/min
Maximum flow monitored	yes	
Pressure	9,80	MPa
Maximum pressure monitored	yes	
Temperature	45,0	°C

Anions

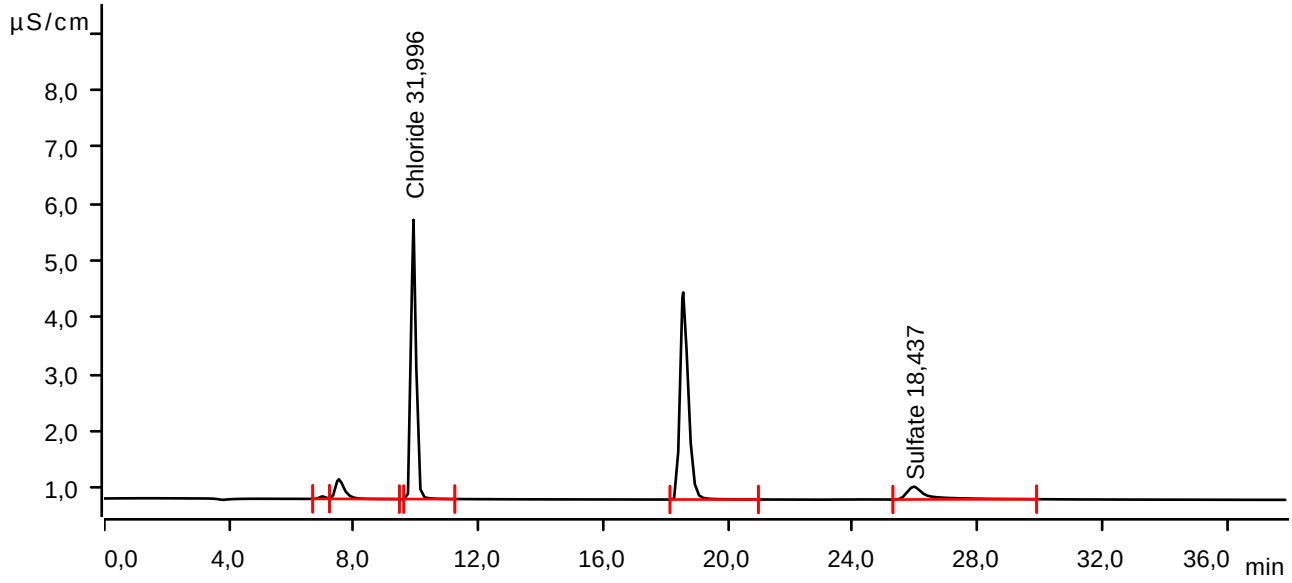

Peak number	Retention time min	Area (µS/cm) x min	Height µS/cm	Concentration mg/L	Component name
1	6,993	0,0093	0,044	invalid	
2	7,518	0,1198	0,346	invalid	
3	9,913	0,8741	4,907	31,996	Chloride
4	18,560	1,1301	3,638	invalid	
5	25,957	0,1694	0,224	18,437	Sulfate

Sample data

Ident	W4D2
Sample type	Sample
Determination start	2022-05-24 16:37:51 UTC+2
Method	Logisk fortynning NTNU Kjemisk
Operator	

Anions

Data source	Conductivity detector 1 (940 Professional IC Vario 1)	
Channel	Conductivity	
Recording time	38,0	min
Integration	Automatically	
Column type	Metrosep A Supp 7 - 250/4.0	
Eluent composition	Anion Eluent - 3,6 mM Na2CO3	
Flow	0,700	mL/min
Maximum flow monitored	yes	
Pressure	9,85	MPa
Maximum pressure monitored	yes	
Temperature	45,0	°C

Anions

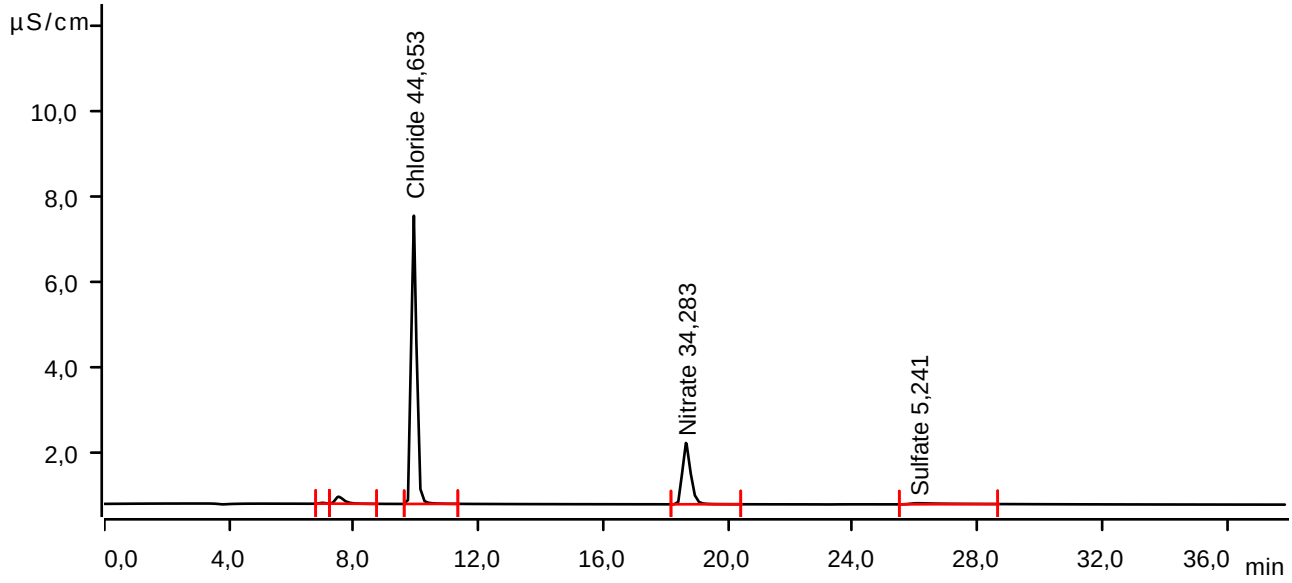

Peak number	Retention time min	Area (µS/cm) x min	Height µS/cm	Concentration mg/L	Component name
1	6,993	0,0039	0,020	invalid	
2	7,515	0,0535	0,165	invalid	
3	9,925	1,2442	6,753	44,653	Chloride
4	18,647	0,4384	1,437	34,283	Nitrate
5	26,098	0,0308	0,025	5,241	Sulfate

Sample data

Ident	W5D1	
Sample type	Sample	
Determination start	2022-05-24 15:55:27 UTC+2	
Method	Logisk fortynning NTNU Kjemisk	
Operator		

Anions

Data source	Conductivity detector 1 (940 Professional IC Vario 1)	
Channel	Conductivity	
Recording time	38,0	min
Integration	Automatically	
Column type	Metrosep A Supp 7 - 250/4.0	
Eluent composition	Anion Eluent - 3,6 mM Na2CO3	
Flow	0,700	mL/min
Maximum flow monitored	yes	
Pressure	9,85	MPa
Maximum pressure monitored	yes	
Temperature	45,0	°C

Anions

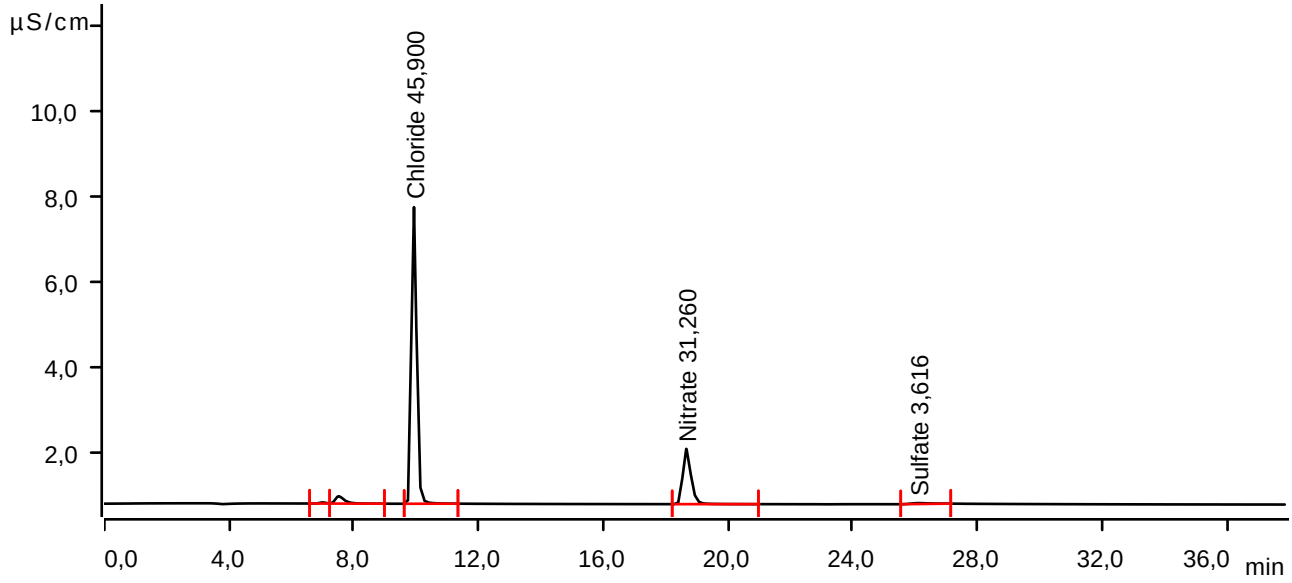

Peak number	Retention time min	Area (µS/cm) x min	Height µS/cm	Concentration mg/L	Component name
1	6,995	0,0062	0,028	invalid	
2	7,518	0,0594	0,174	invalid	
3	9,928	1,2810	6,949	45,900	Chloride
4	18,657	0,3963	1,295	31,260	Nitrate
5	26,097	0,0154	0,021	3,616	Sulfate

Sample data

Ident	W5D2
Sample type	Sample
Determination start	2022-05-24 17:20:16 UTC+2
Method	Logisk fortynning NTNU Kjemisk
Operator	

Anions

Data source	Conductivity detector 1 (940 Professional IC Vario 1)	
Channel	Conductivity	
Recording time	38,0	min
Integration	Automatically	
Column type	Metrosep A Supp 7 - 250/4.0	
Eluent composition	Anion Eluent - 3,6 mM Na2CO3	
Flow	0,700	mL/min
Maximum flow monitored	yes	
Pressure	9,85	MPa
Maximum pressure monitored	yes	
Temperature	45,0	°C

Anions

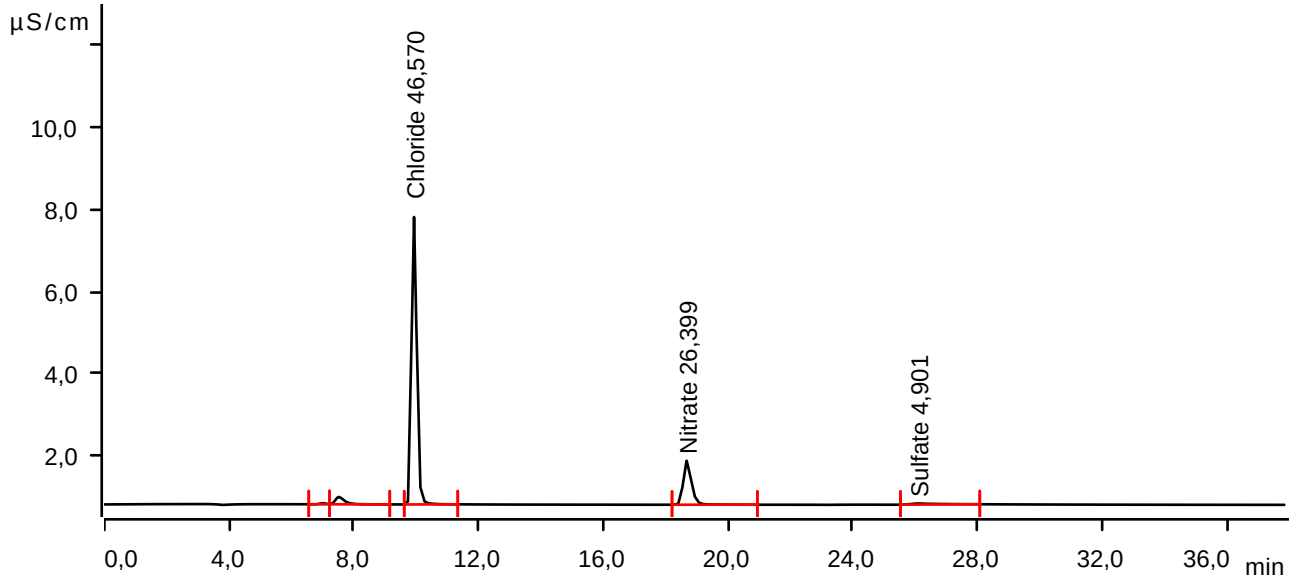

Peak number	Retention time min	Area (µS/cm) x min	Height µS/cm	Concentration mg/L	Component name
1	7,000	0,0059	0,025	invalid	
2	7,522	0,0628	0,181	invalid	
3	9,930	1,3007	7,015	46,570	Chloride
4	18,672	0,3294	1,073	26,399	Nitrate
5	26,108	0,0276	0,027	4,901	Sulfate

Sample data

Ident	W0D0
Sample type	Sample
Determination start	2022-05-24 18:02:41 UTC+2
Method	Logisk fortynning NTNU Kjemisk
Operator	

Anions

Data source	Conductivity detector 1 (940 Professional IC Vario 1)	
Channel	Conductivity	
Recording time	38,0	min
Integration	Automatically	
Column type	Metrosep A Supp 7 - 250/4.0	
Eluent composition	Anion Eluent - 3,6 mM Na2CO3	
Flow	0,700	mL/min
Maximum flow monitored	yes	
Pressure	9,85	MPa
Maximum pressure monitored	yes	
Temperature	45,0	°C

Anions

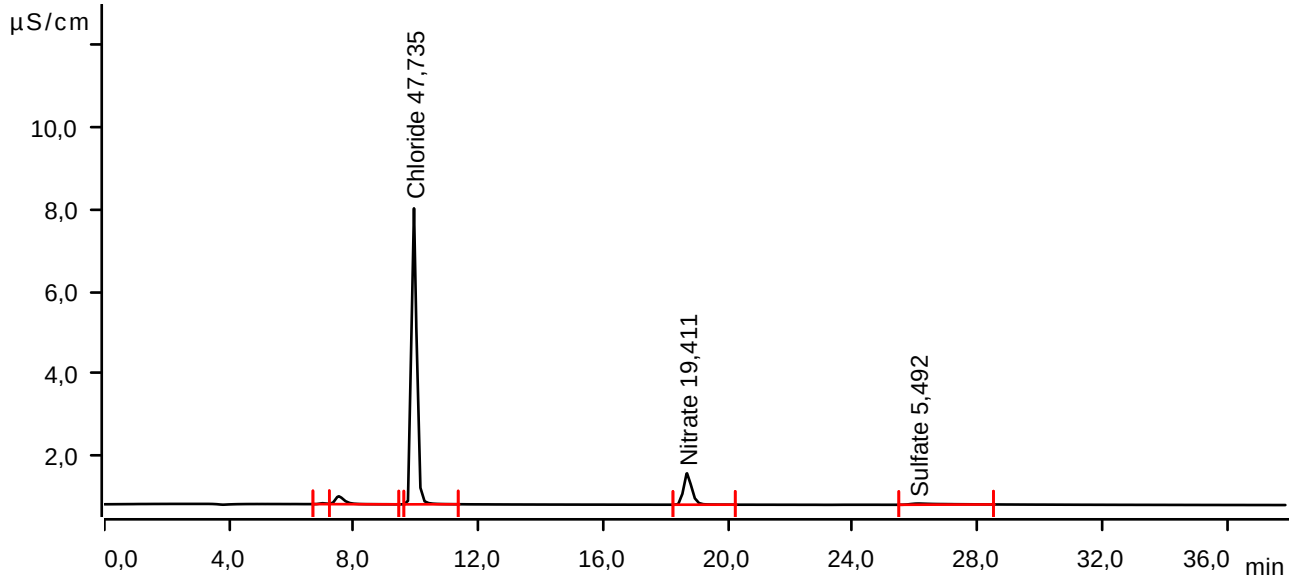

Peak number	Retention time min	Area (µS/cm) x min	Height µS/cm	Concentration mg/L	Component name
1	6,998	0,0053	0,022	invalid	
2	7,518	0,0671	0,193	invalid	
3	9,928	1,3351	7,223	47,735	Chloride
4	18,683	0,2350	0,766	19,411	Nitrate
5	26,105	0,0332	0,029	5,492	Sulfate

A.6 ICP-MS Results

A.6.1 Hydroponic samples, Batch 1&2

The tables on the following pages show the results for the ICP-MS analysis of the two batches of hydroponic samples collected from NTNU Social Research CIRiS. These are labeled EU1 through 8, for samples 1 through 8, and are marked with the date of collection. Batch 1 was collected 30.11.2021, and are marked EUX 30.11., while batch 2 was collected 06.12.2021 and are marked EUX 06.12.

Hydroponic samples, batch 1 & 2, ICP-MS Results page 1

			11 -> 11 B [O2]		23 -> 23 Na [O2]		24 -> 24 Mg [O2]		27 -> 27 Al [H2]		28 -> 44 Si [O2]	
Label	Comment	Total Dil.	Conc. [ug/l]	Conc. RSD	Conc. [ug/l]	Conc. RSD	Conc. [ug/l]	Conc. RSD	Conc. [ug/l]	Conc. RSD	Conc. [ug/l]	Conc. RSD
EU Blank 11.11	BLK1 dil100x	100	<23.545	N/A	27.9	7.0	24.7	0.5	11.64	4.2	155.7	5.2
EU Blank 11.11	BLK1	1	<0.235	131.8	9.5	0.9	7.5	0.4	4.37	0.6	129.7	1.1
EU2 06.12		100	196.0	5.0	8746.0	0.3	14809.4	0.7	71.27	0.7	1572.2	2.2
EU2 06.12		20	212.4	1.5	9731.5	0.9	16146.1	0.5	70.06	1.4	1618.7	0.6
EU1 06.12	Ref	50	191.5	2.0	9621.5	0.6	22199.7	0.4	61.49	1.8	1573.7	0.7
EU1 06.12	Ref	20	194.4	1.0	9750.1	0.5	22268.0	0.3	60.09	0.2	1582.2	0.2
EU6 06.12		20	186.2	1.5	9919.2	0.5	22534.8	1.1	70.36	0.9	1495.7	2.4
EU4 06.12		20	194.5	2.7	121412.0	0.3	16448.3	0.7	50.85	0.2	1339.4	1.2
EU3 06.12		20	211.8	2.0	122645.8	1.7	16308.6	1.6	70.69	0.5	1667.2	1.9
EU5 06.12		20	202.1	0.4	123985.0	0.6	16941.5	0.9	87.45	0.8	1650.2	0.3
EU7 06.12		20	187.9	1.8	10415.4	0.8	30501.5	0.5	66.86	1.4	1621.0	1.6
EU8 06.12		20	190.9	4.3	129256.9	1.1	23867.0	1.0	72.87	0.6	1648.5	1.0
EU2 11.11		30	225.5	1.9	9441.9	0.7	22107.5	1.2	34.28	0.5	1203.4	0.4
EU1 11.11		30	220.4	2.9	9291.8	0.5	28242.0	0.5	25.49	1.5	1161.4	1.5
EU6 11.11		30	219.6	2.6	9120.1	0.6	27656.6	0.9	25.42	1.8	1101.9	0.6
EU4 11.11		30	216.0	1.5	134159.1	0.4	21384.3	0.6	30.86	0.9	1050.7	1.6
EU3 11.11		30	217.2	3.1	134899.4	0.5	21545.6	1.1	34.71	2.2	999.6	0.7
EU5 11.11		30	221.2	1.1	134705.2	0.2	21460.2	0.3	37.47	0.4	1124.4	1.6
EU7 11.11		30	213.8	1.3	9376.9	0.7	35266.6	0.6	19.00	1.4	1109.2	0.4
EU8 11.11		30	214.0	0.1	134697.0	0.1	28129.1	0.4	27.87	1.0	1105.2	0.6

Hydroponic samples, batch 1 & 2, ICP-MS Results page 2

			31 -> 47 P [O2]		32 -> 48 S [O2]		39 -> 39 K [O2]		40 -> 40 Ca [H2]		55 -> 55 Mn [O2]	
Label	Comment	Total Dil.	Conc. [ug/l]	Conc. RSD	Conc. [ug/l]	Conc. RSD	Conc. [ug/l]	Conc. RSD	Conc. [ug/l]	Conc. RSD	Conc. [ug/l]	Conc. RSD
EU Blank 11.11	BLK1 dil100x	100	4.0	14.7	<14.997	143.4	<2.633	N/A	143.6	2.0	<0.079	N/A
EU Blank 11.11	BLK1	1	3.5	1.3	23.7	0.7	1.8	0.8	161.9	0.1	0.05	6.2
EU2 06.12		100	17394.1	1.3	167628.4	2.2	87661.4	0.2	94301.4	0.4	364.05	0.6
EU2 06.12		20	19118.7	1.3	179758.5	1.0	96326.1	0.7	101803.6	2.1	410.44	0.6
EU1 06.12	Ref	50	28823.2	1.2	191096.6	2.1	150606.2	0.5	131668.8	1.9	413.51	0.4
EU1 06.12	Ref	20	28843.7	0.5	191958.9	1.0	151253.8	0.6	132837.4	1.0	424.54	0.4
EU6 06.12		20	28655.8	0.3	192146.1	0.8	152259.6	1.0	134730.9	1.4	424.69	0.7
EU4 06.12		20	19185.7	1.7	159860.1	0.6	51832.5	0.5	101842.1	0.7	313.25	2.0
EU3 06.12		20	18758.4	1.5	200527.7	1.9	93598.6	0.6	103318.0	0.8	344.72	1.2
EU5 06.12		20	19615.4	1.9	274411.9	0.7	116161.1	0.3	105931.2	1.3	437.27	0.5
EU7 06.12		20	40271.4	0.5	216884.2	0.9	215953.9	1.5	170872.1	0.6	447.98	2.6
EU8 06.12		20	29605.6	1.0	216356.6	1.3	150914.6	1.5	140181.7	0.8	439.48	1.9
EU2 11.11		30	34156.2	0.9	204531.9	0.7	179735.7	0.8	121087.5	1.0	714.60	0.3
EU1 11.11		30	42317.6	0.4	204159.5	0.6	231679.4	0.4	147421.1	1.0	672.42	1.0
EU6 11.11		30	42680.1	1.0	206027.2	1.2	230169.3	1.5	142374.0	1.7	666.53	1.3
EU4 11.11		30	32545.0	1.8	172125.5	1.5	173642.4	1.3	115049.5	1.7	665.18	1.5
EU3 11.11		30	32489.4	1.0	213612.9	0.6	175952.8	0.4	114747.8	1.4	672.79	0.7
EU5 11.11		30	32251.2	0.5	288409.5	1.1	175363.3	0.6	115626.5	2.0	676.52	1.2
EU7 11.11		30	53964.3	1.0	224730.3	1.1	289565.1	0.6	177561.6	1.0	666.94	2.0
EU8 11.11		30	41869.4	1.0	223746.4	1.0	231792.6	0.7	146817.0	1.1	668.89	1.5

Hydroponic samples, batch 1 & 2, ICP-MS Results page 3

			56 -> 56 Fe [H2]		63 -> 63 Cu [O2]		66 -> 66 Zn [H2]		95 -> 127 Mo [O2]	
Label	Comment	Total Dil.	Conc. [ug/l]	Conc. RSD	Conc. [ug/l]	Conc. RSD	Conc. [ug/l]	Conc. RSD	Conc. [ug/l]	Conc. RSD
EU Blank 11.11	BLK1 dil100x	100	<4.044	9.3	<0.377	N/A	<4.463	N/A	<0.122	N/A
EU Blank 11.11	BLK1	1	0.5	0.2	0.50	1.2	2.44	1.2	0.00	16.3
EU2 06.12		100	3935.4	1.6	112.88	0.4	325.57	0.8	53.73	2.1
EU2 06.12		20	4160.7	2.1	124.07	0.6	357.24	1.5	58.81	1.5
EU1 06.12	Ref	50	4108.2	1.7	119.64	1.0	339.20	0.6	57.54	1.5
EU1 06.12	Ref	20	4151.4	0.9	119.93	0.8	346.05	0.5	57.69	1.4
EU6 06.12		20	4223.8	2.1	128.42	0.7	328.38	1.8	58.50	1.2
EU4 06.12		20	4218.2	1.1	164.47	0.4	355.46	0.8	59.54	1.0
EU3 06.12		20	4270.4	0.9	140.97	1.0	355.72	0.5	61.65	2.8
EU5 06.12		20	4276.6	1.0	117.27	0.6	341.56	1.1	59.31	1.8
EU7 06.12		20	4309.2	1.6	128.86	1.0	329.50	0.8	63.05	1.2
EU8 06.12		20	4388.2	0.8	128.09	0.7	325.86	0.4	61.28	0.9
EU2 11.11		30	4727.8	1.1	200.95	0.1	411.24	1.1	79.97	0.9
EU1 11.11		30	4504.0	0.8	127.67	0.4	418.28	1.9	74.03	0.7
EU6 11.11		30	4445.0	1.0	113.89	1.4	381.96	0.8	75.23	0.6
EU4 11.11		30	4511.4	1.5	144.74	0.4	419.37	0.4	75.44	1.8
EU3 11.11		30	4499.0	1.2	139.36	1.1	401.39	0.9	76.46	0.8
EU5 11.11		30	4464.9	1.1	116.65	0.4	401.34	1.4	75.34	0.2
EU7 11.11		30	4499.0	0.7	115.01	0.3	394.33	0.7	75.20	0.2
EU8 11.11		30	4500.7	1.4	99.65	0.7	388.99	0.7	73.61	1.3

A.6.2 Flow cell experiment

The table on the following page show the result of the ICP-MS analysis of samples collected from the flow cell experiment. Sampling numbering, related to ISE sampling and nomenclature is as follows:

ICP-MS Sample	Sample, table 4.8
1	1 & 2
2	3
3	4
4	5
5	6
6	7
7	8
8	9 & 10
9	11 & 12

Sample			23 -> 23 Na [O2]		24 -> 24 Mg [O2]		39 -> 39 K [O2]		43 -> 59 Ca [O2]		44 -> 60 Ca [O2]	
Acq. Date-Time	Sample Name	Comment	Conc. [ug/l]	Conc. RSD	Conc. [ug/l]	Conc. RSD	Conc. [ug/l]	Conc. RSD	Conc. [ug/l]	Conc. RSD	Conc. [ug/l]	Conc. RSD
03.06.2022 14:42	1	W2D1	3836.41	0.9	865	0.9	415.14	1.8	19814.39	4.9	19687.17	1.2
03.06.2022 14:44	2 rep1	W2D2	6721.93	2.5	23281	2.9	128953.37	2.6	93975.73	3.1	92814.52	2.5
03.06.2022 14:58	2 rep2	W2D2	7063.75	2.6	24071	2.6	136387.27	2.6	100588.17	3.1	99498.00	2.0
03.06.2022 15:00	3 rep1	W3D1	6898.48	2.1	23241	0.7	130984.94	0.7	94980.65	1.4	95498.39	0.4
03.06.2022 15:02	3 rep2	W3D1	7176.35	2.0	24026	1.2	136922.62	0.8	99438.31	1.4	99291.87	0.8
03.06.2022 15:04	4	W3D2	107784.66	0.7	23007	1.2	128222.40	0.8	96123.24	2.9	95174.38	1.2
03.06.2022 15:06	5	W4D1	111305.16	1.4	23191	0.9	127339.69	0.4	99303.13	5.0	98286.97	1.4
03.06.2022 15:08	6	W4D2	323205.42	0.6	21062	0.9	108790.32	1.0	92565.76	3.3	91056.53	0.5
03.06.2022 15:10	7	W5D1	343470.22	0.9	21887	1.9	88909.28	1.6	97912.78	4.8	96385.49	0.5
03.06.2022 15:12	8	W5D2	349377.42	1.4	21040	2.3	60022.97	1.0	96230.31	1.8	96987.03	2.1
03.06.2022 15:14	9	W6D1	351055.27	1.0	19640	0.7	15063.79	0.8	94380.50	2.1	93057.77	1.3

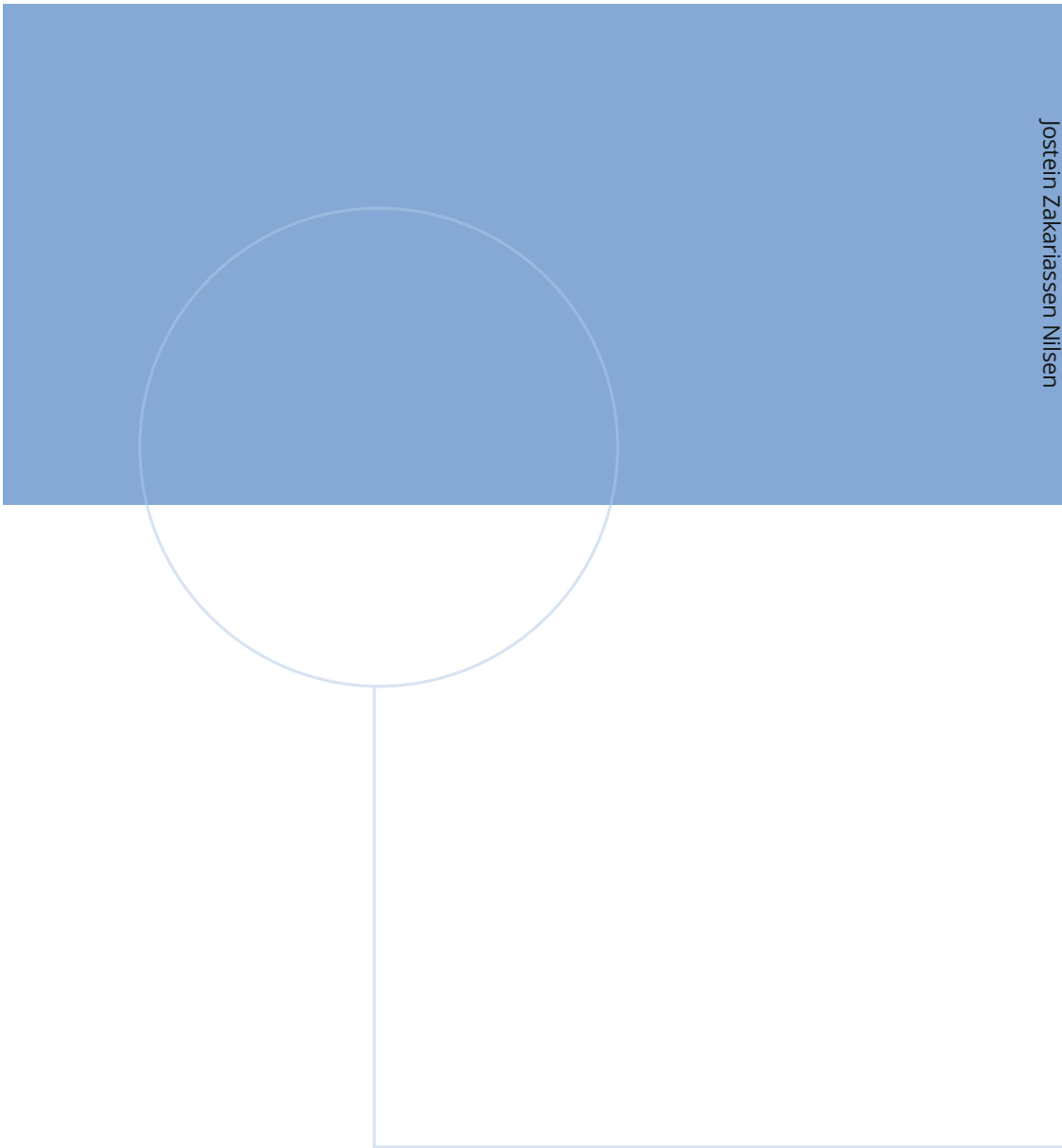

Jostein Zakariassen Nilsen

NTNU
Norwegian University of
Science and Technology